

Going Out on a Limb: Hindlimb loading and muscle activation in three-toed sloths  
(*Bradypus variegatus*, Xenarthra)

by

Andrew J. McKamy

Submitted in Partial Fulfillment of the Requirements

for the Degree of

Master of Science

in the

Biological Sciences

Program

YOUNGSTOWN STATE UNIVERSITY

August, 2022

Going Out on a Limb: Hindlimb loading and muscle activation in three-toed sloths  
(*Bradypus variegatus*, *Xenarthra*)

Andrew J. McKamy

I hereby release this thesis to the public. I understand that this thesis will be made available from the OhioLINK ETD Center and the Maag Library Circulation Desk for public access. I also authorize the University of other individuals to make copies of this thesis as needed for scholarly research.

Signature:

---

*Andrew J. McKamy*, Student

Date

Approvals:

---

*Prof. Michael T. Butcher*, Thesis Advisor

Date

---

*Assist. Prof. Stefania C. Panaitof*, Committee Member

Date

---

*Prof. Kenneth Learman*, Committee Member

Date

---

*Dr. Salvatore A. Sanders*, Dean, College of Graduate  
Studies

Date

©

Andrew J. McKamy

2022

## ABSTRACT

Modern tree-sloths are one of few mammalian taxa for which quadrupedal suspension is obligatory. Sloth limb musculature is specialized for slow velocity, large force contractions that stabilize limb their body below branches, and also conserves energy during locomotion. However, it is unknown if two and three-toed sloths converge in their use of limb biomechanics and whether these patterns are comparable to how primates perform arboreal suspensory locomotion. This study addresses this need by collecting limb loading data in three-toed sloths (*Bradypus variegatus*;  $N=5$ ) during suspensory walking. Sloths performed locomotor trials at their preferred speed on a three-part beam apparatus instrumented with a force platform as the central supporting segment. Peak forces and impulses were recorded and analyzed in three dimensions in the forelimb and hindlimb during suspensory walking. The hindlimbs of *B. variegatus* apply large braking forces comparable in magnitude to forces by the forelimbs in propulsion, a pattern consistent with that of the two-toed sloths. However, *B. variegatus* exhibits hindlimb-biased bodyweight support in vertical peak forces and impulse and appreciable laterally-directed forces in both limb pairs. These patterns of limb force distribution vary from those previously observed in two-toed sloths. Moreover, bodyweight distribution between limb pairs is the opposite of that employed by primates during quadrupedal suspension. There appear to be multiple strategies for achieving suspensory locomotion in arboreal mammals. EMG analyses are expected to provide further insight into how specific hindlimb muscle groups contribute to braking/propulsive forces and stabilizing the center of mass of sloths during suspension.

## **ACKNOWLEDEMENTS**

I sincerely thank my graduate advisor, Dr. Michael Butcher, for his guidance, patience, and mentoring throughout my Thesis research project and Masters Degree. I thank my graduate committee members, Drs. Carmen Panaitof and Ken Learman, for their critical reviews of my Thesis, manuscript, and helpful comments. I am very grateful to Ms. Judy Avey-Arroyo for the opportunity to interact with live sloths during the duration of collecting SRF and EMG data for my Thesis at The Sloth Sanctuary of Costa Rica. Last, I am grateful to my lab mates (former and present) Dakota Morgan, Jordan Fain, Dragan Juzbasich, Michael Deak, Taylor Coblenz, Jamie Stahl, and Christina Tucker, who gave me consistent support throughout my tenure at YSU. The YSU Office of Research and Department of Chemical and Biological Sciences are additionally acknowledged for their support.

## **DEDICATION**

I would like to thank my family, especially my parents and sisters for their support and encouragement during my education. I dedicate this Thesis to them, my advisor Dr. Butcher, and my friends here at Youngstown State University. All of my progression as a student and researcher is owed to them.

# TABLE OF CONTENTS

Approval Page	ii
Copyright Page	iii
Abstract	iv
Acknowledgements	v
Dedication	vi
Table of Contents	vii
List of Tables	viii
List of Figures	ix
Foreword	x
INTRODUCTION	1
MATERIALS and METHODS	2
<i>Animals and permissions</i>	2
<i>Experimental set-up and data collection</i>	3
<i>Kinetic analyses</i>	4
<i>Statistics</i>	5
RESULTS	5
DISCUSSION	7
<i>Limitations</i>	11
<i>Conclusions</i>	12
REFERENCES	13
APPENDIX I	45
<i>EMG analyses</i>	45
APPENDIX II	77
<i>Literature Review/Proposal</i>	77
APPENDIX III	108
<i>MINAE Data Collection Permit</i>	108

## LIST OF TABLES

1. Means ( $\pm$ s.d.) of peak forces (normalized in %BW) for <i>Bradypus variegatus</i>	28
2. Means ( $\pm$ s.d.) of impulses (normalized in %BWS) for <i>Bradypus variegatus</i>	29
3. Intraspecific parameters of statistical importance for fixed effects related to peak limb loading in <i>Bradypus variegatus</i>	30
4. Interspecific parameters of statistical importance for fixed effects related to peak limb-loading in <i>Bradypus variegatus</i>	31

### Supplementary Data Tables

1. Means ( $\pm$ s.d.) of peak forces (normalized in %BW) for $N=5$ individuals of <i>B. variegatus</i>	32
2. Means ( $\pm$ s.d.) of impulses (normalized in %BWS) for $N=5$ individuals of <i>B. variegatus</i>	33
3. Intraspecific parameters of statistical importance for fixed effects related to limb loading impulse in <i>B. variegatus</i>	34
4. Interspecific parameters of statistical importance for fixed effects related to limb loading impulse in <i>B. variegatus</i>	35
5. Subset of means ( $\pm$ s.d.) for impulses (normalized in %BWS) for <i>B. variegatus</i>	36

### Appendix I Data Tables

1. Morphometric data for animals and number of trials/strides/bursts analyzed	64
2. Stride parameters for suspensory walking in <i>B. variegatus</i>	65
3. Individuals, muscles, and functional behaviors for which EMG was recorded and analyzed	66
4. Temporal variables of EMG activation for hindlimb muscles in <i>B. variegatus</i>	67
5. Means of EMG intensity ratios for each individual and muscle analyzed	68
6. Timing of peak EMG activations relative to timings of peak limb force	69
7. Summary of typical limb phase muscle activations during the stride cycle	70



## LIST OF FIGURES

1. Force beam apparatus and suspensory walking limb motion	38
2. Representative single limb forces sampled from <i>Bradypus variegatus</i> and <i>Choloepus didactylus</i> during suspensory walking	40
3. Box and whisker plots of relative peak forces and impulses between limb pairs and species during suspensory walking	42
4. Relative contribution of fore- and hindlimbs to bodyweight support in <i>Bradypus variegatus</i> during suspensory walking	44

### Appendix I Figures

1. Mean EMG burst duration (% stride) for hindlimb muscles during suspensory walking in <i>B. variegatus</i>	72
2. Mean EMG intensity ratios for hindlimb muscles in <i>B. variegatus</i>	74
3. Bi-plots of timing between peaks of muscle activation and limb loading during suspensory walking in <i>B. variegatus</i>	76

## FOREWORD

This thesis contains a thorough evaluation of limb loading in three-toed sloths. The main body text, tables, and figures represent the manuscript from a limb loading study based on force platform data collected from *Bradypus variegatus*. The manuscript containing the kinetics data has been submitted to the *Journal of Experimental Biology* for peer review. Following this work are two appendices. Appendix I is a companion study of simultaneous limb force and muscle EMG activation in ten skeletal muscles. This section is intended to be a manuscript submitted to the *Journal of Experimental Zoology*. The tables and figures for Appendix I are found therein, while the research detailed in the limb loading manuscript is duly cited as McKamy et al. (in review). Appendix II is the original literature review and research proposal. Citations for the main body text and two appendices have been consolidated into a single references list.

## INTRODUCTION

Two-toed sloths (*Choloepus* spp.) and three-toed sloths (*Bradypus* spp.) are rare among mammals in being obligate suspensory taxa (Nyakatura, 2012; Nyakatura and Andrada, 2013; Slater et al., 2016). Moreover, the two modern genera of tree sloths arose from separate lineages that split nearly 29 million years ago (Delsuc et al., 2019; Pant et al., 2014) and thus, the observed similarities in morphology, physiology, and lifestyle between *Choloepus* and *Bradypus* represent one of the most remarkable examples of evolutionary convergence (Nyakatura and Fischer, 2011; Pant et al., 2014).

Although *Choloepus* and *Bradypus* generally share patterns of substrate use, species in each genus have their own ecological and behavioral preferences (Adam, 1999; Hayssen 2009, 2010, 2011), ranging from foraging habits (Montgomery and Sunquist, 1975, 1978) to frequency of suspensory locomotion and posture (Sunquist and Montgomery, 1973; Urbani and Bosque, 2011). Patterns of limb kinematics and kinetics during below-branch locomotion have been previously investigated in *C. didactylus* (Granatosky and Schmitt, 2017; Granatosky et al., 2018b; Nyakatura et al., 2010). Similar to what has been shown for inverted quadrupedalism in primates (Granatosky, 2018a; Granatosky and Schmitt, 2017, 2019; Granatosky et al., 2018a), the available evidence reveals that two-toed sloths employ a diagonal-sequence diagonal-couplet (DSDC; Usherwood and Self Davies, 2017) gait during suspensory walking (SW), wherein their forelimbs act in net propulsion and their hindlimbs in net braking, opposite of the mechanics of upright or pronograde arboreal mammals (Granatosky, 2018b; Granatosky et al., 2018a; Gray, 1944; Usherwood and Self Davies, 2017). Two-toed sloths also demonstrate equal bodyweight support between limb pairs (Granatosky et al., 2018b), with primarily medial forces exerted into the substrate by both the fore- and hindlimbs for arboreal stability (Granatosky and Schmitt, 2017). Furthermore, modeling data predict that sloths do not use pendular exchanges of energy during suspensory locomotion (Nyakatura and Andrada, 2013), therefore suggesting that their locomotion is controlled almost entirely by muscle work. Comparatively fewer studies have examined the locomotor features of *Bradypus* (e.g., Gorvet et al., 2020; Mendel, 1985a, b).

Given the degree of morphological convergence among extant species of tree sloths, it is reasonable to expect that the locomotor mechanics of *Bradypus* would be similar to those

of *Choloepus*. However, while *Choloepus* has limb pairs of nearly equal length (Meritt, 1985; Wislocki, 1928) and feet that are elongate and notably hook-shaped (Mendel 1981a, b), *Bradypus* has elongate forelimbs but retains much shorter hindlimbs with a long calcaneus and short metatarsals (Marshall et al., 2021). These anatomical variations could alter substrate interactions and limb lever mechanics used for suspensory locomotion and posture (Fujiwara et al., 2011; Dickinson et al., 2022). During SW, *Bradypus* flexes its elbow joints, thereby pulling its body towards the substrate to achieve a more level orientation. This position may optimize mechanical advantage of the limb flexor musculature for below-branch stabilization (Olson et al., 2018) and could alter patterns of limb loading relative to *Choloepus*. Also, *B. variegatus* uses a lateral sequence diagonal couplet (LSDC) gait during SW (Gorvet et al., 2020; Mendel 1985a), perhaps further altering limb loading versus that of *C. didactylus*.

The aim of this study is to evaluate locomotor kinetics in *Bradypus* during SW. It was hypothesized that due to the marked physiological convergence observed between genera, patterns of peak forces and impulse application would generally mimic those observed in *Choloepus*. Specifically, it was predicted that both fore-aft and mediolateral limb loading would be similar in magnitude and direction between species, but the morphological variation in limb length observed among species would result in differences in vertical bodyweight support between limb pairs. Moreover, it is expected that magnitudes of propulsive and braking impulses will be equivalently large signifying how counteracting muscular contraction between fore- and hindlimb functional groups restrains locomotion in sloths. Such findings could elucidate multiple strategies by which suspensory taxa interact with the substrate to bring about control of inverted quadrupedalism.

## MATERIALS AND METHODS

### *Animals and permissions*

A total of  $N=5$  (adult and sub-adult:  $3.88\pm 0.3$  kg) brown-throated three-toed tree sloths (*Bradypus variegatus*) were used for this study. Sloths were selected for use and handled entirely by staff at the Sloth Sanctuary of Costa Rica. All animals were healthy with no visible signs of musculoskeletal or gait abnormalities, and no preference was given to male or female individuals (Suppl. Data Tables S1 and S2). All experimental procedures

complied with the protocols approved by the Costa Rica Ministerio Del Ambiente y Energía, Sistema Nacional de Áreas de Conservación, a través del Programa de Investigación del Área de Conservación La Amistad Caribe, (R-SINAC-PNI-ACLAC-012-2021 to M.T. Butcher).

### *Experimental set-up and data collection*

Three-dimensional locomotor kinetics were sampled at 12,000 Hz using a calibrated, medium-load AMTI load cell (model MC3A, 445N maximum load; Watertown, MA) placed in between two un-instrumented beams made of cave brava (a native Costa Rican woody plant). To the load cell was bolted a 3D printed, T-shaped grip attachment (i.e., force platform) that was approximately the same diameter as the cave brava and wrapped with duct tape to provide a frictional pad surface for the animals to grip onto during SW. The end of the T-shaped attachment was suspended level between the two (lower) un-instrumented segments of the beam with ~5cm of clearance on either end (Fig. 1a). The animals were allowed to traverse the entire beam in both directions at their preferred speed while being video-recorded from both sagittal and diagonal views using four GoPro cameras (HERO5; GoPro, San Mateo, CA, USA) set at a frame rate of 60 Hz. Only trials where the individuals moved in a continuous horizontal path and no visual acceleration or deceleration was observed were considered successful. Among these trials, only those with clear footfalls on the force platform were saved for subsequent processing and statistical analysis.

Velocity calculations were performed following procedures described by Young et al. (2022). Briefly, 150-200 video frames of a predetermined center of mass (CoM) position from each individual were labeled (Granatosky et al., 2018a, b; Nyakatura and Andrada, 2013), in addition to two points of a known distance apart (in cm). The position labels were input into markerless pose estimation software (DeepLabCut: Mathis et al., 2018) to train its neural network. The positional outputs as well as the known distance values were used to calibrate the geometric space and provide the conversion factor necessary to calculate the velocity within a stride.

### *Kinetic Analyses*

The forces experienced by the force platform were resolved into vertical (Z), fore-aft (X), and mediolateral (Y) components using the software Bioware v5.4 (Kistler; Michigan,

USA). In total, forces from  $n=69$  forelimb and  $n=98$  hindlimb distinct footfalls on the force platform were successfully recorded and analyzed across all five individuals. These data ( $n=167$  footfalls) were imported into a custom-written MATLAB script and filtered through a low-pass Fourier filter at 15 Hz to calculate peak forces and impulses from each limb: (1) vertical peak force ( $V_{pk}$ ) and impulse ( $J_V$ ); (2) propulsive peak force ( $P_{pk}$ ) and impulse ( $J_P$ ); (3) braking peak force ( $B_{pk}$ ) and impulse ( $J_B$ ); (4) medial peak force ( $M_{pk}$ ) and impulse ( $J_M$ ); (5) lateral peak force ( $L_{pk}$ ) and impulse ( $J_L$ ). All recorded kinetics data were also corrected for direction of travel, orientation, and whether the contact limb was right or left. Specifically, signs of the forces were standardized to reflect those applied by the animal, such that (by convention) vertical forces reflected positive values, fore-aft forces were split into negative braking and positive propulsive forces, and mediolateral forces where medially-directed forces were negative and laterally-directed forces were positive. Additionally, the areas under the horizontal component of the force-time curve were measured to determine braking and propulsive impulses and net fore-aft impulse. The net fore-aft impulse provides a means for differentiating the overall functional role of a limb during locomotor behavior (Granatosky et al., 2018a) such that positive (+) values indicate a net propulsive limb, whereas negative (-) values indicate a net braking limb. Values approximating zero represent single limb forces wherein braking and propulsive impulses are equal.

Peak force in Newtons (N) and impulse (in N.s) in each direction were normalized to percent body weight (%BW) and percent body weight seconds (%BWS), respectively, to allow for normalized comparison between individuals (Granatosky and Schmitt, 2017). All values were averaged across individuals and reported as pooled means  $\pm$  standard deviation (s.d.). Descriptive statistics for each individual sampled are reported in Supplementary Data Tables S1–S4. Last, a separate, more direct evaluation of bodyweight support via vertical impulse was limited to a subset of trials ( $n=25$ ) for which there were consecutive fore- and hindlimb contacts on the force platform to ensure that comparisons between limb pairs were made within a single stride. For this analysis, only values of  $VI_{pk}$  were used to calculate percentages of total vertical impulse to assess the relative contribution of bodyweight support by each limb pair.

### *Statistics*

Statistical tests were conducted using R (R Core Team, 2021). The R packages ‘lmerTest’ (Kuznetsova et al., 2017) and ‘lme4’ (Bates et al., 2014) were used for these analyses. For the purposes of statistical testing, the absolute values of all recorded forces were used, as our goal was to compare magnitudes, rather than direction *per se*. To assess normality and homoscedasticity in the data sets, Shapiro-Wilk and Levene’s tests, respectively, were conducted and peak forces and impulses were rank-transformed prior to conducting statistical testing (Sokal and Rohlf, 2012). A series of linear mixed effect (LME) models were created to assess differences in vertical, fore-aft, and mediolateral peak forces and impulses both between limb pairs (intraspecific variation) and species (interspecific variation) by using available data from *C. didactylus* (Granatosky and Schmitt, 2017; Granatosky et al., 2018b). As velocity is known to influence patterns of limb loading (Granatosky et al., 2020), it was maintained as a fixed covariate in each model tested. Individual idiosyncrasies were also accounted for by using individual as a random effect in each model (Bates et al., 2014; Winter, 2013). Finally, a third LME model was created to test for steady-state locomotion in our sample of sloths. This analysis using *net* impulse for each limb pair within each species verified steady-state locomotion by non-significant findings for each response variable (data not shown).

## **RESULTS**

The overall patterns of limb loading for each limb pair of *B. variegatus* are shown in Figure 2 and mean values of peak force and impulse in each direction are presented in Tables 1 and 2, respectively. The hindlimbs of *B. variegatus* apply larger  $V_{pk}$  force than the forelimbs ( $73.8 \pm 13.7$  %BW vs.  $62.9 \pm 11.2$  %BW, respectively) and this difference is significant ( $p=0.005$ , Tables 1 and 3; Fig. 3a), even after accounting for velocity variation and individual differences. Nonetheless, magnitudes of  $J_v$  between limb pairs in *B. variegatus* did not differ significantly ( $p=0.238$ , Suppl. Data Table 3). Greater  $P_{pk}$  force ( $p=0.001$ ) is exerted by the forelimbs of *B. variegatus* to generate propulsion, whereas greater  $B_{pk}$  force ( $p=<0.001$ ) is applied by the hindlimbs to perform braking (Tables 1 and 3; Fig. 3b), thus the forelimbs are net propulsive (27.9 %BWS) and the hindlimbs are net braking (-34.3 %BWS) during SW (Table 2). This intraspecific trend is consistent with that

in *C. didactylus*, where  $P_{pk}$  and  $B_{pk}$  are the only peak force magnitudes that vary significantly between limb pairs ( $p < 0.001$ , Table 3). Collectively, these data for fore-aft peak forces parallel LME model results for  $J_P$  and  $J_B$  in each limb pair within both species (all  $p$ -values  $< 0.001$ , Suppl. Data Table 3). The hindlimbs of *B. variegatus* also apply larger  $M_{pk}$  force ( $p = 0.013$ ) than the forelimbs, but both limb pairs exert similar  $L_{pk}$  force ( $p = 0.873$ ) (Table 3). The means of  $L_{pk}$  force, however, are appreciable for both the forelimbs and hindlimbs in *B. variegatus* ( $8.5 \pm 6.3$  %BW vs.  $7.2 \pm 7.4$  %BW, respectively) (Table 1; Fig. 3c). In general, mediolateral impulses are not statistically different between limb pairs (all  $p$ -values  $\geq 0.054$ , Table 2 and Suppl. Data Table 3).

Interspecific differences are generally reflective of the variation in peak loading between limb pairs within species. In particular,  $V_{pk}$  force is significantly greater in the hindlimbs of *B. variegatus* than that in *C. didactylus* ( $p = 0.026$ ), whereas equivalent magnitudes of  $V_{pk}$  force are observed in the forelimbs of both species ( $p = 0.693$ ) (Table 4). Although there are mean differences in limb pairs between species (all  $p$ -values  $> 0.640$ , Suppl. Data Table 4), the elevated values of  $J_V$  for the hindlimbs of *B. variegatus* (Table 2; Suppl. Data Table 5) correspond with a greater percentage of bodyweight support relative to the forelimbs (range: 54.6–56.4% for the hindlimbs vs. 45.9–47.1% for the forelimbs) (Fig. 4). In addition,  $P_{pk}$  force exerted by the forelimbs ( $p = 0.019$ ) and  $B_{pk}$  force by the hindlimbs ( $p < 0.001$ ) were larger in *B. variegatus* than *C. didactylus* (Table 4). However, the hindlimbs in *C. didactylus* generate significantly larger  $J_P$  ( $p = 0.016$ ) but smaller  $J_B$  ( $p = 0.017$ ) than those in *B. variegatus* (Suppl. Data Table 4). Despite greater  $M_{pk}$  force applied by the forelimbs of *C. didactylus* ( $p < 0.001$ ), yet comparable  $M_{pk}$  force ( $p = 0.780$ ) in the hindlimbs of both species, the mean magnitudes of  $L_{pk}$  force for both the forelimbs ( $p < 0.001$ ) and hindlimb ( $p = 0.022$ ) in *B. variegatus* are significantly larger than those in *C. didactylus* (Table 4). Significant LME model results for  $J_M$  and  $J_L$  in the forelimbs and hindlimbs of both species match those of the mediolateral peak forces (all  $p$ -values  $< 0.001$ , Suppl. Data Table 4).



## DISCUSSION

Existing data on suspensory locomotor kinetics in tree sloths reveal three major findings. First, like *C. didactylus*, there is a functional difference between the limb pairs of *B. variegatus*, with the forelimbs and the hindlimbs serving as the propulsive and braking appendages, respectively. Second, although bodyweight and impulse are equally distributed between limb pairs during SW in *C. didactylus* (Granatosky et al., 2018b), this feature may be exclusive to two-toed sloths (Dickinson et al., 2022) because *B. variegatus* demonstrates a hindlimb bias in vertical bodyweight support, as predicted. Third, *C. didactylus* mainly exerts medially-directed forces with both limb pairs (Granatosky and Schmitt, 2017), whereas medial peak force predominates in the hindlimbs of *B. variegatus*, and surprisingly, both of its limb pairs exert significant magnitudes of laterally-directed forces. This latter finding is novel, as neither two-toed sloths nor suspensory primates apply appreciable magnitudes of lateral peak force during inverted quadrupedalism.

Limb loading patterns resolved for SW in both genera indicate that the hindlimbs act as the main braking and stabilizing limbs during SW as originally hypothesized by Goffart (1971), a convergent trait among tree sloths (Granatosky and Schmitt, 2017; Nyakatura and Andrada, 2013), bats (Granatosky, 2018a) and numerous primates (e.g., lemurs and monkeys: Dickinson et al., 2022; Granatosky et al., 2016; Granatosky and Schmitt, 2019). Thus, use of the forelimbs to provide primary propulsion during inverted quadrupedalism appears to be a universal locomotor strategy for suspensory taxa. Sloths also employ slow, intermittent locomotion as an adaptive strategy to conserve metabolic energy (Gorvet et al., 2020; McDonald and De Iuliis, 2008) and this movement pattern matches well with a broad distribution of slow-contracting muscle fibers dependent on anaerobic metabolism (Spainhower et al., 2018, 2021). For example, the hindlimbs of *B. variegatus* are composed of several muscles that are homogenous in their expression of slow-contracting MHC-1 fibers (Spainhower et al., 2021) and these may be the most extremely well-suited for applying braking and stabilizing forces.

Animals in this study were noted to reach with their forelimbs ahead of their body position to test the beam for adequate strength/stiffness prior to committing to support of their bodyweight. It is not known, however, if *Choloepus* is as deliberate with their purchase of the substrate (at touchdown) as *Bradypus*. It was additionally observed that

compared with *C. didactylus* during the contact phase of SW, the hindlimb of *B. variegatus* initially provides modest, but significantly greater propulsive impulse, and transitions early rather and later in support to applying comparatively larger braking force. Conversely, its forelimbs provide large propulsive force/impulse and transition late in contact phase to exert equally modest braking force prior to lift-off (Fig. 2). Because these patterns of fore-aft limb loading are generally similar to that seen in *Choloepus* (Granatosky and Schmitt, 2017), this may be the mechanism by which sloths minimize swinging in the sagittal plane at the beginning and end of contact phase during SW and precisely control their forward horizontal velocity. As previously posited by Nyakatura and Andrada (2013), sloth locomotion may be entirely driven by muscle work and the transitions of propulsive to braking forces observed between limb pairs likely reflect this type of limb muscle function. Previous work in *B. variegatus* showed the possibility for co-activation of selected flexor/adductor muscles in each limb pair (Gorvet et al., 2020) that may ensure that there is minimal horizontal acceleration of the CoM via balancing of the propulsive and braking forces as was suggested for inverted quadrupedalism in slow lorises (*Nycticebus*: Ishida et al., 1990). In sloths, large but very slow-contracting motor units can be selectively recruited (Gorvet et al., 2020) to provide equal propulsion and braking across a stride, thus producing controlled movements that reduce oscillations of the substrate and minimize energy loss.

A divergent pattern between genera of tree sloths is related to limb proportions. Three-toed sloths have elongate forelimbs relative to both their body and hindlimb lengths, a morphological trait that they share with suspensory primates (Granatosky, 2018c), and one that also might be related to vertical climbing performance on larger diameter substrates (Jungers, 1978). For example, *B. variegatus* has a higher intermembral index (IMI:  $1.65 \pm 0.11$  vs.  $1.11 \pm 0.03$ ) and ankle extensor index (AEI:  $0.73 \pm 0.04$  vs.  $0.63 \pm 0.07$ ) relative to those of *C. didactylus* (Marshall et al., 2021). Greater trochanter height index and crural index, however, are both lower in *B. variegatus*, jointly suggesting that the hindlimbs of three toed sloths have enhanced limb mechanical advantage (MA) and large out-force application to the substrate during locomotion and posture (Marshall et al., 2021) consistent with a greater role in support of the bodyweight in suspension. Retention of shorter hindlimbs could have contributed to convergence of support postures (e.g., tripodal posture) in suspensory mammals with a high IMI. Nevertheless, having greatly elongate

forelimbs may limit the options in which *Bradypus* achieves support via vertical limb loading, and although their forelimb bones are stronger (compressive and bending strength) than their hindlimb bones (Mossor et al., 2022), both limb pairs are capable for resisting routine tensile loading and this capacity is equivalent between two and three-toed forms. Therefore, large MA of the well-developed flexor musculature in *B. variegatus* (Mendel, 1985a; Morgan et al., *in review*) by modified origins and insertions (Butcher et al., 2022) could be the most critical factor for a greater reliance on the hindlimbs for vertical bodyweight support.

Notably, primates exhibit hindlimb-biased support during pronograde arboreal locomotion accounting for 55–70% of the bodyweight (Demes et al., 1994; Larson and Demes, 2011), values matching hindlimb loading during SW in *B. variegatus* (Table 1). Yet, the available data for primates based on vertical peak force and impulse (Ishida et al., 1990; Granatosky et al., 2016; Dickinson et al., 2022) indicate a shift to forelimb-biased support during inverted quadrupedalism (Granatosky and Schmitt, 2019; Larson, 2018). Indeed, a hindlimb-biased support distribution is rare among inverted quadrupeds with the giant flying fox (*Pteropus vampyrus*) being the only other species besides *B. variegatus* to exhibit such a pattern, and the mechanisms for support vary considerably among suspensorial species. For two-toed sloths, the position of the CoM and limb kinematics relative to the CoM provide a good explanation for bodyweight support distribution equally between the limbs. In primates, however, the mechanism is less well-known, and it remains unclear whether CoM position or relative contact duration between the limbs determines patterns of forelimb versus hindlimb bodyweight distribution. More explicit tests of CoM position during suspensory locomotion are required to determine the mechanism and ecological advantage of hindlimb-biased support in *B. variegatus*.

Though the magnitudes of vertical peak force in the hindlimbs of *B. variegatus* are significantly larger compared with their forelimbs, as well as those from the hindlimbs of *C. didactylus* (Tables 3, 4), the vertical impulses evaluated across a stride provide the most direct evidence of hindlimb-biased support in three-toed sloths (Fig. 4). The suggestion of hindlimb-biased suspensory support in *Bradypus*, however, could be a consequence of selection for climbing ability. For example, appreciable MA at the hip and knee joints versus high velocity of joint rotation, but especially large MA at the ankle joint (Marshall

et al., 2021) is beneficial for slow, stealthy climbing behavior that involves prolonged vertical clinging. Gripping the substrate via low velocity, high force contractions of distal hindlimb musculature (Spainhower et al., 2021) would also provide stability in both vertical and horizontal directions.

Another divergent pattern between genera of tree sloths is reflected in the magnitudes of both peak braking and medial forces exerted on the substrate by the hindlimbs of *B. variegatus* that are nearly double those of *C. didactylus*. In particular, significantly greater braking forces may prevent cranial shifting of position of the CoM and bodyweight onto the forelimb (i.e., horizontal levering: Granatosky et al., 2018b), especially in three-toed sloths that move at consistently slower average velocities (Britton, 1941; Gorvet et al., 2020). The *m. sartorius* (hip flexor/knee flexor) and *m. iliopsoas* (hip flexor), as well as the bellies of *m. adductor longus*, were formerly hypothesized as the muscles with potentially the greatest capacity for applying braking and medial forces, respectively (Spainhower et al., 2021; Butcher et al., 2022). It is also possible that the *m. quadriceps* (knee extensors) in *B. variegatus* enhance the strut-like function of the hindlimb by undergoing isometric (or eccentric) loading (adding to the net braking forces), in addition to a role in stabilizing the knee joint by counteracting large flexor torques applied by the massive, forceful knee flexor musculature (Butcher et al., 2022). However, muscle fiber architecture (Morgan et al., *in review*) and EMG activation analyses in the hindlimb of three-toed sloths are needed to verify such roles of these functional muscle groups.

The finding of significantly elevated lateral peak forces and impulse by the fore- and hindlimbs of *Bradypus* (7.2–8.5 %BW) as opposed to minimal lateral peak forces in *Choloepus* (1.0–1.4 %BW), is another distinction in the way that the feet of tree sloths interact with the substrate. Initial purchase of the substrate varies between species with *B. variegatus* placing the entire plantar/palmar aspect of its feet in contact with the upper surface of the substrate with flexion of the claws to secure the purchase (Gorvet et al. 2020; Mendel, 1985a) (see Fig. 1b), whereas *C. didactylus* prefers contacting the substrate with only its claws (Granatosky et al., 2018b; Mendel 1981b). The magnitudes of peak laterally-directed forces observed could be caused by the claws first pulling laterally against the substrate to secure the limb contact just before the entire foot contours to the substrate and the limb supports full weight. Some amount of the lateral peak forces observed may also

represent simultaneous abduction as the limbs are retracted during intervals of propulsion (Fig. 1b), whereas medially-directed forces are those that stabilize the body by contralateral limbs as previously found in *C. didactylus* (Granatosky and Schmitt, 2017).

The limb placement of the LSDC gait in *B. variegatus* (Gorvet et al., 2020) also serves to diagonally balance sloths during suspensory locomotion, such that the detached and protracted forelimb is afforded the freedom to test for purchase of new substrates, in addition to allowing for a large range of motion needed in a complex arboreal environment. As *Bradypus* prefers the high-canopy and/or emergent level of the rainforest, and they must navigate a more vertical strata niche than *Choloepus* (Hayssen, 2010, 2011), a greater range of motion for the forelimbs may be more critical to their locomotor success. During functional use of tripodal support, both hindlimbs have the role of anchoring the animal to the substrate, which is realized by their large grip forces that approximate or slightly exceed bodyweight force, especially on larger diameter substrates (Young et al., *in review*). Moreover, this posture mirrors that of hang-feeding behavior in orangutans (Hunt, 2016), as well as that of spider monkeys (Youlatos, 2002), which support their bodyweight by grasping the substrate with their hindlimbs and prehensile tail (i.e., tail assisted hindlimb hanging) to free the forelimbs for foraging on fruit.

### *Limitations*

Despite the adequate sample size and large number of single limb contacts on the force platform, there are still several possible limitations to this study. One such consideration is that the animals in this study were not always undergoing steady-state locomotion. Those trials were excluded from analysis and were from mainly one individual (Bv2) for which we had a disproportionately large number of recorded footfalls (see Suppl. Data Tables 1 and 2). That said, data for this individual still represent the highest measured velocities in the data set. Minor accelerations and decelerations, however, are typical of intermittent sloth locomotion, but our statistical analysis of mean net impulse differences between the fore- and hindlimb pairs for each species verified that in the trials selected for analysis the animals were undergoing steady state locomotion with large duty factors. Another potential limitation is the sedation effects of the drug Dexdomitor injected prior to experimentation, which was necessary for implantation of fine wire EMG electrodes used in our companion study and the benefit of collecting simultaneous *in vivo* data. This sedative, though

countered with a reversal agent (Antisedan) prior to trials of SW, may have initially reduced performance if the individuals were not able to fully metabolize the drug within the time given to recover. Nevertheless, these two drugs were used in a prior EMG study (Gorvet et al., 2020) with no obvious performance impairment. Furthermore, the sloths used in our study are routinely exposed to sedation/reversal for health checks, claw trimmings, and various veterinary medical procedures. A final possible limitation involves the construction of the force beam apparatus. Although composed of a local woody plant (cave brava), the beam is not typical of the substrate (i.e., *Cecropia* trees) that *Bradypus* uses. The small diameter and smooth surface of the beam were therefore unnatural and may have altered how the sloths gripped and walked (or were motivated to walk) across the substrate.

### *Conclusions*

Despite their numerous shared physiological traits, suspension in sloths exemplifies a combination of convergent and divergent locomotor kinetics. Consistent between genera, and suspensory primates, is the use of the forelimbs for propulsion and the hindlimbs for both braking and stability. However, appreciable magnitudes of medial and lateral peak forces and impulses exerted by both limb pairs and being hindlimb-biased in bodyweight support signify limb loading patterns in *Bradypus* that not only diverge from those in *Choloepus*, but also from primates. Thus, inverted quadrupedalism involves a continuum of mechanics that are employed across suspensorial taxa, which is dependent on several factors, including limb proportions, bone strength, modifications to the flexor musculature for enhanced mechanical advantage, behavioral flexibility, and ecological preferences. In addition, an overriding consideration for tree sloths is slow, deliberate substrate use that ensures stability realized when testing and traversing arboreal supports.

## REFERENCES

- Abbott, B. C., Bigland, B. and Ritchie, J. M. (1952). The physiological cost of negative work. *J. Physiol.*, **117**, 380–390.
- Adam, P. J. (1999). *Choloepus didactylus*. *Mammal. Spec.* **621**, 1–8.
- Aiello, B. R., Olsen, A. M., Mathis, C. E., Westneat, M. W. and Hale, M. E. (2020). Pectoral fin kinematics and motor unit patterns are shaped by fin ray mechanosensation during steady swimming in *Scarus quoyi*. *J. Exp. Biol.* **223**.
- Alexander, R. M. (1984). Stride length and speed for adults, children, and fossil hominids. *Am. J. Phys. Anthropol.* **63**, 23–27.
- Barrat, E. S. (1965). EEG correlates of tonic immobility in the opossum (*Didelphis virginiana*). *Electro. Clin. Neuro.* **18**, 709–711.
- Bates, D., Mächler, M., Bolker, B. and Walker, S. (2014a). Fitting Linear Mixed-Effects Models using lme4. *arXiv:1406.5823 [stat]*.
- Beltman, J. G. M., Van Der Vliet, M. R., Sargeant, A. J. and De Haan, A. (2004). Metabolic cost of lengthening, isometric and shortening contractions in maximally stimulated rat skeletal muscle. *Acta Physiol. Scand.* **182**, 179–187.
- Bertram, J. E. A. and Chang, Y. H. (2001). Mechanical energy oscillations of two brachiation gaits: measurement and simulation. *Am. J. Phys. Anthropol.* **115**, 319–326.
- Bertram, J. E. A., Ruina, A., Cannon, C. E., Chang, Y. H. and Coleman, M. J. (1999). A point-mass model of gibbon locomotion. *J. Exp. Biol.* **202**, 2609–2617.
- Biewener, A. A. (1998). Muscle-tendon stresses and elastic energy storage during locomotion in the horse. *Comp. Biochem. Physiol. Part B*, **120**, 73–87.
- Biewener, A. A., Farley, C. T., Roberts, T. J. and Temaner, M. (2004). Muscle mechanical advantage of human walking and running: implications for energy cost. *J. Appl. Physiol.* **97**, 2266–2274.
- Biewener, A.A., and Roberts, T.J., (2000). Muscle and tendon contributions to force, work, and elastic energy savings: a comparative perspective. *Exerc. Sport. Sci. Rev.* **28**, 99–107.
- Bottinelli, R. (2001). Functional heterogeneity of mammalian single muscle fibres: Do myosin isoforms tell the whole story? *Pflügers Arch.* **443**, 6–17.
- Britton, S. W. (1941). Form and function in the sloth. *Q. Rev. Biol.* **16**, 13–34.

- Britton, S. W. and Atkinson, W. E. (1938). Poikilothermism in the sloth. *J. Mammal.* **19**, 94–99.
- Brooks, S. V., and Faulkner, J. A. (1988). Contractile properties of skeletal muscle from young, adult and aged mice. *J. Physiol.* **404**, 71–82.
- Butcher, M. T., Hermanson, J. W., Ducharme, N. G., Mitchell, L. M., Soderholm, L. V. and Bertram, J. E. A. (2009) Contractile behavior of the forelimb digital flexors during steady-state locomotion in horses (*Equus caballus*): an initial test of muscle architectural hypotheses about in vivo function. *Comp. Biochem. Physiol. Part A Mol. Integr. Physiol.* **152**, 100–114.
- Butcher, M. T., Morgan, D. M., Spainhower, K. B., Chadwell, B. A., Thomas, D. R., Kennedy, S. P., Avey-Arroyo, J. A. and Cliffe, R. N. (2022). Myology of the pelvic limb of the brown-throated three-toed sloth (*Bradypus variegatus*). *J. Anat.* **240**, 1048–1074. <https://doi.org/10.1111/joa.13626>
- Cartmill, M., Lemelin, P. and Schmitt, D. (2002). Support polygons and symmetrical gaits in mammals. *Zool. J. Linn. Soc.* **136**, 401–420.
- Clarke, A. and Rothery, P. (2007). Scaling of body temperature in mammals and birds. *Func. Ecol.* **22**, 58–67.
- Cliffe, B. N., Haupt, R. J., Avey-Arroyo, J. A. and Wilson, R. P. (2015). Sloths like it hot: Ambient temperature modulates food intake in the brown-throated sloth (*Bradypus variegatus*). *PeerJ* **3**, e875.
- Cliffe, B. N., Scantlebury, M. D, Kennedy, S. J, Avey-Arroyo, J. A, Mindich, D. and Wilson R. P. (2018). The metabolic cost of the *Bradypus* sloth to temperature. *PeerJ* **6**, e5600.
- Cohen, A. H., and Gans, C. (1975). Muscle activity in rat locomotion: Movement analysis and electromyography of the flexors and extensors of the elbow. *J. Morphol.* **146**, 177–196.
- Delsuc, F., Kuch, M., Gibb, G. C., Gibb, G. C., Karpinski, E., Hackenberger, D., Szpak, P., Martinez, J. G., Mead, J. I., McDonald, H. G., MacPhee, R. D. E., Billet, G., Lionel, H. and Poinar, H. N.. (2019). Ancient mitogenomes reveal the evolutionary history and biogeography of sloths. *Cur. Biol.* **29**, 2031–2042.
- DeLuca, C. J. (1997). The use of surface electromyography in biomechanics. *J. Appl. Biomech.* **13**, 135–136.



- Demes, B., Larson, S. G., Stern, J.T., Jr., Jungers, W. L., Biknevicius, A. R. and Schmitt, D. (1994). The kinetics of primate quadrupedalism: "hindlimb drive" reconsidered. *J. Human Evol.* **26**, 353–374.
- Dickinson, E., Young, M. W. and Granatosky, M. C. (2022). Testing mechanisms for weight support distribution during inverted quadrupedalism in primates. <https://doi.org/10.1002/jez.2605>
- Diniz J.A.R.A., Falcão B.M.R., Rocha E.F., de Souza J.G., da Nobrega Carreiro A., Medeiros G.X. and de Menezes D.J.A. (2018). Descrição anatômica dos músculos do membro torácico da preguiça-comum (*Bradypus variegatus*) *Acta Sci. Vet.* **46**, 1601.
- Enders, R. K. (1935). Mammalian life histories from Barro Colorado Island, Panama. *Bull. Mus. Comp. Zool.* **78**, 383–502.
- Enger, P. S. and Bullock, T. (1965). Physiological basis of slothfulness in the sloth, *Hvalradets Skrifter* **48**, 143.
- Fujiwara, S. I., Endo, H. and Hutchinson, J. R. (2011). Topsy-turvy locomotion: biomechanical specializations of the elbow in suspended quadrupeds reflect inverted gravitational constraints. *J. Anat.* **219**, 176–191.
- Gans, C. (1982). Fiber architecture and muscle function. *Exerc. Sport Sci. Rev.* **10**, 160–207.
- Gans, C. (1992). Electromyography. In *Biomechanics – structures and systems: A practical approach* (ed. A.A. Biewener), pp. 175-204. New York: Oxford University Press.
- Gardner, A. L. (2005). Order Pilosa. In: *Mammal species of the world: A taxonomic and geographic reference* (eds. D. E. Wilson and D. M. Reeder) pp. 100–103. Baltimore: Johns Hopkins University Press.
- Gardner, A. L. (2008). *Mammals of South America, Vol. 1: Marsupials, Xenarthrans, Shrews, and Bats*. Chicago: University of Chicago Press.
- Garla, R. C., Setz, E. Z. F. and Gobbi, N. (2001). Jaguar (*Panthera onca*) food Habits in Atlantic rain Forest of southeastern Brazil *Biotropica* **33**, 691–696.
- Gaudin, T. J. (2004). Phylogenetic relationships among sloths (Mammalia, Xenarthra, Tardigrada): The craniodental evidence. *Zool. J. Linn. Soc., Lond.* **140**, 255–305.
- Gaudin, T. J. and McDonald, H. G. (2008). Morphology-based investigations of the phylogenetic relationships among extant and fossil xenarthrans. In *The biology of the*

- Xenarthra (eds. S. F. Vizcaíno and W. J. Loughry), pp. 24–36. Gainesville: University Press of Florida.
- Gaudin, T. J. and Croft, D. A. (2015). Palogene xenarthra and the evolution of South American mammals. *J. Mammal.* **96**, 622–634.
- Genoways, H. H. and Timm, R. M. (2003). The Xenarthrans of Nicaragua. *J. Neotrop. Mamm.* **10**, 231–253.
- Gillespie, D. S. (2003). Xenarthra: Edentata. In *Zoo and wild animal medicine* (eds. M. E. Fowler and E. Miller), pp. 397–407. Philadelphia: W.B. Saunders Company.
- Gillis, G. B. and Biewener, A. A. (2001). Hindlimb muscle function in relation to speed and gait: in vivo patterns of strain and activation in a hip and knee extensor of the rat (*Rattus norvegicus*). *J. Exp. Biol.* **204**, 2717–2731.
- Gillis, G. B. and Biewener, A. A. (2002). Effects of surface grade on proximal hindlimb muscle strain and activation during rat locomotion. *J. Appl. Physiol.* **93**, 1731–1743.
- Goffart, M. (1971). *Function and form in the sloth*. Oxford: Pergamon Press.
- Goffart, M. and Gerebtzoff, M. A., (1964) *J. Physiol. (Paris)*, **56**, 563
- Goffart, M., Gerebtzoff, M. A. and Duchesne, P. Y. (1967). The spinal roots in the sloth (*Choloepus hoffmanni peters*). *J. Comp. Neuro.* **131(3)**, 393–403.  
<https://doi.org/10.1002/cne.901310309>
- Goffart, M., Holmes, O. and Bacq, Z. M. (1962). Some mechanical properties of skeletal muscle in the sloth. *Arch. Physiol. and Biochem.* **70(1)**, 103–106.  
<https://doi.org/10.3109/13813456209092846>
- Gordon, G. and Holbourn, A. H. S. (1949). The mechanical activity of single motor units in reflex contractions of skeletal muscle. *J. Physiol.* **110**, 26–35.  
<https://doi.org/10.1113/jphysiol.1949.sp004418>
- Gorvet, M. A., Wakeling, J. M., Morgan, D. M., Hidalgo Segura, D., Avey-Arroyo, J. A. and Butcher, M. T. (2020). Keep calm and hang on: EMG activation in the forelimb musculature of three-toed sloths. *J. Exp. Biol.* **223**, jeb218370.
- Grand, T. I. (1978). Adaptations of tissue and limb segments to facilitate moving and feeding in arboreal folivores. In *The ecology of arboreal folivores* (ed. G. G. Montgomery), pp. 231–241. Washington, DC: Smithsonian Institution Press.

- Granatosky, M. C. (2018a). Forelimb and hindlimb loading patterns during quadrupedal locomotion in the large flying fox (*Pteropus vampyrus*) and common vampire bat (*Desmodus rotundus*). *J. Zool.* **305**, 63–72.
- Granatosky, M. C. (2018b). Quadrupedal. In *Encyclopedia of Animal Cognition and Behavior* (ed. Vonk, J.) and Shackelford, T.), pp. 1–6. Cham: Springer International Publishing.
- Granatosky, M. C. (2018c). A review of locomotor diversity in mammals with analyses exploring the influence of substrate use, body mass and intermembral index in primates. *J. Zool.* **306**, 207–216.
- Granatosky, M. C. (2020). Testing the propulsive role of m. peroneus longus during quadrupedal walking in *Varanus exanthematicus*. *J. Exp. Zool. A: Ecol. Integr. Physiol.*
- Granatosky, M. C., Fitzsimons, A., Zeininger, A. and Schmitt, D. (2018a). Mechanisms for the functional differentiation of the propulsive and braking roles of the forelimbs and hindlimbs during quadrupedal walking in primates and felines. *J. Exp. Biol.* **221**, 1–11.
- Granatosky, M. C., Karatanis, N. E., Rychlik, L. and Youlatos, D. (2018b). A suspensory way of life: integrating locomotion, posture, limb movements, and forces in two-toed sloths *Choloepus didactylus* (Megalonychidae, Folivora. Pilosa). *J. Exp. Zool.* **329**, 570-588. doi:10.1002/jez.2221
- Granatosky, M. C., McElroy, E. J., Lemelin, P., Reilly, S. M., Nyakatura, J. A., Andrada, E., Kilbourne, B. M., Allen, V. R., Butcher, M. T., Blob, R. W. and Ross C. F.. (2020). Variation in limb loading magnitude and timing in tetrapods. *J. Exp. Biol.* **223**, jeb201525.
- Granatosky, M. C. and Schmitt, D. (2017). Forelimb and hind limb loading patterns during below branch quadrupedal locomotion in the two-toed sloth. *J. Zool.* **302**, 271–278.
- Granatosky, M. C. and Schmitt, D. (2019). The mechanical origins of arm-swinging. *J. Human Evol.* **130**, 61–71.
- Granatosky, M.C., Schmitt, D. and Hanna, H (2019). Comparison of spatiotemporal gait characteristics between vertical climbing and horizontal walking in primates. *J. Exp. Biol.* **222**, jeb185702.
- Granatosky M. C., Tripp, C. H. and Schmitt, D. (2016). Gait kinetics of above- and below-branch quadrupedal locomotion in lemurid primates. *J. Exp. Biol.* **219**, 53–63.

- Gray, J. (1944). Studies in the Mechanics of the Tetrapod Skeleton. *Journal of Experimental Biology* **20**, 88–116.
- Hanna, J. B., Schmitt, D. and Griffin, T. M. (2008). The energetic cost of climbing in primates. *Science* **320**, 898.
- Hanna, J. B., Granatosky, M. C., Rana, P. and Schmitt, D. (2017). The evolution of vertical climbing in primates: evidence from reaction forces. *J. Exp. Biol.* **220**, 3039–3052.
- Hayssen, V. (2009). *Bradypus tridactylus* (Pilosa: Bradypodidae). *Mammal. Spec.* **839**, 1–9. doi:10.1644/839.1
- Hayssen, V. (2010). *Bradypus variegatus* (Pilosa: Bradypodidae). *Mammal. Spec.* **42**, 19–32. doi:10.1644/850.1
- Hayssen, V. (2011). *Choloepus hoffmanni* (Pilosa: Megalonychidae). *Mammal. Spec.* **43**, 37–55. doi:10.1644/873.1
- Henneman, E. (1957). Relation between size of neurons and their susceptibility to discharge. *Science*. **126**, 1345–1347.
- Henneman, E., and Olson, C. B. (1965). Relations between structure and function in the design of skeletal muscles. *J. Neurophysiol.* **28**, 581–598.
- Hermanson, J.W. and Cobb, M.A. (1992). Four forearm flexor muscles of the horse, *Equus caballus*: *Anat. Histochem. J. Morphol.* **212**, 269–280.
- Hildebrand, M. (1960). How animals run. *Sci. Am.* **202**, 148–157.
- Hildebrand, M. (1985). Walking and running. (Hildebrand, M., Bramble, D. M., Liem, K. F., Wake, D. B. eds.), *Functional Vertebrate Morphology*, pp. 38–58. Harvard University Press, Cambridge.
- Hill, A. V. (1938). The heat of shortening and the dynamic constants of muscle. *Proc. R. Soc. B.* **126**, 136–195.
- Hill, R. W., Wyse, G. A. and Anderson, M. (2004). *Muscle. Anim. Physiol.* 523-547. Sunderland: Sinauer Associates.
- Hodson-Tole, E. F. and Wakeling, J. M. (2007). Variations in motor unit recruitment patterns occur within and between muscles in the running rat (*Rattus norvegicus*). *J. Exp. Biol.* **210**, 2333–2345.
- Hodson-Tole, E. F., Wakeling, J. M. and Dick, T. J. M. (2016). Passive muscle-tendon unit gearing is joint dependent in human medial gastrocnemius. *Front. Physiol.* **7**, 1–8.

- Humphrey, G. M. (1870). The myology of the limbs of the Unau, the Ai, the two-toed anteater, and the Pangolin. *J. Anat. Physiol.* **3**, 2–78.
- Hunt, K. D. (2016). Why are there apes? Evidence for the co-evolution of ape and monkey ecomorphology. *J. Anat.* **228**, 630–685.
- Ishida, H., Jouffroy, F. K. and Nakano, Y. (1990). Comparative dynamics of pronograde and upside down horizontal quadrupedalism in the slow loris (*Nycticebus coucang*). In Gravity, Posture and Locomotion in Primates (ed. F. K. Jouffroy, M. H. Stack and C. Niemitz), pp. 209-220. Florence: Il Sedicesimo.
- Jenkins, F. A. and Weijstouch, W. A. (1979). The functional anatomy of the shoulder in the Virginia opossum (*Didelphis virginiana*). *J. Zool. Lond.* **188**, 379–410.
- Jouffroy, F. K. and Medina, M. F. (2004). Comparative fiber-type composition and size in the antigravity muscles of primate limbs. In Shaping Primate Evolution Form, Function, and Behavior (eds. F. Anapol, R. Z. German, and N. G. Jablonski), pp. 134–161. Cambridge: Cambridge University Press.
- Jouffroy, F. K. and Petter, A. (1990). Gravity-related kinematic changes in lorine horizontal locomotion in relation to position of the body. In Gravity, Posture and Locomotion in Primates (ed. F. K. Jouffroy, M. H. Stack and C. Niemitz), pp. 199–208. Florence: Il Sedicesimo.
- Jouffroy, F. K. and Stern, J. T., Jr. (1990). Telemetered EMG study of the antigravity versus propulsive actions of knee and elbow muscles in the slow loris (*Nycticebus coucang*). In Gravity, Posture and Locomotion in Primates (ed. F. K. Jouffroy, M. H. Stack and C. Niemitz), pp. 221–236. Florence: Il Sedicesimo.
- Jouffroy, F. K., Stern, J. T., Médina, M. F. and Larson, S. G. (1999). Functional and cytochemical characteristics of postural limb muscles of the rhesus monkey: a telemetered EMG and immunofluorescence study. *Folia Primatologica* **70**, 235–253.
- Jungers, W. L. (1978). The functional significance of skeletal allometry in *Megaladapis* in comparison to living prosimians. *Am. J. Phys. Anthropol.* **49**, 303–314.
- Jungers, W. L. and Stern, J. T. (1980). Telemetered electromyography of forelimb muscle chains in gibbons (*Hylobates lar*). *Science* **208**, 617–619.
- Jungers, W. L. and Stern, J. T. (1981). Preliminary electromyographical analysis of brachiation in gibbon and spider monkey. *Int. J. Primatol.* **2**, 19–33.

- Kohn, T.A. (2014). Insights into the skeletal muscle characteristics of three southern African antelope species. *Biol. Open* **3**, 1037–1044.
- Kohn, T. A., Curry, J. W. and Noakes, T. D. (2011). Black wildebeest skeletal muscle exhibits high oxidative capacity and a high proportion of type IIx fibres. *J. Exp. Biol.* **214**, 4041–4047.
- Kohn, T. A., Hoffman L. C. and Myburgh, K. H. (2007). Identification of myosin heavy chain isoforms in skeletal muscle of four African ruminants. *Comp. Biochem. Phys. A.* **148**, 399–407.
- Kuznetsova, A., Brockhoff, P. B. and Christensen, R. H. B. (2017). lmerTest Package: Tests in Linear Mixed Effects Models. *J. Stat. Software* **82**, 1–26.
- Larson, S. G. and Demes, B. (2011). Weight support distribution during quadrupedal walking in *Ateles* and *Cebus*. *Am. J. Phys. Anthropol.* **144**, 633–642.
- Larson, S. G. (2018). Nonhuman Primate Locomotion. **165**, 705–725. <https://doi.org/10.1002/ajpa.23368>
- Lee, S. H., Lee, C. K., Park, J. B. and Choi, Y. H. (2013). Diagnostic method for insulated power cables based on wavelet energy. *IEICE Electronics Express*. **10**, 335.
- Lieber, R. L. (2002). Skeletal muscle structure, function, and plasticity (ed. T. Julet). Baltimore: Lippincott Williams & Wilkins.
- Lieber, R. L. (2009). Skeletal muscle, structure, function, and plasticity, 3rd ed. Baltimore: Lippincott Williams & Wilkins: 369.
- Macalister, A. (1869). On the myology of *Bradypus tridactylus*; with remarks on the general muscular anatomy of the Edentata. *Trans. R. Irish Acad.* **25**, 51–67.
- Mackintosh, H. W. (1875). On the muscular anatomy of *Choloepus didactylus*. *Proc R Irish Acad. Sci.* **2**, 66–79.
- Mackintosh, H. W. (1875). On the Myology of the Genus *Bradypus*. *Proc. R. Irish Acad. Sci.* **1**, 517–529.
- Malcolm, J. L., Saraiva, P. and Spear, P. J. (1967). Cholinergic and adrenergic inhibition in the rat cerebral cortex. *Neuropharm.* **6**, 509–527. [https://doi.org/10.1016/0028-3908\(67\)90051-2](https://doi.org/10.1016/0028-3908(67)90051-2)

- Marechal, G., Goffart, M., Reznik, M. and Gerebtzoff, M. A. (1976). The striated muscles in a slow-mover, *Perodicticus potto* (prosimii, lorisidae, lorisinae). *Comp. Biochem. Physiol. Part A: Physiol.* **54**, 81–93. [https://doi.org/10.1016/S0300-9629\(76\)80075-8](https://doi.org/10.1016/S0300-9629(76)80075-8)
- Marshall, S. K., Spainhower, K. B., Sinn, B. T., Diggins, T. P. and Butcher, M. T. (2021). Hind limb bone proportions reveal unexpected morpho- functional diversification in xenarthrans. *J. Mammal. Evol.* **28**, 599–619.
- Mathis, A., Mamidanna, P., Cury, K. M., Abe, T., Murthy, V. N., Mathis, M. W. and Bethge, M. (2018). DeepLabCut: markerless pose estimation of user-defined body parts with deep learning. *Nat. Neurosci.* **21**, 1281–1289.
- McDonald, H. G. and De Iuliis, G. (2008). Fossil history of sloths. In *The Biology of the Xenarthra* (ed. S. F. Vizcaíno and W. J. Loughry), pp.39-55. Gainesville: University Press of Florida.
- McPhedran, A. M., Wuerker, R. B. and Henneman, E. (1965a). Properties of motor units in a heterogeneous pale muscle (M. Gastrocnemius) of the cat. *J. Neurophysiol.* **28**, 85–99.
- McPhedran, A. M., Wuerker, R. B. and Henneman, E. (1965b). Properties of motor units in a homogeneous red muscle (Soleus) of the cat. *J. Neurophysiol.* **28**, 71–84.
- McKamy, A. J., Young, M. W., Mossor, A. M., Young, J. W., Avey-Arroyo, J. A., Granatosky, M. C. and Butcher, M. T. (2022). Pump the Brakes! The hindlimbs of three-toed sloths control suspensory locomotion. In review, *J. Exp. Biol.*
- Mendel, F. C. (1981a). Use of hands and feet of two-toed sloths (*Choloepus hoffmanni*) during climbing and terrestrial locomotion. *J. Mammal.* **62**, 413–421.
- Mendel, F. C. (1981b). The hand of two-toed sloths (*Choloepus*): its anatomy and potential uses relative to size of support. *J. Morphol.* **169**, 1–19.
- Mendel, F. C. (1985a). Use of hands and feet of three-toed sloths (*Bradypus variegatus*) during climbing and terrestrial locomotion. *J. Mammal.* **66**, 359–366.
- Mendel, F. C. (1985b). Adaptations for suspensory behavior in the limbs of two-toed sloths. In: Montgomery, G.G. (Ed.) *The evolution and ecology of armadillos, sloths, and vermilinguas*. Washington DC: Smithsonian Institution Press, pp. 151–162.
- Meritt, D. A. Jr. (1985). The two-toed hoffmann's sloth, *Choloepus hoffmanni* Peters. In *The Evolution and Ecology of Armadillos, Sloths, and Vermilinguas*, pp. 333–341.

- Washington, DC: Smithsonian Institution Press.
- Miller R.A. (1935). Functional adaptations in the forelimb of the sloths. *J Mammal.* **16**, 38–51.
- Montgomery, G. G., Cochran W. W. and Sunquist M.E. (1973). Radiolocating arboreal vertebrates in tropical forest. *J. Wildl. Manag.* 37:426–428
- Montgomery, G. G. (1983). *Bradypus variegatus* (perezoso de tres dedos, three-toed sloth). In Costa Rican natural history (ed. D. H. Janzen), pp. 453–456. Chicago: University of Chicago Press.
- Montgomery, G. G. and Sunquist, M. E. (1975). Impact of sloths on neotropical forest energy flow and nutrient cycling. In *Tropical Ecological Systems: Trends in Terrestrial and Aquatic Research*, pp. 69–98. New York, NY: Springer-Verlag Inc.
- Montgomery, G. G. and Sunquist, M. E. (1978). Habitat selection and use by two-toed and three-toed sloths. In *The Ecology of Arboreal Folivores*, pp. 329–359. Washington, DC: Smithsonian Press.
- Morgan, D. M., Spainhower, K. B., Mossor, A. M., Avey-Arroyo, J. A. and Butcher, M. T. (2022). Architectural properties of the hindlimb musculature of sloths (*Bradypus*, Pilosa, Xenarthra). In review, *J. Anat.*
- Mossor, A. M., Austin, B. L., Avey-Arroyo, J. A. and Butcher, M.T. (2020) Horses hanging upside down?: Tensile strength and elasticity of sloth flexor tendons. *Integr. Org. Biol.* **2**, 1–11. <https://doi.org/10.1093/iob/obaa032>
- Mossor, A. M., Young, J. W. and Butcher, M. T. (2022). Does a suspensory lifestyle result in increased tensile strength?: Organ level material properties of sloth limb bones. *J Exp. Biol.* **225**, jeb242866. <https://doi.org/10.1242/jeb.242866>
- Muchlinski, M. N., Snodgrass, J. J. and Terranova, C. J. (2012). Muscle mass scaling in primates: An energetic and ecological perspective. *Am. J. Primatol.* **74**, 395–407.
- Muscolino, J. E. (2011). *Kinesiology: The skeletal system and muscle function*, 15th ed. Chicago, Illinois: Mosby/Elsevier: 704.
- Muybridge, E. (1887). *The Horse in motion*. "Sallie Gardner," owned by Leland Stanford; running at a 1:40 gait over the Palo Alto track. California Palo Alto, ca.
- Nyakatura, J. A. (2012). The convergent evolution of suspensory posture and locomotion in tree sloths. *J. Mamm. Evol.* **19**, 225–234. doi:10.1007/s10914-011- 9174-x



- Nyakatura, J. A. and Andrada, E. (2013). A mechanical link model of two-toed sloths: No pendular mechanics during suspensory locomotion. *Acta Theriol.* **58**, 83–93.
- Nyakatura, J. A. and Fischer, M. S. (2010). Three-dimensional kinematic analysis of the pectoral girdle during upside-down locomotion of two-toed sloths (*Choloepus didactylus*, Linné 1758). *Front. Zool.* **7**, 21.
- Nyakatura, J. A. and Fischer, M. S. (2011). Functional morphology of the muscular sling at the pectoral girdle in tree sloths: convergent morphological solutions to new functional demands? *J. Anat.* **219**, 360–374.
- Nyakatura, J. A., Petrovitch, A. and Fischer, M. S. (2010). Limb kinematics during locomotion in the two-toed sloth (*Choloepus didactylus*, Xenarthra) and its implications for the evolution of the sloth locomotor apparatus. *Zoology* **113**, 221–234. doi:10.1016/j.zool.2009.11.003
- Olson, R. A., Glenn, Z. G., Cliffe, R. N. and Butcher, M. T. (2018). Architectural properties of sloth forelimb muscles (Pilosa: Bradypodidae). *J. Mamm. Evol.* **25**, 573–588. doi:10.1007/s10914-017-9411-z
- Pant, S. R., Goswami, A. and Finarelli, J. A. (2014). Complex body size trends in the evolution of sloths (Xenarthra: Pilosa). *BMC Evol. Biol.* **14**, 184.
- Patel, B. A., Wallace, I. J., Boyer, D. M., Granatosky, M. C., Larson, S. G. and Stern Jr., J. T. (2015). Distinct functional roles of primate grasping hands and feet during arboreal quadrupedal locomotion. *J. Hum. Evol.* **88**, 79–84.
- Pauli, J. N., Peery, M. Z., Fountain, E. D. and Karasov, W. H. (2016). Arboreal folivores limit their energetic output, all the way to slothfulness. *Am. Nat.* **188**, 196–204.
- Presslee, S., Slater, G., Pujos, F., Forasiepi, A., Fischer, R., Molloy, K. Mackie, M., Olsen, J., Kramarz, A., Taglioretti, M., Scaglia, F., Lezcano, M., Lanata, J., Southon, J., Feranec, R., Bloch, J., Hajduk, A., Martin, F., Salas-Gismondi, R. and Macphee, R. (2019). Palaeoproteomics resolves sloth relationships. *Nat. Ecol. Evol.* **3**, 1–10.
- Preuschoft, H. and Demes, B. (1984). Biomechanics in brachiation. In *The lesser apes: Evolutionary and behavioral biology* (eds. H. Preuschoft, D.J. Chivers, W.Y. Brockelman, N Creel), pp. 96–118. Edinburgh: Edinburgh University Press.

- Pujos, F., Gaudin, T. J., De Iuliis, G. and Cartelle, C. (2012). Recent advances on variability, morpho-functional adaptations, dental terminology, and evolution of sloths. *J. Mamm. Evol.* **19**, 159–169.
- R Core Team (2021). *R: A language and environment for statistical computing*. Vienna, Austria: R Foundation for Statistical Computing.
- Reynolds, T. R. (1985). Mechanics of increased support of weight by the hindlimbs in primates. *Am. J. Phys. Anthropol.* **67**, 335–349.
- Roberts, T. J. and Gaboldon, A. M. (2008). Interpreting muscle function from EMG: lessons learned from direct measurements of muscle force. *Integr. Comp. Biol.* **48**, 312–320.
- Roberts, T. J., Marsh, R. L., Weyand, P. G. and Taylor, C. R. (1997). Muscular force in running turkeys: the economy of minimizing work. *Science* **275**, 1113–1115.
- Rome, L. C., Sosnicki, A. A. and Goble, D. O. (1990). Maximum velocity of shortening of three fibre types from horse soleus muscle: implications for scaling with body size. *J. Physiol.* **431**, 173–185.
- Schiaffino, S. and Reggiani, C. (1996). Molecular diversity of myofibrillar proteins: gene regulation and functional significance. *Physiol. Rev.* **76**, 371–423.
- Schmitt, M. (2008). Forelimb proportions and kinematics: How are small primates different from other small mammals? *J. Exp. Biol.* **211**, 3775–3789.
- Schmitt, D. and Lemelin, P. (2002). Origins of primate locomotion: gait mechanics of the woolly opossum. *Am. J. Phys. Anthro.* **118**, 231–238.
- Schmitt, D. and Lemelin, P. (2004). Locomotor mechanics of the slender loris (*Loris tardigradus*). *J. Hum. Evol.* **47**, 85–94.
- Sickles, D.W. and Pinkstaff, C.A. (1981a). Comparative histochemical study of prosimian primate hindlimb muscles. I. Muscle fiber types. *Am. J. Anat.* **160**, 175–186.
- Sickles, D.W. and Pinkstaff, C.A. (1981b). Comparative histochemical study of prosimian primate hindlimb muscles. II. Populations of fiber types. *Am. J. Anat.* **160**, 187–194.
- Slater G. J., Pin, C., Forasiepi, A. M., Lenz, D., Tsangaras, K., Voirin, B., de Moraes-Barros N., MacPhee, R. D. E. and Greenwood, A. D. (2016). Evolutionary Relationships among Extinct and Extant Sloths: The Evidence of Mitogenomes and Retroviruses. *Genome Biol. Evol.* **14**, 607–621.

- Sokal, R. R. and Rohlf, F. J. (2012). *Biometry : the principles and practice of statistics in biological research*. 6th ed. New York: Freeman & Company.
- Spainhower, K. B., Cliffe, R. N., Metz, A. K., Barkett, E. M., Kiraly, P. M., Thomas, D. R., Kennedy, S. J., Avey-Arroyo, J. A. and Butcher, M. T. (2018). Cheap Labor: Myosin fiber type expression and enzyme activity in the forelimb musculature of sloths (Pilosa: Xenarthra). *J. Appl. Physiol.* **125**, 799–811.
- Spainhower, K. B., Metz, A. K., Yusuf, A.-R.-S., Johnson, L. E., Avery-Arroyo, J. A. and Butcher, M. T. (2021). Coming to grips with life upside down: how myosin fiber type and metabolic characteristics of sloth hindlimbs contribute to suspensory function. *J. Comp. Physiol. B.* **191**, 207–224.
- Stevens, N. J. (2008). The effect of branch diameter on primate gait sequence pattern. *Am. J. Primatol.* **70**, 356–362.
- Sugi, Haruo, and Tetsuo Ohno. Physiological Significance of the Force-Velocity Relation in Skeletal Muscle and Muscle Fibers. (2019). *Int. J. Mol. Sci.* **20**, 3075.
- Sunquist, M. E. and Montgomery, G. G. (1973). Activity patterns and rates of movement of two-toed and three-toed sloths (*Choloepus hoffmanni* and *Bradypus infuscatus*). *Am. Soc. Mammal.* **54**, 946–954.
- Thomas, D. R., Chadwell, B. A., Walker, G. R., Budde, J. E., VandeBerg, J. L. and Butcher, M.T. (2017). Ontogeny of myosin isoform expression and prehensile function in the tail of the gray short-tailed opossum (*Monodelphis domestica*). *J. Appl. Physiol.* **123**, 513–525.
- Touchton, J. M., Hsu, Y. C. and Palleroni, A. (2002). Foraging ecology of reintroduced captive-bred sub-adult harpy eagles (*Harpia harpyja*) on Barro Colorado Island, Panama. *Ornithol. Neotrop.* **13**, 365–379.
- Urbani, B. and Bosque, C. (2007). Feeding ecology and postural behaviour of the three-toed sloth (*Bradypus variegatus*) in northern Venezuela. *Mamm. Biol.* **72**, 321–329.
- Usherwood, J. R. and Self Davies, Z. T. (2017). Work minimization accounts for footfall phasing in slow quadrupedal gaits. *eLife Sciences* **6**, e29495.
- Vaughn, C., Ramírez, O., Herrera, G. and Guries, R. (2007). Spatial ecology and conservation of two sloth species in a cacao landscape in Limón, Costa Rica. *Biodivers. Conserv.* **16**, 2293–2310.

- Vizcaíno, S. F., Bargo, M. S. and Fariña, R. A. (2008). Form, function, and paleobiology in xenarthrans. In: *The biology of the xenarthra* (eds. S. F. Vizcaíno and W. J. Loughry), pp. 86–99. Gainesville: University Press of Florida.
- Vizcaíno, S. F. (2009). The teeth of the "toothless": Novelties and key innovations in the evolution of xenarthrans (Mammalia, Xenarthra). *Paleobiol.* **35**, 343–366.
- Voirin, B., Scriba, M. F., Martinez-Gonzalez, D., Vyssotski, A. L., Wikelski, M. and Rattenborg, N. C. (2014). Ecology and Neurophysiology of Sleep in Two Wild Sloth Species. *Sleep.* **37**, 753–761.
- von Tscherner, V. (2000). Intensity analysis in time-frequency space of surface myoelectric signals by wavelets of specified resolution. *J. Electromyogr. Kinesiol.* **10**, 433–445.
- Wakeling, J. M. (2009). Patterns of motor recruitment can be determined using surface EMG. *J. Electromyogr. Kinesiol.* **19**, 199–207.
- Wakeling, J. M., Lee, S. S. M., Arnold, A. S., Miara, M. D. B. and Biewener, A. A. (2012). A muscle's force depends on the recruitment patterns of its fibers. *Ann. Biomed. Eng.* **40**, 1708–1720.
- Wakeling, J. M., Pascual, S. A., Nigg, B. M. and Tscherner, V. (2001). Surface EMG shows distinct populations of muscle activity when measured during sustained sub-maximal exercise. *Eur. J. Appl. Physiol.* **86**, 40–47.
- Wakeling, J. M. and Rozitis, A. I. (2004). Spectral properties of myoelectric signals from different motor units in the leg extensor muscles. *J. Exp. Biol.* **207**, 2519–2528.
- Winter, B. (2013). Linear models and linear mixed effects models in R with linguistic applications. *arXiv:1308.5499 [cs]*.
- Windle, B. C. A. and Parsons, F. G. (1899). On the myology of the Edentata. *Proc. Zool. Soc., Lond.* 990–1017.
- Wislocki, G. B. (1928). Observation on the gross and microscopic anatomy of the sloths (*Bradypus griseus* Gray and *Choloepus hoffmani* Peters). *J. Morphol. Physiol.* **46**, 317–397.
- Youlatos, D. (2002). Positional Behavior of Black Spider Monkeys (*Ateles paniscus*) in French Guiana. *Int. J. Primatol.* **23**, 1071–1093.

Young, M. W., Dickinson, E., Flaim, N. D. and Granatosky, M. C. (2022). Overcoming a “forbidden phenotype”: the parrot’s head supports, propels and powers tripedal locomotion. *Proc Biol Sci* **289**, 20220245.

Young, M. W., Granatosky, M. C., Avey-Arroyo, J. A., Butcher, M. T. and Dickinson, E. (2022). Grip it good: *in vivo* grip strength across substrate diameters in the brown-throated three-toed sloth (*Bradypus variegatus*). In review, *J. Zool.*

**Table 1.** Means ( $\pm$ s.d.) of peak forces (normalized in %BW) for *Bradypus variegatus*.

Velocity (ms <sup>-1</sup> )	Limb	N	Contact Time (s)	V <sub>pk</sub> (%BW)	P <sub>pk</sub> (%BW)	B <sub>pk</sub> (%BW)	M <sub>pk</sub> (%BW)	L <sub>pk</sub> (%BW)
0.09 $\pm$ 0.04	FL	69	5.16 $\pm$ 2.72 (5.09-5.24)	62.9 $\pm$ 11.2 (62.6-63.2)	16.6 $\pm$ 6.7 (16.4-16.8)	-4.7 $\pm$ 5.3 (-4.8- -4.5)	-7.5 $\pm$ 6.6 (-7.8- -7.2)	8.5 $\pm$ 6.3 (8.2-8.8)
	HL	98	5.12 $\pm$ 3.98 (5.06-5.18)	73.8 $\pm$ 13.7 (73.6-74.1)	5.8 $\pm$ 5.3 (5.7-5.9)	-18.0 $\pm$ 7.0 (-18.1- -17.9)	-14.0 $\pm$ 7.6 (-14.3- -13.8)	7.2 $\pm$ 7.4 (6.9-7.4)

N, number of single limb forces analyzed; FL, forelimb; HL, hindlimb; BW, bodyweight; V<sub>pk</sub>, vertical peak force; P<sub>pk</sub>,

propulsive peak force; B<sub>pk</sub>, braking peak force; M<sub>pk</sub>, medial peak force; L<sub>pk</sub>, lateral peak force.

In parentheses are 95% confidence intervals.

Vertical force applied by the animals is shown as positive (absolute) values by convention, as well as (+) propulsive force and (-) braking force.

**Table 2.** Means ( $\pm$ s.d.) of impulses (normalized in %BWS) for *Bradypus variegatus*.

Velocity (ms <sup>-1</sup> )	Limb	<i>N</i>	Contact Time (s)	<i>J<sub>V</sub></i> (%BWS)	<i>J<sub>P</sub></i> (%BWS)	<i>J<sub>B</sub></i> (%BWS)	Net <i>J</i> (%BWS)	<i>J<sub>M</sub></i> (%BWS)	<i>J<sub>L</sub></i> (%BWS)
0.09 $\pm$ 0.04	FL	69	4.48 $\pm$ 2.46 (4.28-4.67)	148.6 $\pm$ 88.8 (146.1-151.2)	32.1 $\pm$ 26.7 (31.3-32.9)	-4.23 $\pm$ 13.3 (-4.61- -3.85)	27.9 $\pm$ 33.2 (26.9- -28.8)	-10.7 $\pm$ 12.1 (-11.3- -10.2)	15.5 $\pm$ 18.5 (14.6-16.3)
	HL	98	4.43 $\pm$ 2.97 (4.20-4.66)	181.2 $\pm$ 108.9 (179.1-183.4)	2.07 $\pm$ 10.7 (1.85-2.28)	-36.4 $\pm$ 30.9 (-37.0- -35.8)	-34.3 $\pm$ 34.1 (-35.0- -33.7)	-27.5 $\pm$ 31.6 (-28.4- -26.5)	11.9 $\pm$ 21.3 (11.3-12.6)

*N*, number of trials for which consecutive fore- and hindlimb forces were collected; FL, forelimb; HL, hindlimb; BWS, bodyweight seconds;

*J<sub>V</sub>*, vertical impulse; *J<sub>P</sub>*, propulsive impulse; *J<sub>B</sub>*, braking impulse; Net*J*, net impulse; *J<sub>M</sub>*, medial impulse; *J<sub>L</sub>*, lateral impulse.

In parentheses are 95% confidence intervals.

Vertical force applied by the animals is shown as positive (absolute) values by convention, as well as (+) propulsive force and (-) braking force.

**Table 3.** Intraspecific parameters of statistical importance for fixed effects related to peak limb loading in *Bradypus variegatus*.

Species	Response Variable	Fixed Effect	Estimate	Standard Error	df	t-value	p-value
<i>Bradypus variegatus</i>	Peak Vertical Force	Velocity	133.93	92.53	157.76	1.45	0.150
		Limb (hindlimb)	42.54	11.91	9.75	3.57	<b>0.005</b>
	Peak Propulsive Force	Velocity	37.74	77.24	135.05	0.49	0.626
		Limb (hindlimb)	-72.50	10.60	5.09	-6.84	<b>0.001</b>
	Peak Braking Force	Velocity	-154.65	74.01	150.27	-2.09	<b>0.038</b>
		Limb (hindlimb)	-71.38	6.55	4.52	-10.90	<b>&lt;0.001</b>
	Peak Medial Force	Velocity	-464.28	105.93	156.25	-4.38	<b>&lt;0.001</b>
		Limb (hindlimb)	-17.45	6.96	159.99	-2.51	<b>0.013</b>
	Peak Lateral Force	Velocity	-452.31	107.85	162.10	-4.19	<b>&lt;0.001</b>
		Limb (hindlimb)	-1.13	7.05	160.60	-0.16	0.873
<i>Choloepus didactylus</i>	Peak Vertical Force	Velocity	-84.00	63.95	41.20	-1.31	0.196
		Limb (hindlimb)	-1.03	3.79	41.81	-0.27	0.788
	Peak Propulsive Force	Velocity	-116.03	50.87	43.00	-2.28	<b>0.028</b>
		Limb (hindlimb)	-13.27	3.01	43.00	-4.41	<b>&lt;0.001</b>
	Peak Braking Force	Velocity	-43.38	54.31	43.00	-0.80	0.429
		Limb (hindlimb)	-13.52	3.13	43.00	-4.21	<b>&lt;0.001</b>
	Peak Medial Force	Velocity	126.85	62.12	43.00	2.04	<b>0.047</b>
		Limb (hindlimb)	2.37	3.68	43.00	0.64	0.523
	Peak Lateral Force	Velocity	-30.40	64.66	43.00	-0.47	0.641
		Limb (hindlimb)	4.51	3.83	43.00	1.18	0.245

Significant interaction *p*-values are in bold.

Forelimb not listed because it was used as the reference variable.



**Table 4.** Interspecific parameters of statistical importance for fixed effects related to peak limb-loading in *Bradypus variegatus*.

Limb	Response Variable	Fixed Effect	Estimate	Standard Error	df	t-value	p-value
Fore	Peak Vertical Force	Velocity	31.38	79.36	88.22	0.40	0.693
		Species ( <i>C. didactylus</i> )	-10.22	8.99	5.41	-1.14	0.304
	Peak Propulsive Force	Velocity	-3.66	72.47	84.08	-0.05	0.960
		Species ( <i>C. didactylus</i> )	-25.03	7.58	5.42	-3.30	<b>0.019</b>
	Peak Braking Force	Velocity	-178.84	72.49	93.89	-2.47	<b>0.015</b>
		Species ( <i>C. didactylus</i> )	8.14	12.87	6.79	0.63	0.548
	Peak Medial Force	Velocity	-213.67	66.99	94.00	-319.00	<b>0.002</b>
		Species ( <i>C. didactylus</i> )	-24.43	5.48	94.00	-4.46	<b>&lt;0.001</b>
	Peak Lateral Force	Velocity	-181.33	58.02	94.00	-3.13	<b>0.002</b>
		Species ( <i>C. didactylus</i> )	-36.98	4.75	94.00	-7.79	<b>&lt;0.001</b>
Hind	Peak Vertical Force	Velocity	18.92	85.46	111.78	0.22	0.825
		Species ( <i>C. didactylus</i> )	-29.01	11.40	11.64	-2.54	<b>0.026</b>
	Peak Propulsive Force	Velocity	13.98	89.39	115.87	0.16	0.876
		Species ( <i>C. didactylus</i> )	4.06	14.97	7.48	0.27	0.794
	Peak Braking Force	Velocity	-103.63	76.91	116.00	-1.35	0.180
		Species ( <i>C. didactylus</i> )	44.83	7.62	116.00	5.88	<b>&lt;0.001</b>
	Peak Medial Force	Velocity	-132.53	86.73	116.00	-1.53	0.129
		Species ( <i>C. didactylus</i> )	-2.41	8.59	116.00	-0.28	0.780
	Peak Lateral Force	Velocity	-150.05	82.02	65.15	-1.83	0.072
		Species ( <i>C. didactylus</i> )	-37.25	9.38	3.47	-3.97	<b>0.022</b>

Significant interaction *p*-values are in bold.

*B. variegatus* is not listed because it was used as the reference variable.

**Suppl. Table 1.** Means ( $\pm$ s.d.) of peak forces (normalized in %BW) for  $N=5$  individuals of *Bradypus variegatus*.

	Body Mass (kg)	Sex	Velocity ( $\text{ms}^{-1}$ )	Limb	$N$	Contact Time (s)	$V_{\text{pk}}$ (%BW)	$P_{\text{pk}}$ (%BW)	$B_{\text{pk}}$ (%BW)	$M_{\text{pk}}$ (%BW)	$L_{\text{pk}}$ (%BW)
BV1	3.4	M	0.08 $\pm$ 0.03	FL	17	5.12 $\pm$ 2.11 (4.88-5.36)	68.3 $\pm$ 8.5 (87.3-69.3)	14.4 $\pm$ 8.1 (13.5-15.3)	-9.7 $\pm$ 7.0 (10.5-8.8)	-4.6 $\pm$ 6.4 (-6.0-3.2)	12.2 $\pm$ 6.5 (10.8-13.7)
				HL	21	4.74 $\pm$ 2.31 (4.52-4.95)	66.4 $\pm$ 10.3 (65.4-67.4)	7.0 $\pm$ 7.0 (6.4-7.7)	-19.1 $\pm$ 7.6 (-19.8-18.4)	-13.2 $\pm$ 6.9 (-14.3-12.1)	5.2 $\pm$ 6.4 (4.2-6.3)
BV2	4.0	M	0.11 $\pm$ 0.04	FL	26	3.78 $\pm$ 2.32 (3.61-3.96)	61.4 $\pm$ 11.3 (60.5-62.2)	17.3 $\pm$ 6.1 (16.9-17.8)	-2.9 $\pm$ 2.7 (-3.1-2.7)	-9.3 $\pm$ 6.9 (-10.0-8.6)	7.3 $\pm$ 5.8 (6.8-7.9)
				HL	45	4.72 $\pm$ 2.84 (4.60-4.85)	78.9 $\pm$ 12.5 (78.4-79.5)	6.7 $\pm$ 4.9 (6.4-6.9)	-19.6 $\pm$ 6.4 (-19.9-19.3)	-13.2 $\pm$ 7.7 (-13.7-12.7)	8.9 $\pm$ 7.8 (8.4-9.4)
BV3	4.2	M	0.03 $\pm$ 0.02	FL	3	11.6 $\pm$ 1.45 (10.6-12.5)	65.4 $\pm$ 5.2 (62.0-68.7)	12.4 $\pm$ 3.5 (10.1-14.7)	-1.7 $\pm$ 2.6 (-3.4-0.03)	-4.2 $\pm$ 6.1 (-8.2-0.02)	10.6 $\pm$ 3.5 (8.3-12.9)
				HL	5	9.85 $\pm$ 2.33 (8.94-10.8)	76.4 $\pm$ 2.3 (75.5-77.3)	1.3 $\pm$ 1.0 (1.0-1.7)	-17.6 $\pm$ 2.3 (-18.5-16.6)	-16.1 $\pm$ 9.1 (-19.7-12.6)	5.2 $\pm$ 8.3 (2.0-8.5)
BV4	3.9	F	0.08 $\pm$ 0.02	FL	17	4.99 $\pm$ 1.29 (4.84-5.13)	64.2 $\pm$ 9.5 (63.1-65.3)	19.9 $\pm$ 5.9 (19.2-20.6)	-4.2 $\pm$ 4.5 (-4.8-3.7)	-8.0 $\pm$ 5.8 (-9.9-6.7)	8.2 $\pm$ 7.9 (5.6-10.7)
				HL	18	4.53 $\pm$ 1.42 (4.38-4.69)	69.0 $\pm$ 19.1 (66.9-71.0)	3.4 $\pm$ 2.5 (3.1-3.7)	-18.1 $\pm$ 9.7 (-19.2-17.1)	-16.6 $\pm$ 6.7 (-18.2-14.9)	6.6 $\pm$ 5.5 (5.3-8.0)
BV5	3.7	M	0.07 $\pm$ 0.02	FL	6	8.57 $\pm$ 2.12 (7.88-9.26)	49.2 $\pm$ 14.0 (44.6-53.8)	12.5 $\pm$ 3.4 (11.4-13.6)	-1.1 $\pm$ 1.2 (-1.5-0.7)	-7.1 $\pm$ 6.2 (-9.5-4.7)	5.5 $\pm$ 6.4 (3.0-8.0)
				HL	9	8.76 $\pm$ 3.03 (8.09-9.42)	74.2 $\pm$ 5.9 (72.9-75.5)	1.6 $\pm$ 1.3 (1.3-1.9)	-14.3 $\pm$ 3.2 (-14.9-13.6)	-9.7 $\pm$ 8.0 (-11.5-8.0)	10.2 $\pm$ 8.6 (8.3-12.1)

$N$ , number of single limb forces analyzed; FL, forelimb; HL, hindlimb; BW, bodyweight;  $V_{\text{pk}}$ , vertical peak force;  $P_{\text{pk}}$ , propulsive peak force;

$B_{\text{pk}}$ , braking peak force;  $M_{\text{pk}}$ , medial peak force;  $L_{\text{pk}}$ , lateral peak force.

In parentheses are 95% confidence intervals.

**Suppl. Table 2.** Means ( $\pm$ s.d.) of impulses (normalized in %BWS) for  $N=5$  individuals of *Bradypus variegatus*.

	Body Mass (kg)	Sex	Velocity ( $\text{ms}^{-1}$ )	Limb	$N$	Contact Time (s)	$J_V$ (%BWS)	$J_P$ (%BWS)	$J_B$ (%BWS)	$J_M$ (%BWS)	$J_L$ (%BWS)
BV1	3.4	M	0.08 $\pm$ 0.03	FL	17	5.12 $\pm$ 2.11 (4.88-5.36)	165.6 $\pm$ 83.6 (155.9-175.2)	21.6 $\pm$ 15.3 (19.8-23.4)	-14.4 $\pm$ 23.3 (-17.1-11.7)	-6.20 $\pm$ 12.0 (-8.83-3.63)	20.8 $\pm$ 13.0 (18.0-23.7)
				HL	21	4.74 $\pm$ 2.31 (4.52-4.95)	157.7 $\pm$ 84.7 (149.8-165.6)	4.39 $\pm$ 15.6 (2.93-5.85)	-30.2 $\pm$ 24.0 (-32.4-27.9)	-20.3 $\pm$ 12.6 (-22.4-18.2)	9.31 $\pm$ 21.2 (5.85-12.8)
BV2	4.0	M	0.11 $\pm$ 0.04	FL	26	3.78 $\pm$ 2.32 (3.61-3.96)	104.9 $\pm$ 86.6 (98.4-111.4)	17.3 $\pm$ 6.06 (16.9-17.8)	-2.91 $\pm$ 2.71 (-3.11-2.70)	-10.6 $\pm$ 9.89 (-11.6-9.61)	6.95 $\pm$ 7.51 (6.21-7.69)
				HL	45	4.72 $\pm$ 2.84 (4.60-4.85)	189.7 $\pm$ 100.3 (185.3-194.0)	6.66 $\pm$ 4.91 (6.45-6.88)	-19.6 $\pm$ 6.39 (-19.9-19.3)	-24.3 $\pm$ 29.8 (-26.3-22.4)	6.26 $\pm$ 11.5 (5.51-7.01)
BV3	4.2	M	0.03 $\pm$ 0.02	FL	3	11.6 $\pm$ 1.45 (10.6-12.5)	361.9 $\pm$ 38.2 (336.9-386.8)	67.1 $\pm$ 13.1 (58.5-75.6)	-2.46 $\pm$ 4.31 (-5.27-0.36)	-12.3 $\pm$ 20.6 (-25.7-1.18)	50.5 $\pm$ 30.2 (30.8-70.2)
				HL	5	9.85 $\pm$ 2.33 (8.94-10.8)	399.1 $\pm$ 100.2 (359.9-438.4)	0.48 $\pm$ 0.85 (0.15-0.18)	-94.9 $\pm$ 32.8 (-107.8-82.1)	-81.1 $\pm$ 55.1 (-102.7-59.5)	14.8 $\pm$ 30.1 (3.02-26.6)
BV4	3.9	F	0.08 $\pm$ 0.02	FL	17	4.99 $\pm$ 1.29 (4.84-5.13)	138.6 $\pm$ 30.0 (135.2-142.1)	34.9 $\pm$ 25.2 (32.0-37.8)	-2.06 $\pm$ 7.00 (-2.86-1.25)	-11.3 $\pm$ 11.4 (-15.1-7.58)	13.8 $\pm$ 15.4 (8.81-18.9)
				HL	18	4.53 $\pm$ 1.42 (4.38-4.69)	133.1 $\pm$ 53.5 (127.3-139.0)	0.40 $\pm$ 2.48 (0.13-0.67)	-32.5 $\pm$ 25.6 (-35.3-29.7)	-21.6 $\pm$ 11.6 (-24.4-18.7)	7.37 $\pm$ 10.5 (4.78-9.95)
BV5	3.7	M	0.07 $\pm$ 0.02	FL	6	8.57 $\pm$ 2.12 (7.88-9.26)	212.0 $\pm$ 24.1 (204.1-219.8)	53.3 $\pm$ 34.5 (42.0-64.5)	-0.11 $\pm$ 0.16 (-0.17-0.05)	-17.7 $\pm$ 17.1 (-24.4-11.0)	20.8 $\pm$ 29.4 (9.27-32.3)
				HL	9	8.76 $\pm$ 3.03 (8.09-9.42)	300.5 $\pm$ 72.2 (284.8-316.2)	0.55 $\pm$ 0.70 (0.40-0.70)	-50.4 $\pm$ 20.4 (-54.9-46.0)	-29.1 $\pm$ 28.3 (-35.3-22.9)	32.9 $\pm$ 36.3 (25.0-40.8)

$N$ , number of trials for which consecutive fore- and hindlimb forces were collected; FL, forelimb; HL, hindlimb; BWS, bodyweight seconds;  $J_V$ , vertical impulse;  $J_P$ , propulsive impulse;  $J_B$ , braking impulse;  $J_M$ , medial impulse;  $J_L$ , lateral impulse.

In parentheses are 95% confidence intervals.

**Suppl. Table 3.** Intraspecific parameters of statistical importance for fixed effects related to limb loading impulse.

Species	Response Variable	Fixed Effect	Estimate	Standard Error	df	t-value	p-value	
<i>Bradypus variegatus</i>	Peak Vertical Impulse	Velocity	-638.75	83.05	163.10	-7.69	<b>&lt;0.001</b>	
		Limb (hindlimb)	13.00	9.91	6.03	1.31	0.238	
	Peak Propulsive Impulse	Velocity	-200.07	72.50	120.41	-2.76	<b>0.007</b>	
		Limb (hindlimb)	-70.72	7.05	7.14	-10.03	<b>&lt;0.001</b>	
	Peak Braking Impulse	Velocity	99.39	77.79	165.39	1.28	0.203	
		Limb (hindlimb)	-75.20	12.49	8.70	-6.02	<b>&lt;0.001</b>	
	Peak Medial Impulse	Velocity	-381.19	106.89	166.69	-3.57	<b>&lt;0.001</b>	
		Limb (hindlimb)	-13.40	6.91	161.25	-1.94	0.054	
	Peak Lateral Impulse	Velocity	-511.74	104.19	130.98	-4.91	<b>&lt;0.001</b>	
		Limb (hindlimb)	-6.21	6.98	159.66	-0.89	0.375	
	Peak Net Fore-Aft Impulse	Velocity	33.50	72.67	162.05	0.46	0.645	
		Limb (hindlimb)	-83.61	10.66	7.11	-7.84	<b>&lt;0.001</b>	
	<i>Choloepus didactylus</i>	Peak Vertical Impulse	Velocity	14.93	62.66	41.19	0.24	0.813
			Limb (hindlimb)	6.92	3.71	41.69	1.86	0.070
Peak Propulsive Impulse		Velocity	-77.67	46.25	43.00	-1.68	0.100	
		Limb (hindlimb)	-16.52	2.74	43.00	-6.04	<b>&lt;0.001</b>	
Peak Braking Impulse		Velocity	37.66	62.13	43.00	0.61	0.548	
		Limb (hindlimb)	-8.31	3.68	43.00	-2.26	<b>0.029</b>	
Peak Medial Impulse		Velocity	138.25	61.51	43.00	2.25	<b>0.030</b>	
		Limb (hindlimb)	2.35	3.64	43.00	0.65	0.522	
Peak Lateral Impulse		Velocity	-3.66	64.69	43.00	-0.06	0.955	
		Limb (hindlimb)	4.53	3.83	43.00	1.18	0.244	
Peak Net Fore-Aft Impulse		Velocity	-61.52	45.83	43.00	-1.34	0.186	
		Limb (hindlimb)	-17.07	2.71	43.00	-6.29	<b>&lt;0.001</b>	

Significant interaction *p*-values are in bold.

Forelimb not listed because it was used as the reference variable.

**Suppl. Table 4.** Interspecific parameters of statistical importance for fixed effects related to limb loading impulse.

<b>Limb</b>	<b>Response Variable</b>	<b>Fixed Effect</b>	<b>Estimate</b>	<b>Standard Error</b>	<b>df</b>	<b>t-value</b>	<b>p-value</b>	
Fore	Peak Vertical Impulse	Velocity	-232.56	64.10	93.38	-3.63	<b>0.001</b>	
		Species ( <i>C. didactylus</i> )	-6.28	12.73	5.89	-0.49	0.640	
	Peak Propulsive Impulse	Velocity	-261.24	72.07	94.00	-3.63	<b>0.001</b>	
		Species ( <i>C. didactylus</i> )	-6.55	5.90	94.00	-1.11	0.269	
	Peak Braking Impulse	Velocity	-58.50	68.44	93.88	-0.86	0.395	
		Species ( <i>C. didactylus</i> )	-23.39	12.28	7.35	-1.91	0.095	
	Peak Medial Impulse	Velocity	-131.60	64.82	94.00	-2.03	<b>0.045</b>	
		Species ( <i>C. didactylus</i> )	-31.27	5.30	94.00	-5.90	<b>&lt;0.001</b>	
	Peak Lateral Impulse	Velocity	-246.09	54.88	94.00	-4.48	<b>&lt;0.001</b>	
		Species ( <i>C. didactylus</i> )	-37.10	4.49	94.00	-8.26	<b>&lt;0.001</b>	
	Peak <i>Net</i> Fore-Aft Impulse	Velocity	-173.51	74.46	89.44	-2.33	<b>0.022</b>	
		Species ( <i>C. didactylus</i> )	-18.59	8.79	5.06	-2.12	0.087	
	Hind	Peak Vertical Impulse	Velocity	-485.42	77.82	115.97	-6.24	<b>&lt;0.001</b>
			Species ( <i>C. didactylus</i> )	-0.62	13.45	7.07	-0.05	0.964
Peak Propulsive Impulse		Velocity	-147.85	86.91	102.46	-1.70	0.919	
		Species ( <i>C. didactylus</i> )	29.55	10.41	11.13	2.84	<b>0.016</b>	
Peak Braking Impulse		Velocity	283.69	80.60	116.00	3.52	<b>0.001</b>	
		Species ( <i>C. didactylus</i> )	19.34	7.98	116.00	2.42	<b>0.017</b>	
Peak Medial Impulse		Velocity	-34.42	92.49	106.03	-0.37	0.711	
		Species ( <i>C. didactylus</i> )	-10.65	12.47	4.43	-0.85	0.437	
Peak Lateral Impulse		Velocity	-182.84	78.52	116.00	-2.33	<b>0.022</b>	
		Species ( <i>C. didactylus</i> )	-34.34	7.78	116.00	-4.41	<b>&lt;0.001</b>	
Peak <i>Net</i> Fore-Aft Impulse		Velocity	245.48	80.71	116.00	3.04	<b>0.003</b>	
		Species ( <i>C. didactylus</i> )	23.33	8.00	116.00	2.92	<b>0.004</b>	

Significant interaction *p*-values are in bold.

*B. variegatus* is not listed because it was used as the reference variable.

**Suppl. Table 5.** Subset of means ( $\pm$ s.d.) for impulses (normalized in %BWS) for *Bradypus variegatus*.

Velocity ( $\text{ms}^{-1}$ )	Limb	N	Contact	$J_V$ (%BWS)	$J_P$ (%BWS)	$J_B$ (%BWS)	$J_M$ (%BWS)	$J_L$ (%BWS)
			Time (s)					
0.09 $\pm$ 0.04	FL	25	4.48 $\pm$ 2.46 (4.28-4.67)	131 $\pm$ 72.5 (125-136)	29.1 $\pm$ 25.6 (27.1-31.1)	-3.0 $\pm$ 6.5 (-3.5- -2.5)	-11.2 $\pm$ 12.7 (-12.5- -9.9)	14.4 $\pm$ 16.8 (16.1-19.0)
	HL	25	4.43 $\pm$ 2.97 (4.20-4.66)	173 $\pm$ 105 (164-181)	1.5 $\pm$ 8.3 (0.09-2.2)	-39.5 $\pm$ 31.9 (-42.0- -37.0)	-21.1 $\pm$ 20.2 (-23.2- -19.1)	10.0 $\pm$ 21.8 (7.8-12.3)

N, number of trials for which consecutive fore- and hindlimb forces were collected; FL, forelimb; HL, hindlimb; BWS, bodyweight seconds;  $J_V$ , vertical impulse;  $J_P$ , propulsive impulse;  $J_B$ , braking impulse;  $J_M$ , medial impulse;  $J_L$ , lateral impulse.

In parentheses are 95% confidence intervals.

Vertical impulse applied by the animals is shown as positive (absolute) values by convention.

**Fig. 1 Force beam apparatus and suspensory walking limb motion.** **a**, two parallel sections of cave brava wood were secured together with 0.25” threaded rods and suspended from the rafters of an overhang with heavy-duty plastic wrap ties. The beam apparatus was reinforced by horizontally oriented heavy-duty plastic wrap ties fastened to animal enclosures. An AMTI force plate (inset) was affixed to the upper beam and bolted to it was a T-shaped grip attachment positioned central to the two lower beam segments. The grip attachment was wrapped in duct tape (and veterinary wrap) to approximate the diameter of cave brava and was positioned with approximately a 5 cm gap between it and either of the two lower beam segments; **b**, a three-toed sloth performing suspensory walking. Note the abducted posture of the limbs and placement of the entire palmar/plantar surface of the foot on the dorsal aspect of the beam (inset). Grip on the substrate is anchored by strong flexion of the claws.

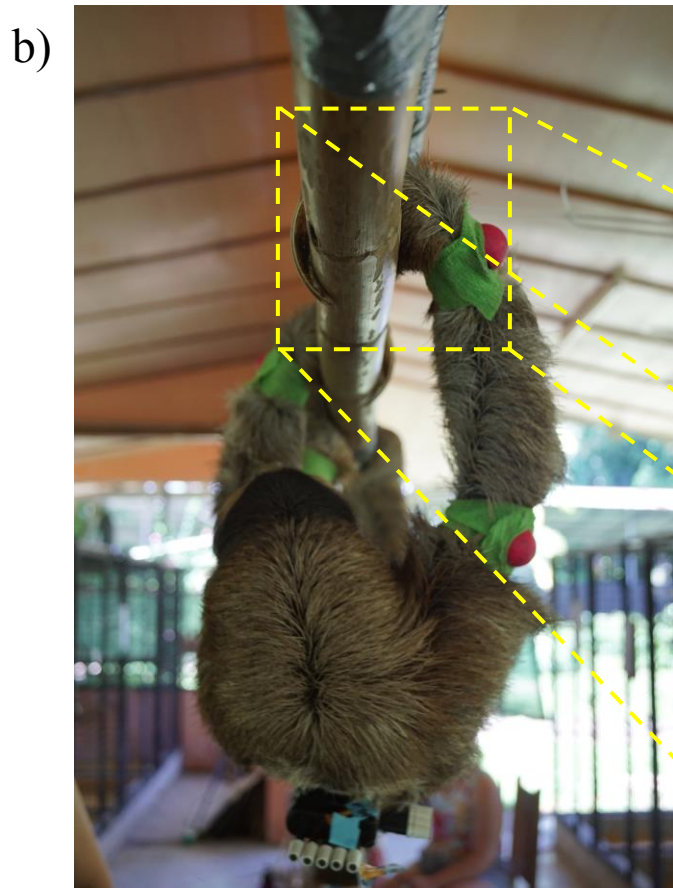
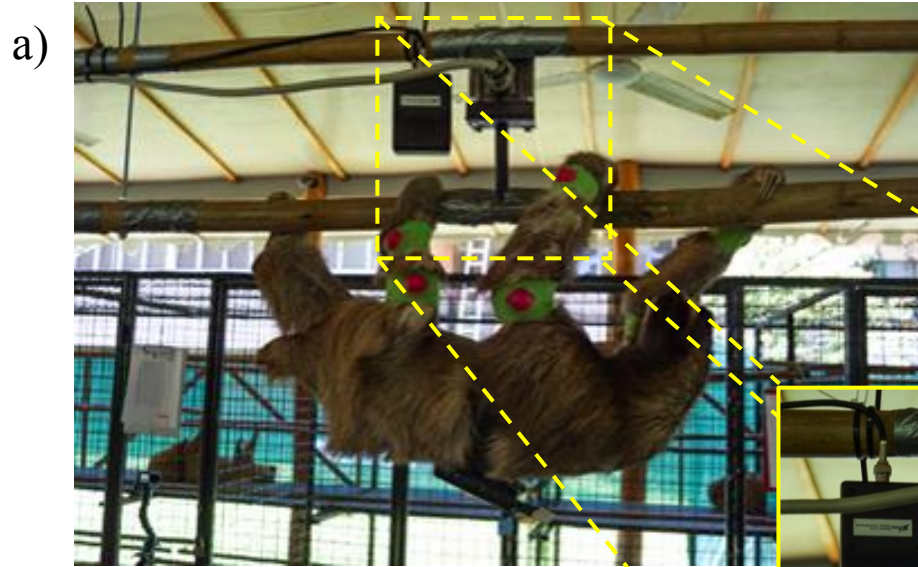




**Fig. 2 Representative single limb forces sampled from *Bradypus variegatus* and *Choloepus didactylus* during suspensory walking.** Vertical (blue, z-axis), fore-aft (red, x-axis), and mediolateral (green, y-axis) forces applied by the forelimbs (above, grey shading) and hindlimbs (below, not shaded) of sloths. Vertical force is shown as positive (absolute) values by convention, as well as (+) propulsive force and (-) braking force. All values are normalized in percentage bodyweight (%BW) and these data shown are from consecutive limb contacts within the same trial.

*Choloepus didactylus*

*Bradypus variegatus*

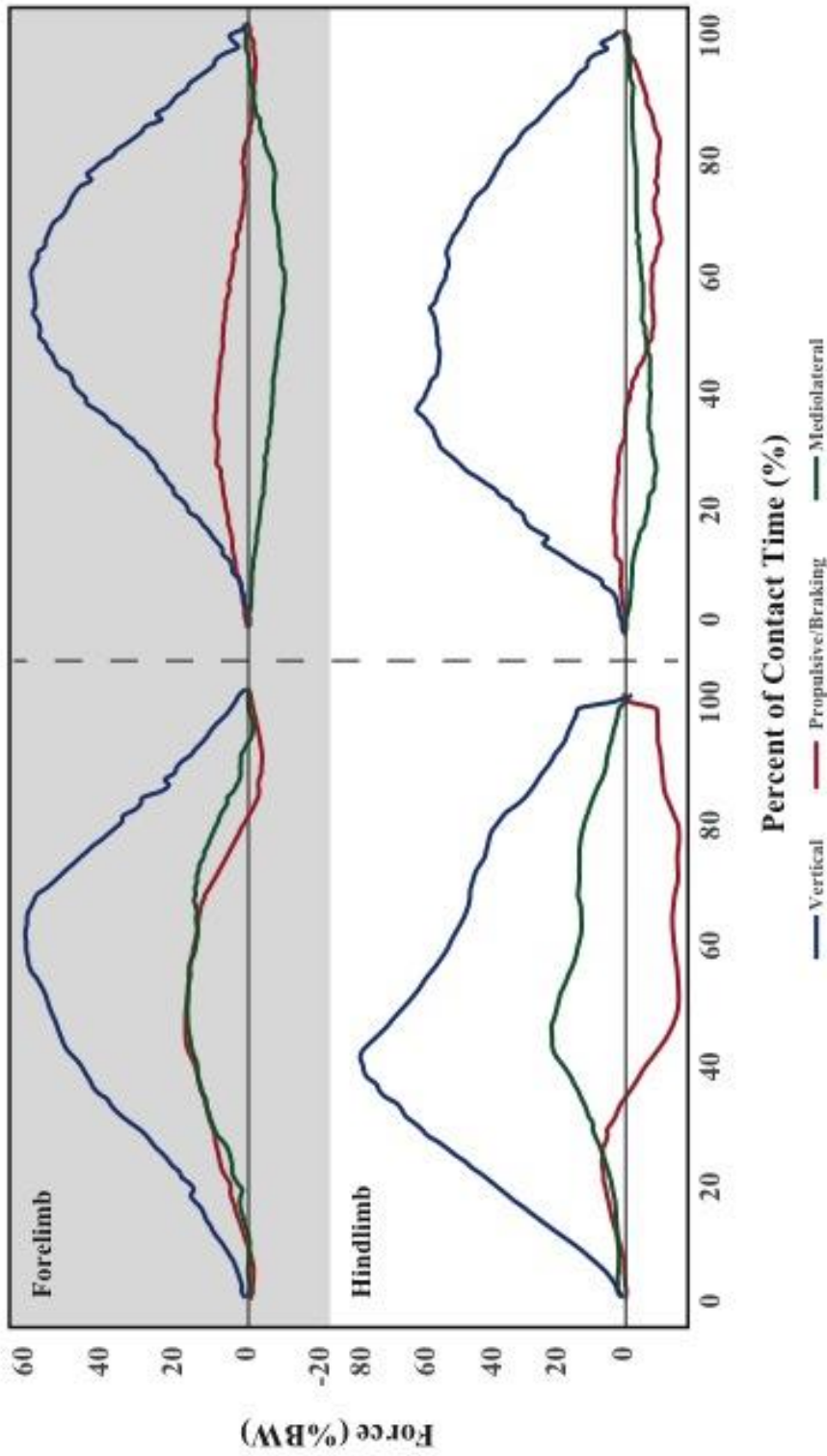


**Fig. 3 Box and whisker plots of relative peak forces and impulses between limb pairs and species during suspensory walking.** **a**, comparisons of vertical peak forces (left) and impulse (right) between forelimbs (grey shaded) and hindlimbs (not shaded) for both species; **b**, comparisons of peak (+) propulsive vs. (-) braking forces (left) and impulses (right) between forelimbs (grey shaded) and hindlimbs (not shaded) for both species; **c**, comparisons of peak (-) medial vs. (+) lateral forces (left) and impulses (right) between forelimbs (grey shaded) and hindlimbs (not shaded) for both species. Color coding the same as in Fig. 2. All values of force are normalized in percentage bodyweight (%BW) and those for impulse in bodyweight seconds (%BWS). Means represent data from *Bradypus* ( $N=5$ ) and *Choloepus* ( $N=2$ ). The number of single-limb contacts for each limb pair are listed in Table 1.

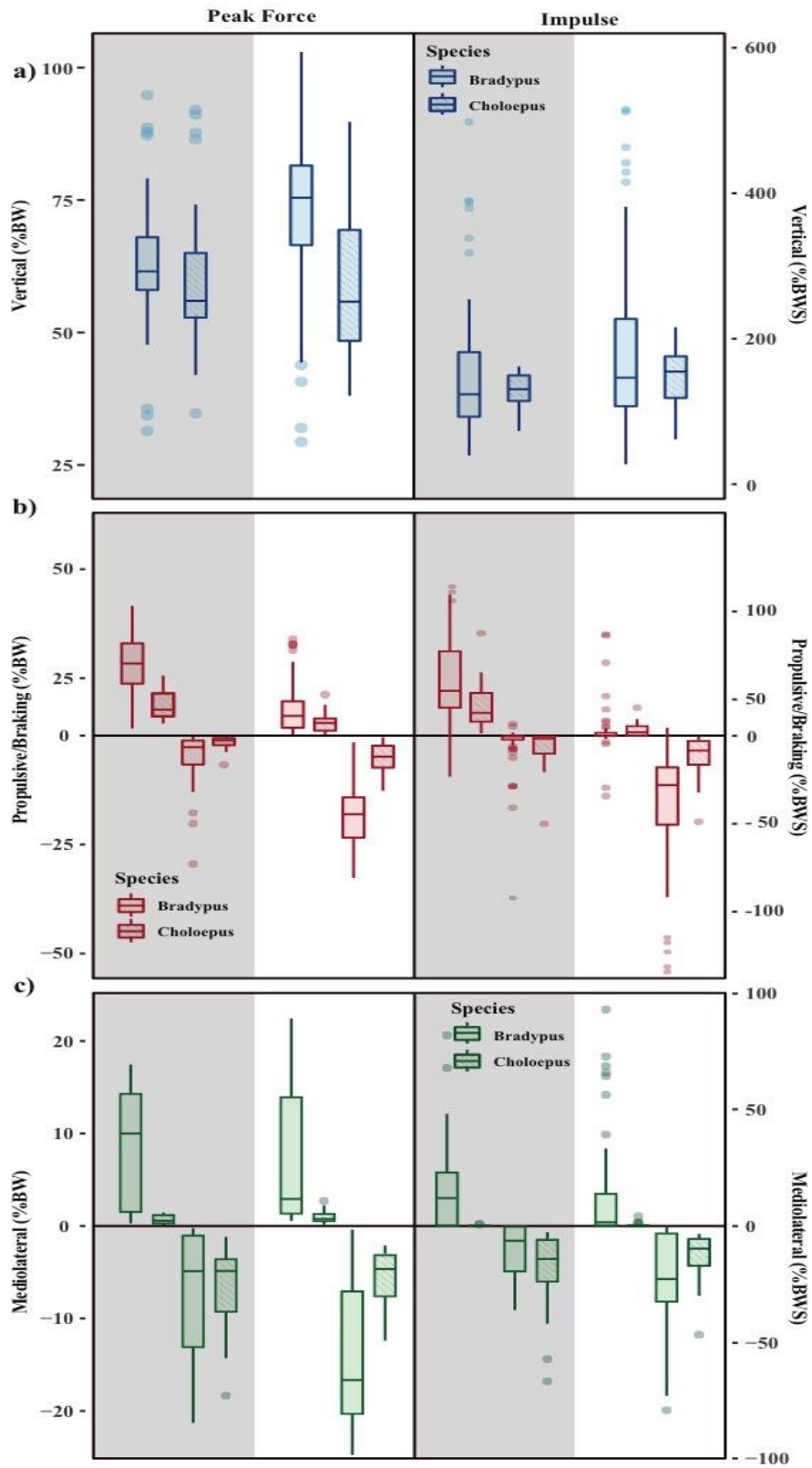
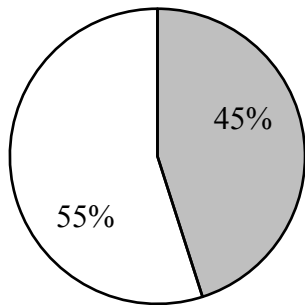
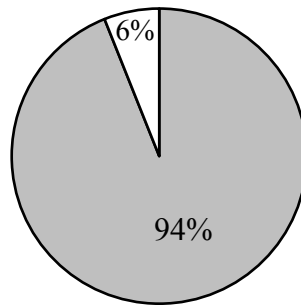


**Fig. 4 Relative contribution of fore- and hindlimbs to bodyweight support in *Bradypus variegatus* during suspensory walking.** Percentage of vertical, propulsive, and braking impulse (single limb impulse/total impulse) applied by the forelimbs (grey shaded) and hindlimbs (not shaded). Values of relative impulse were determined as the quotient of impulse in each direction per limb and total vertical impulse across limb pairs during a single stride. Data shown represent a subset of  $n=25$  strides.

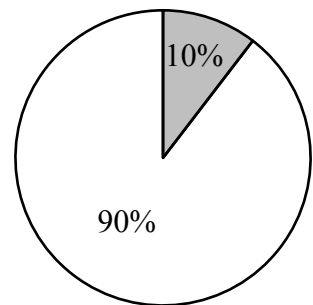
Vertical Impulse



Propulsive Impulse



Braking Impulse



Forelimb  Hindlimb 

## APPENDIX I: EMG ANALYSES

### INTRODUCTION

Tree sloths are obligate suspensory taxa with some of the lowest body temperatures (Pauli et al., 2016) and basal metabolisms among placental mammals (Cliffe et al., 2015, 2018). As such, energy savings are critical to their locomotor success and sloths employ slow, intermittent locomotion as a strategy to conserve metabolic energy during functional behaviors. Slow and deliberate movements are also important for evading predators, as well as avoidance of wasteful oscillations of the substrate, further emphasizing the necessity for highly controlled movement. The two genera of modern tree sloths, *Choloepus* (two-toed) and *Bradypus* (three-toed) diverged nearly 29 million years ago (Presslee et al., 2019), and therefore, arboreal suspensory habits arose separately in each lineage, making the acquisition of similar morphological and physiological traits one of the most striking examples of convergent evolution within Mammalia (Nyakatura, 2012).

Sloths primarily use suspensory walking (SW) and vertical climbing (VC) on arboreal substrates as their main locomotor behaviors. Resting postures range from suspensory hanging (SH) to reclining in tree branch junctions and laying supine across branches (Hayssen 2009, 2010). In fact, sloths are inactive for large portions of their awake time (Sunquist and Montgomery, 1973; Urbani and Bosque, 2007). Nonetheless, arboreal locomotor activity is both necessary and costly (Hanna et al., 2008), and two- and three-toed forms vary in their frequency of SH, SW, and VC, which coincides with their ecological/behavioral preferences (or constraints) and body size. For example, the smaller *Bradypus* are specialized folivores (Montgomery, 1983) and prefer to occupy the canopy and emergent levels of their native neotropical rainforests in Central and South America (Hayssen, 2010), whereas *Choloepus* prefer to occupy the understory to canopy levels of vertical strata (Adam, 1999; Hayssen, 2011). Despite their differences in substrate use, the flexor musculature of sloths is generally well-developed (e.g., Humphrey, 1870; Mackintosh, 1875; Miller, 1935; Diniz et al., 2018; Butcher et al., 2022) and areas of origin/insertion are modified for greater mechanical advantage to support the bodyweight in suspension (Mendel, 1985; Olson et al., 2018; Morgan et al., in review). In addition, limb musculature in both *Choloepus* and *Bradypus* demonstrate a predominant expression

of slow, anaerobic myosin heavy chain (MHC-1) fibers in (Spainhower et al., 2018, 2021). Thus, their muscle physiology is specialized for, or perhaps constrained to, intermittent, slow, large force contractile activity that typifies the locomotion and gait patterns of tree sloths. These slow-contracting, anaerobic fibers may also constrain sloth locomotion to being highly controlled and intermittent in nature.

Locomotor mechanics are essential to the understanding of limb muscle function. Several studies have shown that both genera have large duty factors and slow average velocity of locomotion approximating  $0.1 \text{ ms}^{-1}$  (Nyakatura et al., 2010; Granatosky and Schmitt, 2017; Gorvet et al., 2020). Specifically, previous evaluations of limb kinematics and kinetics in *C. didactylus* (Nyakatura and Andrada, 2013; Granatosky and Schmitt, 2017; Granatosky et al., 2018), and a recent study in *B. variegatus* (McKamy et al., in review), revealed that the fore- and hindlimbs of sloths primarily act as propulsive and braking appendages, respectively, during SW. These functional roles of the limb pairs are consistent with those of primates performing inverted quadrupedalism (Ishida et al., 1990; Dickenson et al., 2022). However, unlike suspensory primates that utilize pendular exchanges of potential and kinetic energy (e.g., brachiating gibbons and siamangs) (Bertram et al., 1999) for metabolic economy, locomotor modeling data from *C. didactylus* (Nyakatura and Andrada, 2013) indicate that these mechanics are unavailable to sloths suggesting that their mode of locomotion is driven entirely by muscular work.

Electromyography (EMG) is a well-established technique for measurement of muscle activation and is often correlated with the underlying mechanisms of locomotion. EMG duration and intensity (i.e., EMG amplitude) are representative of the volume of muscle activation and thusly can be used to infer the metabolic energy cost of contraction (Roberts et al., 1997), as well as function of specific limb muscles or groups. Moreover, wavelet analysis of EMG (Wakeling et al., 2001; Wakeling et al., 2012; Gorvet et al., 2020) is capable of resolving the spectral frequency properties of the EMG signals specific to the recruitment patterns of slow and fast motor unit (MU) and/or muscle fibers during locomotion. Foundational EMG studies in suspensory taxa such as those in the slow loris (*Nycticebus coucang*) established muscle activation patterns for antagonistic flexor/extensor muscles in each limb pair during SW and VC (Jouffroy and Stern, 1990). Large muscle activations in the flexor musculature were correlated with muscle fiber type



(Sickles and Pinkstaff, 1981a, b) and clearly demonstrated burst activations of muscle functional groups for either a role in limb propulsion or braking during inverted quadrupedalism. The timing and magnitudes of peak EMG intensity in targeted muscles and have additionally been shown to correlate with magnitudes of maximum force of muscular contractions in fish (Aiello et al., 2020) and the application of peak forces by the limbs during locomotion in varanid lizards (Granatosky, 2020). In particular, a previous review of animal locomotion utilizing simultaneous EMG and limb loading measurements found that force is linearly correlated with EMG intensities (Roberts and Gabaldon, 2008). It is therefore suggested that the timing of peak EMG intensity is also likely to be correlated with peak limb forces in the direction in which limb muscles apply force. As such, evaluations of simultaneous EMG and limb loading can uncover which muscles and/or muscle functional groups are responsible for specific locomotor contributions during the contact phase of a stride. However, these types of studies are limited in the literature, and none are currently available for suspensory taxa.

Gorvet et al. (2020) found that in the forelimbs of *Bradypus* the lowest volumes of active muscle are recruited during SH, whereas the elbow flexor muscles (e.g., m. biceps brachii and m. brachioradialis) are recruited most intensely and for long durations during SW. Alternatively, the elbow and carpal/digital extensors of *B. variegatus* showed biphasic activations during a stride and are most active during VC (potentially to propel the body upward). In addition, wavelet analysis indicated that fast (MHC-2A) fibers are recruited at low intensities during SH (e.g., distal digital flexors), but slow (MHC-1) fibers (e.g., proximal flexor muscles) are recruited at larger intensities during SW and VC (Gorvet et al., 2020). It was concluded that the economy of sloth locomotion is potentially dependent to selective recruitment of large, slow-contracting MU during locomotion, but smaller fast MU during suspensory posture in *Bradypus*. The reduction in overall EMG intensity observed during SH in sloth forelimbs was further related to passive support provided by tensile loading of compliant digital flexor tendons in both limb pairs (Mossor et al., 2020). Furthermore, Granatosky (2018) and Gorvet et al. (2020) hypothesized that co-activation of m. pectoralis superficialis and selected flexor/adductor muscles of the hindlimb in sloths may be a mechanism by which sloths ensure stable, controlled movement during SW and may explain the limb loading patterns observed in *Choloepus*.

As such, it is necessary to further evaluate limb loading patterns and EMG activation timings and intensities in sloths to address this hypothesis.

In general, less is known about structure/function in the hindlimbs of sloths, especially in *Bradypus*. Yet, recent reports of hindlimb myology (Butcher et al., 2022) and muscle architectural properties (Morgan et al., in review) in *B. variegatus* identified several strong hip and knee flexor muscles with large mass/volume and long muscle moment arms that can slowly rotate or stabilize their respective limb joints against gravity during suspension. Notably, the hip flexors *m. iliopsoas* and *m. sartorius* appear to be best suited to perform braking during locomotion (Butcher et al., 2022), whereas the *m. gluteus medius* is likely the most capable of propelling the body upward during VC (Butcher et al., 2022; Morgan et al., in review). Butcher et al. (2022) also predicted that the main role of the knee extensors is to stabilize the knee joint to counteract large flexor torques produced by massive knee flexor musculature. Moreover, *Bradypus* has longer forelimbs than hindlimbs (i.e., high intermembral index: Marshall et al., 2021) and this trait has been suggested to contribute to greater bodyweight support on its hindlimbs during suspension (McKamy et al., in review) versus equal bodyweight support roles by the fore- and hindlimb in *Choloepus* (Granatosky et al., 2018; Dickinson et al., 2022).

This study is designed to verify the potential for co-activation of selected fore- and hindlimb muscle pairs by evaluating EMG activation in the hindlimb of *B. variegatus*, and it will be the first to correlate EMG intensity with peak limb loading patterns in a suspensory mammal. It is specifically hypothesized that braking function (via lengthening contractions) of the slow-contracting *m. sartorius* during hindlimb retraction will coordinate with activation timing of *m. pectoralis superficialis* to control the horizontal advancement of body during SW. To this end, hindlimb muscle activations coupled with patterns of limb loading in both the fore-aft and vertical directions will not only further understanding of sloth locomotor mechanics, but also suspensory adaptations in mammals, more generally. Moreover, it is unknown if specific hindlimb muscles in *Bradypus* will show similar patterns of activation as those in the forelimbs during suspensory locomotion and posture, although prolonged, moderate activations of notably slow-contracting hindlimb flexor/extensors (Spainhower et al., 2021) are predicted due to the important

braking, joint stability, and bodyweight support functions of the hindlimb in sloths as determined in the prior companion study (McKamy et al., in review).

## **MATERIALS AND METHODS**

### **Study Animals**

A total of  $N=5$  brown-throated three-toed sloths (*Bradypus variegatus*, Shinz 1825) were used for this study. All animals (adults and sub-adults;  $3.84\pm 0.3$  kg) were healthy and showed no obvious musculoskeletal or gait abnormalities. Individuals were selected and handled by staff at The Sloth Sanctuary of Costa Rica and no preference was given to the sex of the sloths (4 males and 1 females: Table A1). This work was conducted at The Sloth Sanctuary in Peshurst-Límon, Costa Rica in Spring 2022. All experimental procedures complied with the protocols approved by the Costa Rica Ministerio Del Ambiente y Energía, Sistema Nacional de Áreas de Conservación, a través del Programa de Investigación del Área de Conservación La Amistad Caribe, (R-SINAC-PNI-ACLAC-012-2021 to M.T. Butcher).

### **Implantation of Electrodes**

Protocols for sedation and electrode implantation were based on those used in Gorvet et al. (2020). Sloths were sedated with an injection of Dexdomitor (0.1 mL/kg, injected into the left m. gluteus medius) prior to electrode implantation. Following a titration period of 20 min, on average, custom fine-wire bipolar EMG electrodes (0.002 bifilar: California Fine Wire, Grover Beach, CA, USA) were sterilized in 100% ethanol and implanted into two suites of four selected muscles for trials of suspensory walking (SW): a proximal suite consisting of m. sartorius (SRT), gluteus medius (GLM), m. biceps femoris (BF), and vastus lateralis (VL); a distal suite consisting of m. adductor longus (ADDL), m. tibialis cranialis (TCN), m. lateral gastrocnemius/m. soleus (LG/SOL) and m. flexor digitorum profundus (FDP); a modified suite consisting of VL, BF, m. rectus abdominis (RA), and m. longissimus dorsi (LD). Electrodes for proximal and distal suites were consistently implanted across all individuals, whereas implantation in the modified suite of muscles was performed in only one individual to account for prior electrode failures in two proximal suite muscles. See Butcher et al. (2022) for a review of hindlimb myology in *B. variegatus*.

Pairs of four EMG electrodes were implanted percutaneously into muscles of the right hindlimb using 26-gauge needles. Following piercing the skin, needles were inserted into the muscle belly, twisted 180°, and then withdrawn to leave the barred, hooked end of the electrode fine-wire implanted in the muscle belly. Muscle targets were identified via careful palpation of the sloth hindlimb after sedation. The electrode wires were then cabled and connected to +/- paired twist-pot connectors, which were inserted into a wireless EMG unit (BioRadio™, Great Lakes NeuroTechnologies, Cleveland, OH, USA) that was harnessed to the thorax/abdomen of the animal. After the electrodes were secured, sedation was reversed via injection of Antisedan (0.05 mL kg) again into the left m. gluteus medius. Sloths were tested for alertness by lifting their bodies by their forelimbs to elicit vocalizations and/or digital flexion. After the animals had adequately recovered, they were then moved to the force beam apparatus for experimentation.

### **EMG Recordings**

Individuals were placed below a horizontal beam apparatus composed of cave brava (a native Costa Rican woody plant) and containing a central force platform segment as previously described (McKamy et al., in review). Sloths were allowed to move freely and select their preferred speed along the length of the beam in either direction. A total of  $n=37$  trials of SW recorded while the instrumented right hindlimb was in contact with the force platform (Table A1). Videos (frame rate: 60 Hz) of each trial were recorded with four GoPro cameras (HERO5 San Mateo, CA, USA) positioned approximately 1 m from the beam in both the sagittal and diagonal planes. EMG (2000 Hz) and force platform (12,000 Hz) data recordings were synchronized using footfall event markers in the BioCapture™ software (Great Lakes NeuroTechnologies, Cleveland, OH, USA) run on laptop computer where EMG signals were live streamed via Bluetooth.

EMG recordings between the proximal and distal suite of muscles during SW occurred on consecutive days. Muscles targeted for the modified suite were sampled on the final day of SW trials. Thus, each individual was given a minimum of 24 hr to recover from a previous set of experimental trials before another was performed. After EMG signals were recorded (~1 hr) the fidelity of each implant was inspected before the fine wire electrodes were removed from the muscle bellies, after which the sloths were placed back into their enclosures by The Sloth Sanctuary staff and observed to ensure full recovery.

## EMG Analyses

Video analysis involved extraction of frame numbers that marked the touchdown and lift-off events of the right hindlimb. Touchdown was defined as the first frame in which the hindfoot and all three claws were in contact with the substrate, while lift-off was the first frame where the claws were no longer in contact with the substrate and the hindfoot began to move cranially in the sagittal plane. From these video data, velocity for all trials from each individual was determined following the procedures described in detail by Young et al. (2022). A mean value of  $0.09 \pm 0.04 \text{ ms}^{-1}$  was reported in the prior companion study of limb loading (McKamy et al., in review). Stride parameters for each individual are presented in Table A2.

Temporal EMG variables were determined using BioCapture™. Briefly, both and high- and low-pass noise was first removed from the EMG signals using the automated routines available in BioCapture™. Cursors were used to mark and measure the absolute times (in s) of EMG onset ( $\text{EMG}_{\text{on}}$ ) and offset ( $\text{EMG}_{\text{off}}$ ). All temporal variables were normalized to percent stride cycle (%cycle) by designating the time of footfall on the force platform as 0% and the next consecutive contact of the right hindlimb as 100%. Force platform data provided an exact time interval of the contact phase, while the time interval of swing phase was calculated as the difference between contact and stride durations (contact + swing = stride). EMG signals were then set to fill the channel parameters to bracket the scale for maximum/minimum burst amplitudes (in millivolts, mV). Rectified (positive signal only) EMG intensity was measured for each burst in a signal. An EMG burst was considered as a muscle activation greater than or equal to 2x baseline voltage. The single highest value of EMG intensity (a proxy for maximal voluntary contraction) was also determined for each muscle and used to calculate activation intensity ratios of 0–1 (burst intensity/peak intensity) for each burst analyzed, where zero indicates no activation and a value of 1 indicates maximal activation (Gillis and Biewener, 2001; Gorvet et al., 2020).

The timing peak EMG activation was additionally measured for each burst and muscle, and normalized to percent contact (%contact). Complimentary measurements of the times of peak propulsive, braking, and vertical forces (in %contact) were determined as output variables from the prior analyses of limb loading reported in the companion study (McKamy et al., in review). These combined temporal data set from the hindlimb muscles

were analyzed as a series of bi-plots for each muscle and direction of applied force during SW to determine the strength of the correlations between peaks of EMG activation and limb loading. Correlation of peak EMG intensity timings and peak forces during the contact phase assists in identifying a role in force production by the limb muscles, as force production has been previously shown to increase linearly with EMG activation intensity (Roberts and Gabaldon, 2008).

### **Methodological Limitations**

The exact placement of EMG electrode wires was not verified in the present study because there was not access to an ultrasound to ensure that the electrodes were implanted into the intended muscle belly. As targeted muscles are part of functional groups (e.g., knee flexors or knee extensors), insertion of electrodes into specific regions of the hindlimb is adequate to test the hypotheses proposed. Electrodes also failed during trials of SW (see Table A3), as expected for an *in vivo* study using percutaneous EMG electrode implants during locomotion. However, enough locomotor trial replicates were performed for each muscle and each behavior across individuals to account any missing data from failures. Not all individuals performed locomotor trials at the same time of day, which could have potentially impacted performance. However, *B. variegatus* is a diurnal and performed out of direct sunlight. The sloths may have also been influenced by the effects of the sedative/reversal drugs administered before trial recordings due to their slow metabolism. A large number of trials (15–30 trials) were performed to account for this potential impact on performance, although all trials do not represent contacts on the force platform by the right hindlimb only. A final consideration is that sloths naturally employ intermittent, non-steady-state locomotion; however, the individuals in this study were used simultaneously for data collection with the companion study (see McKamy et al., in review) for which steady-state locomotion was required and verified statistically.

## **RESULTS**

### **EMG Activation Patterns**

A total of 37 strides and 165 individual EMG bursts were analyzed across the ten muscles sampled (Table A1). The means for stride duration and duty factor are  $6.84 \pm 3.88$  s and  $0.74 \pm 0.11$  (Table A2), respectively, along with an average velocity of  $0.09 \text{ ms}^{-1}$ . EMG

onset and offset times, as well as burst durations of each muscle for each individual are presented in Table A4. Most muscles have long activations approximating 40–50% of the stride cycle, including several that display a second activation late in the contact interval that persisted into swing phase (e.g., SRT, GLM, ADDL, FDP), while the extensors VL and LG/SOL exhibit bi-phasic activations that are distinct to both the contact and swing phases of the stride (Fig. A1). In particular, EMG<sub>on</sub> of the flexors SRT and RA is nearly simultaneous and delayed (8–10 %cycle), followed by activation the VL, which has the latest EMG<sub>on</sub> at a mean of  $11.0 \pm 25.1$  %cycle (Table A4). With the exception of BF, all other hindlimb muscles activate either at or immediately after footfall. The flexors BF (bi-articular, hip extensor/knee flexor), RA, and TCN are most typically activated during contact only, whereas the epaxial LD has the longest activation accounting for nearly 90% of the stride cycle (Fig. A1). The proximal GLM and distal FDP also have long total EMG activation durations averaging 70% of the stride cycle (Table A4).

### **EMG Burst Intensities**

Mean EMG intensities across for all muscles and individuals are presented in Table A5. On average, SRT and ADDL are the two most intensely activated hindlimb muscles during contact, with mean EMG activation ratios greater than 0.60, followed by that of the vertebral extensor LD (Fig. A2). The knee extensor VL has a mean activation ratio of  $0.45 \pm 0.30$ , which is larger than the average ratios for each of the three flexors muscles FDP, BF, and TCN. Notably, the hip extensor GLM has the lowest average intensity ratio at 0.23 of all muscles sampled during SW (Fig. A2). Moderate-to-strong correlations between the timing of peak limb forces in three directions (i.e., propulsive, braking, and vertical) and peak EMG activation for selected muscles are shown in Figure A3. Peak propulsive force is applied by the hindlimb early in the contact and is most strongly related to the time of peak activation in GLM ( $R=0.438$ ). The time of peak braking force occurs near mid-contact and most strongly correlates with peak activations of SRT ( $R=0.510$ ) and TCN ( $R=0.730$ ). In addition to ADDL with a correlation coefficient of  $R=0.456$ , the ankle flexor TCN ( $R=0.839$ ) also shows the strongest relationship between the time of peak vertical force and muscle activation.

The relative timing in % difference of peak EMG activations and limb forces for all muscles sampled are presented in Table A6. Again, only SRT and TCN approximate the

timing of peak braking force application by the hindlimb. All extensor muscles, in addition to ADDL, FDP, and the bi-articular BF, have peak activations less than 10% different during the contact interval than the time of peak propulsive force (Table A6). The pattern for vertical support time peaks by muscle activations matches that of propulsive force application, except for extensors GLM and VL, which both have relative timings greater than 20% different than peak vertical force on average.

## DISCUSSION

Previous research into sloth locomotion has analyzed gait (Mendel 1981a, 1985; Gorvet et al., 2020), suspensory walking kinematics (Nyakatura et al., 2010; Nyakatura and Fischer, 2010; Granatosky et al., 2018), limb loading (Nyakatura and Andrada, 2013; Granatosky and Schmitt, 2017; McKamy et al., in review), and forelimb muscle activation (Gorvet et al., 2020). And although some studies have assessed functional capacity of the pelvic limb musculature in *Bradypus*, including analyses of myology (Butcher et al., 2022), muscle architectural properties (Morgan et al., in review), and grip strength (Young et al., in review), no *in vivo* data are available for hindlimb muscle activation. This study provides complementary EMG activation data to that of the forelimb in *Bradypus* reported by Gorvet et al. (2020).

Analysis of burst durations and peak EMG activation timings clarifies the roles of specific muscles and functional groups as it pertains to braking, propulsion, and bodyweight support in suspensory locomotion. In general, the flexor musculature of the hindlimb is primarily activated during the contact phase of SW, whereas extensor and adductor muscle activations exhibit either biphasic or distinct contact and swing activations (see Table A7). Specifically, and as previously hypothesized, the bi-articular m. sartorius (SRT: hip flexor and limb abductor) is activated during a similar portion of the contact interval as m. pectoralis superficialis anterior (PSA) in the forelimb and has peak EMG activations that correlate with the application of peak braking force by the hindlimb. The correspondence in timing of peak events suggests that SRT may be primarily responsible for providing braking forces during the mid-to-latter portion (44–84 %contact) of the contact phase. It is also possible that the well-developed and powerful m. iliopsoas (Morgan et al., in review) provides a substantial amount of braking force over the contact



interval by either strong isometric (or lengthening) contractions as previously proposed for SRT. Thus, the available EMG activation data herein provide additional support for the hypothesis that SRT, or more generally, the hip flexor muscles, including the m. iliopsoas, co-activate with PSA as a mechanism for enhanced strut-like function of fore- and hindlimb pairs to control movement during suspensory locomotion in tree sloths.

Limb extensor muscles m. gluteus medius (GLM), VL, and LG/SOL activate during both the contact and swing phases of suspensory walking, with low percent differences observed between peak EMG activations and the application of peak propulsive forces by the hindlimb. These findings are evidence their roles in propulsion forces during early contact phase (peak propulsion: 26 %contact). In particular, early EMG onset activation of LG/SOL immediately following the footfall could provide propulsive force, whereas a swing activations of GLM likely counterbalance flexor moments at the hip joint acting to 'quickly' advance (i.e., swing phase is only 0.25 of the stride) the limb forward during limb protraction throughout swing phase. Moreover, the lowest average EMG intensities were observed in GLM, which further implies it serving a primary role as an antagonistic hip joint stabilizer and secondary role as propulsive muscle during SW. A main role in controlling joint position and joint rotational velocity during SW is consistent with the homogenous expression of slow-contracting myosin heavy chain (MHC-1) fibers in the GLM of *B. variegatus* (Spainhower et al., 2021). The LG/SOL and VL were the only two muscles to display distinct swing phase activations. As such, swing activations of both muscles match their functional roles to extend the ankle and knee joints, respectively, in preparation for the next footfall. Nonetheless, the delayed EMG onset of VL during the contact phase was somewhat surprising, and its relative lower intensity of activation indicates that the pennate-fibered m. quadriceps femoris have to be strong to not only counterbalance large flexor torques of the massive knee flexors (Butcher et al., 2022; Morgan et al., in review), but also the VL could be functioning equally as strongly in the exertion of braking force at the propulsion-to-braking transition late in contact.

Considering the apparent extended position of the knee joint during contact phase, the VL indeed may be in a favorable position for applying supplemental braking force by isometric or eccentric loading represented by less intense activations (i.e., lower volume of muscle recruited during isometric/lengthening contractions). Previous studies of human

lower limb muscle activations across varying joint angles have shown that for some muscles, EMG activation intensities are lowest for lengthening contractions regardless of joint angle, whereas for other muscles (e.g., mm. brachioradialis and biceps brachialis), lengthening contractions resulted in the lowest recorded EMG intensities with the upper limb in an extended posture (Nakazawa et al., 1993). It is therefore possible that VL enhances the strut-like function of the hindlimb (an expected role of the pelvic limb during SW) in coordination with the initial deactivation of SRT prior to mid-contact. This hypothesized means of VL applying braking forces also relates to it being composed of entirely slow MHC-1 fibers that hydrolyze ATP at a low rate while producing appreciable force (Spainhower et al., 2021). Future evaluations of limb kinematics and joint powers in *B. variegatus*, however, are needed to verify degrees of relative flexion/extension at the knee joint and function of the knee joint in braking/propulsion during suspensory walking to verify this supposition. It may be the *Bradypus* maintains an extended position of the knee joint during contact mainly due to their short hindlimb length relative to their notably elongated forelimbs (Marshall et al., 2021).

In contrast, the m. biceps femoris (BF) and ankle flexor/foot supinator m. tibialis cranialis (TCN) are primarily activated during contact phase and likely serve an anti-gravity role of bodyweight support. The BF both extends the hip and flexes the leg at the knee joint, and as such, the EMG onset and activation duration are similar to that of VL. The patterns observed typify antagonistic muscle group function. Nevertheless, fine-wire electrodes were most often placed in the bi-articular ischial head of BF, thus action at either joint is difficult to discern from measurements of EMG activation reported herein. The femoral head of BF (knee flexor) was the original intended muscle target, but accuracy implantation of the electrodes in this belly proved to be ungainly do the amount of fascia in the knee and leg region of the pelvic limb (Butcher et al., 2022). Ergo, equal percent differences for the timing of peak EMG activation and peaks in both propulsive force (via hip extension) and vertical force (via knee flexion) application exemplify the expected actions of the bi-articular ischial head. It is also acknowledged that potentially mistaken implantation of EMG electrodes into the adjacent m. semimembranosus would have resulted in similar activation patterns, and further indicate dual functional roles of the hamstring musculature during suspension. With respect to TCN, production of flexor joint

torque and supination of the hindfoot to bring a the entire plantar foot in contact with the substrate are the roles designated by the myology of the muscle (Butcher et al., 2022). That said, maximum EMG activation of TCN occurs near the time of peak braking force during contact indicating a potential role in braking, in addition to its contribution to bodyweight support. Additionally, the role of TCN in vertical support should be supplemented by the m. extensor digitorum longus, which is a modified ankle flexor in *B. variegatus* with an insertion onto only metatarsal III (Butcher et al., 2022).

While m. rectus abdominus (RA) and BF have relatively short total activations that are nearly synchronous with one another, those of SRT, TCN, and FDP are active for over 50% of the stride, and the epaxial m. longissimus dorsi (LD) is essentially constantly activated. Specifically, the antagonistic actions of RA and LD likely aid in stiffening and stabilizing the long axis of the body during SW. Although, the MHC isoform fiber type expression is unknown for the hypaxial/epaxial musculature in sloths, prolonged co-activations of slow-contracting muscles through limb contact would allow for highly controlled movements to prevent unnecessary body swinging and reduce energetically wasteful oscillations of the substrate. In turn, maintaining a rigid body core should also contribute to behavioral stealth for evading predators.

EMG activation for selected extrinsic and intrinsic flexors of the hindlimb also suggest the possibility of antagonistic functions dependent on the percentage contact of their activation. For example, limb flexor muscles may initially activate at lower intensities to counteract propulsive extensor moments in early contact, but then maximally activate to provide braking during mid-to-late contact as indicated by limb loading patterns in *B. variegatus* (McKamy et al., in review). Limb flexor muscles in sloths (e.g., SRT and BF) can additionally activate at overall lower intensities to more strictly provide bodyweight support, especially the flexors in the distal limb with a greater expression of smaller, fast-contracting MHC-2A fibers, as proposed by both Gorvet et al. (2020) and Spainhower et al. (2021). Low intensity activations are again more typically indicative of muscles counteracting large moments, thereby controlling joint position and joint rotational velocity (Kingma et al., 2004). The moments applied by hip and knee extensors during early contact and swing must be counterbalanced by activation of the antagonistic flexors,

either to protect tendons from excess force (Kingma et al., 2004), or to ensure stability while distal limb segments rotate about the joint.

In addition, the bi-phasic activation patterns of flexor musculature at the hip (SRT, more frequently) and knee (BF, infrequently) that occur during swing are thought to stabilize the hip joint in a retracted position near the end of contact and control knee joint extension during second half of swing phase, respectively. However, the infrequency of swing activation by BF may be indicative the other knee flexors (e.g., m. bicep femoris femoral head) serving a stabilizing role during advancement of the hindlimb. At the hip joint, the timing of the second activation of SRT is also indicative of stretch-shortening muscle behavior. The SRT muscle belly likely undergoes lengthening contractions by activating late in contact when the hindlimb is near its maximally retracted position, but then shortens to flex the hip and protract the limb through swing as evidenced by its continued activation (see Fig. A1). This type of contractile function would both produce appreciable braking forces and allow for ‘quick’ limb recycling during the short swing phase. Furthermore, the metabolic energy expenditure expected from long duration, intense muscle activations of SRT may be offset, or economized, by its homogeneous expression of slow MHC-1 fibers in *B. variegatus* (Spainhower et al., 2021).

The digital flexor musculature is active during the majority of contact phase and also during swing phase. Reactivation of FDP at the end of contact phase and persistence through swing phase was unexpected. A second phase of muscle activation may be necessary to ensure that the claws of the pes are in the correct conformation for the next purchase of the substrate. Notably, the digits of the hindfoot appear relaxed upon lift-off, but are again flexed prior to substrate purchase (McKamy et al., personal observations). However, due to the following three factors: 1. large maximum force production capacity of FDP (Morgan et al., in review), 2. grip strength of the hindlimbs in *B. variegatus* approximating 100% of their bodyweight force (Young et al., in review), and 3. support from digital tendons with elevated safety factors of 4–10 (Mossor et al., 2020), the hindlimb FDP may weakly activate, or deactivate prior to the end of contact and still have enough passive force necessary to appreciably contribute to support of the bodyweight. Moreover, vertical support is distributed across multiple limbs during suspensory locomotion, including diagonal limb pairs, thereby reducing limb loading on any single limb at the end

of the contact interval. A similar distribution of bodyweight support between limbs in contact with the substrate is posited by Jouffroy and Stern (1990) to explain patterns of EMG activations in the forelimbs of the slow loris (*Nycticebus coucang*). Reduced activation intensity, or deactivation of FDP, additionally may be related to lower metabolic expenditures via reduced cost of active force production by the distal flexor musculature (Gorvet et al., 2020).

Last, the m. adductor longus (ADDL) has a similar activation pattern as FDP, albeit its initial EMG duration is shorter by ~20% of the contact interval. Activation of limb adductors were expected based on evidence of moderate medially-directed forces exerted by sloths into the substrate (Granatosky and Schmitt, 2007), presumably to align the limbs in the parasagittal plane and placing the body in a stable conformation below-branch. However, appreciable laterally-directed forces, accompanied by lateral rotations and abducted posture of the limbs were observed during SW in *B. variegatus* (McKamy et al., in review). This slightly non-parasagittal limb conformation may be caused by activation of abductor (e.g., GLM) and lateral rotator (e.g., BF) musculature and/or joint rotational effects of suspensory limb-loading due to gravity (Jouffroy and Stern, 1990). As such, multiple heads of the m. adductor likely are intensely activated to counterbalance the actions of abductor/lateral rotator muscles to stabilize the hip joint during both (early) contact and swing phases of SW. Moreover, the calculated mean EMG activation intensity ratio of ADDL is the highest of all muscle sampled (Fig. A2), and rivals those of the forelimb elbow flexors in *B. variegatus* (Gorvet et al., 2022). Again, intense activations of muscles that express entirely slow-contracting MHC-1 fibers such as ADDL (Spainhower et al., 2021) exemplifies an effective means of reducing the metabolic cost of contraction. This is especially critical for sloth hindlimb muscles with a primary role in stabilizing joints with economic, slow (large force) contractions occurring over the majority of the stride cycle. Taken together, EMG activation, limb loading, and MHC isoform fiber type data suggest how important the actions of limb adduction and elbow flexion are for limb joint stabilization against abductor and extensor moments, respectively, during suspension in three-toed sloths.

## New Insights into Suspensory Muscle Function

Suspensory locomotion gait patterns, as well as observed EMG activation timings and intensities in both the fore- and hindlimbs of *B. variegatus*, show demonstrable similarities with those of *N. coucang* (Jouffroy and Stern, 1990), the only other known mammal for which limb muscle EMG has been sampled during inverted quadrupedalism. First, the limb flexor musculature in *N. coucang* acts in bodyweight support as it does in *Bradypus*. These results were independently predicted in sloths through studies of MHC isoform fiber type and metabolism (Spainhower et al., 2018, 2021) and muscle architectural properties (Olson et al., 2018), and previously verified by EMG studies (Gorvet et al., 2020). Second, the limbs of *Nycticebus* are flexed and laterally rotated of during suspensory locomotion and posture, matching observations from limb loading analyses in *B. variegatus* (McKamy et al., in review). The elongate forelimbs of *Bradypus* (Intermembral Index, IMI = 1.71: Marshall et al., 2021b) are strongly flexed to elevate and maintain the body in a position parallel to the substrate. This common behavior across suspensory taxa was argued to place the elbow (and possibly the knee) joint at a joint angle to optimize mechanical advantage for bodyweight support by limb flexors (Fujiwara et al., 2011). Third, extensor activations that occurred late in contact (proximal, GLM) and during swing (distal, VL and LG/SOL) as observed in *Bradypus* and comparable with late extensor activations in *Nycticebus* during SW. Nevertheless, it is noted that longer contact activation durations are more typical of extensor musculature in the hindlimbs of *B. variegatus*. Fourth, antagonistic muscle activations occurred at the knee joint in *Nycticebus* between the VL and BF (same head, previously identified as m. flexor crurus lateralis: Jouffroy and Stern, 1990), thus establishing a precedent for co-activation of selected antagonistic muscle pairs to stabilize the knee joint during SW as they do for upright locomotion (Jouffroy and Stern, 1990). Similar patterns were demonstrated between VL and BF in *Bradypus*, although EMG onset of all muscle sampled herein occurred relatively early in the contact interval and only a second (bi-phasic) activation of GLM occurred late in the contact when no other extensors (except for LD) were concurrently active.

While similarities of EMG activations help establish convergent patterns among slow-moving suspensory mammals that share numerous ecological, physiological, and behavioral traits, the observable differences in limb muscle function between sloths and

slow lorises provide novel insight into the diversity of locomotor features among suspensory taxa. For example, in *Nycticebus* the m. semitendinosus displayed a delayed activation following the footfall, whereas m. flexor cruris lateralis (BF in this study) was active upon touchdown. In *Bradypus*, however, delayed EMG onset is observed in both SRT (hip/knee flexor) and BF (hip extensor/knee flexor), which likely overlaps with braking force applied by the hindlimbs of sloths later in the contact (contribution to propulsion by the hindlimbs occurs immediately after contact), as opposed to the hindlimb extensors of *Nycticebus* generating propulsion during late contact phase (Jouffroy and Stern, 1990). Another important and related distinction between these two taxa is that *Nycticebus* (like other suspensory primates) may be utilizing pendular mechanics during SW involving some amount of forward swinging through the first half of contact (Jouffroy and Stern, 1990), whereas limb loading (McKamy et al., in review) and muscle EMG activation data (Gorvet et al., 2020; this study) for *B. variegatus* convincingly verify that suspensory locomotion in sloths is powered solely by muscle work as predicted by modeling data of Nyakatura and Andrada (2013). Moreover, whereas a *B. variegatus* maintains hindlimb-biased support during SW, *Choloepus* shows equally bodyweight support between the fore- and hindlimbs, and thus no shifting (or horizontal levering: Granatosky et al., 2018) of support distribution between limb pairs. The latter being further indicative of no pendulum-like swinging mechanics in sloths.

Finally, the differences in muscle EMG activation patterns described may be indicative of salient differences in locomotor mechanics between arboreal primates and sloths which might be driven by morphological and behavioral constraints, at least in tree sloths. Perhaps the most marked difference between *Bradypus* and *Nycticebus* (and perhaps all suspensory primates) is that the forelimb flexors in sloths produce primary propulsion, whereas the hindlimbs act as the main braking limbs by activation of both flexors (e.g., SRT, primary) and extensors (e.g., VL, secondary). In *Nycticebus*, the main role of the hindlimb extensor muscles such as VL is indicated to be propulsion, though fore- and hindlimbs can each act as propulsive appendages during SW (Jouffroy and Stern, 1990); propulsion from the hindlimb extensors occurs late in contact, opposite of the pattern observed in *Bradypus*. Based on average activation durations, the GLM is the only extensor muscle in *B. variegatus* that could actively extend the hip to provide propulsion late in the contact at a

point when the hindlimb nearly fully retracted. Greater hindlimb pushing versus less forelimb pulling in *Nycticebus* is reflective of a shift to forelimb-biased weight support in primates during inverted quadrupedalism (Granatosky and Schmitt, 2019). Notably, this feature is not observed in tree sloths and the forelimb must provide propulsion in addition to vertical support. Thus, the collective observations on muscle activations in *Bradypus* and limb loading in both genera of tree sloths elucidate fundamental differences from the primate condition (Jouffroy and Stern, 1990; Granatosky and Schmitt, 2017; Granatosky, 2018c) and represent an alternative, entirely muscular driven mechanism by which suspensory locomotor success is achieved.

### **Concluding Remarks and Future Directions**

The inverse orientation of sloth locomotion necessitates modifications of limb morphology and the roles of limb musculature. Specifically, functional roles of the flexor and extensor muscles are segregated: the hindlimb flexor musculature generally activates intensely during mid-to-late contact phase to produce braking forces in addition to providing vertical support to ensure stable suspensory locomotion, whereas extensor musculature activates most intensely early in contact when propulsive forces predominate, before transitioning to a less active state to counteract flexor torques late in the contact. Extensor musculature also activates in tandem to either control protraction of the hindlimb or actively extend the knee and ankle joints during swing phase. Limb adductor musculature activates during swing and early contact most likely to counteracting the abducted position of the limb, thus ensuring a stability below-branch. In sum, these EMG activation patterns observed for the hindlimb of *B. variegatus* provide support for the hypothesis of co-activation of fore- and hindlimb flexors as the mechanism to control horizontal velocity of the center of mass in sloths. The SRT (and m. iliopsoas) appear to be the hindlimb muscles responsible for providing strong braking forces during suspensory locomotion, although prolonged activations from hypaxial/epaxial muscles likely enhance body stability and control.

Future studies are required to conduct wavelet analyses and identify motor unit recruitment patterns in *Bradypus* hindlimb musculature during suspensory locomotion. These analyses will elucidate the recruitment of fast (high frequency) and slow, forceful motor units (low frequency) within specific muscles and muscle groups. Additionally, force and EMG data for suspensory hanging and vertical climbing will be analyzed to



further evaluate the roles of hindlimb musculature during these behaviors, specifically burst durations, EMG intensities, and timings of peak force.

**Table A1.** Morphometric data for animals and number of strides and bursts analyzed during suspensory walking.

<b>Sloth</b>	<b>Sex</b>	<b>Limb</b>	<b>Body Mass (kg)</b>	<b><i>N</i> Strides</b>	<b><i>N</i> Bursts</b>
BV1	M	R	3.4	8	35
BV2	M	R	4.0	17	81
BV3	M	R	4.2	4	19
BV4	F	R	3.9	5	12
BV5	M	R	3.7	3	18
<b>mean±s.d.;</b>			<b>3.84±0.3</b>	<b>37</b>	<b>165</b>
<b>totals</b>					

*N*= number

In bold are either pooled mean±s.d. or total counts.

**Table A2.** Stride parameters for suspensory walking in *B. variegatus*.

<b>Sloth</b>	<b>Contact Duration (s)</b>	<b>Stride Duration (s)</b>	<b>Duty factor (ratio)</b>	<b>Velocity (ms<sup>-1</sup>)</b>
BV1	4.07±0.98	5.56±1.29	0.74±0.14	0.08±0.01
BV2	4.24±2.74	5.92±3.70	0.72±0.12	0.11±0.04
BV3	10.7±1.56	14.4±1.39	0.75±0.14	0.04±0.02
BV4	3.59±0.57	5.06±0.19	0.71±0.10	0.09±0.02
BV5	6.74±1.33	9.46±1.16	0.71±0.07	0.07±0.01
<b>mean±s.d.</b>	<b>4.95±2.97</b>	<b>6.84±3.88</b>	<b>0.74±0.11</b>	<b>0.09±0.04</b>

In bold are pooled means±s.d.

**Table A3.** Individuals, muscles, and functional behaviors for which EMG was recorded and analyzed.

<b>Sloth</b>	<b>SRT</b>	<b>GLM</b>	<b>ADDL</b>	<b>BF</b>	<b>VL</b>	<b>TCN</b>	<b>LG/SOL</b>	<b>FDP</b>	<b>LD</b>	<b>RA</b>
BV1	X	X	X	X	--	--	X	X		
BV2	X	X	X	X	X	X	X	X	X	X
BV3	--	X	†	X	X	†	†	†		
BV4	--	X	--	X	X	X	X	X		
BV5	X	X	†	X	X	†	†	†		

†EMG data to be analyzed in future.

Muscle abbreviations: SRT, sartorius; GLM, gluteus medius; ADDL, adductor longus; BF, biceps femoris; VL, vastus lateralis; TCN, tibialis cranialis; LG/SOL, lateral gastrocnemius/soleus; FDP, flexor digitorum profundus; LD, longissimus dorsi; RA, rectus abdominus.

**Table A4.** Temporal variables of EMG activation of hindlimb muscles in *B. variegatus*.

	SRT	GLM	ADDL	BF	VL	TCN	LG/SOL	FDP
<b>Suspensory Walking</b>								
EMG Onset 1 (%)	8.2±20.4	1.1±3.2	1.3±3.0	6.2±10.0	11.0±25.1	0.8±2.4	1.0±2.7	0.0±0.0
EMG Offset 1 (%)	41.9±28.3	41.6±22.1	31.3±18.9	45.6±19.7	52.1±27.1	53.2±6.3	41.7±11.1	49.3±19.6
EMG Burst Duration 1 (%Cycle)	33.7±18.4	40.4±21.4	30.0±19.0	39.5±13.8	41.1±21.3	52.4±7.0	40.7±11.9	49.3±19.6
EMG Onset 2 (%)	59.6±21.4	†61.5±22.3	†69.1±18.7	72.8±19.2	†75.2±10.7	93.3±2.9	†80.3±16.0	73.7±18.1
EMG Offset 2 (%)	91.2±15.3	96.8±10.1	98.5±2.9	93.3±13.3	100.0±0.0	98.0±4.0	98.7±2.4	98.7±3.8
EMG Burst Duration 2 (%Cycle)	21.5±12.0	35.3±19.5	29.5±19.2	20.6±13.8	24.8±10.7	4.8±3.9	18.4±14.2	25.3±17.1
Total EMG Activation (%Cycle)*	58.2±24.1	71.5±19.9	53.6±20.7	43.8±9.3	56.2±20.7	54.8±6.3	51.4±11.5	69.9±16.7

Values are pooled means of all data per EMG burst.

\*Total activation duration across all bursts when muscles showed multiple bursts per stride (most typical for SRT, GLM, ADDL, VL and LG/SOL).

Muscle abbreviations are the same as those in Table A3.

†Muscles that activate during swing phase and are considered muscles with true contact and swing activations.

**Table A5.** Means of EMG intensity ratios for each individual and muscle analyzed.

<b>Sloth</b>	<b>SRT</b>	<b>GLM</b>	<b>ADDL</b>	<b>BF</b>	<b>VL</b>	<b>TCN</b>	<b>LG/SOL</b>	<b>FDP</b>	<b>LD</b>	<b>RA</b>
BV1	<b>0.73±0.17</b>	0.08±0.01	<b>0.79±0.22</b>	0.15±0.06	--	--	0.10±0.06	0.09±0.40	--	--
BV2	<b>0.78±0.17</b>	0.19±0.07	0.54±0.19	0.17±0.10	0.39±0.28	0.33±0.31	0.56±0.23	0.53±0.31	0.58±0.32	0.38±0.36
BV3	--	0.18±0.09	†	0.92±0.11	0.36±0.43	†	†	†	--	--
BV4	--	<b>0.65±0.54</b>	--	0.44±0.0	0.52±0.30	0.02±0.0	0.24±0.09	0.09±0.04	--	--
BV5	0.55±0.20	0.10±0.04	†	0.32±0.13	<b>0.67±0.08</b>	†	†	†	--	--

In bold are the largest mean±s.d. ratios (0.60–0.80).

Muscle abbreviations are the same as those in Table A3.

†Data to be analyzed in future study.

**Table A6.** Timing of peak EMG activations relative to timings of peak limb force.

	<b>SRT</b>	<b>GLM</b>	<b>ADDL</b>	<b>BF</b>	<b>VL</b>	<b>TCN</b>	<b>LG/SOL</b>	<b>FDP</b>	<b>LD</b>	<b>RA</b>
Peak EMG Intensity (% Contact)	57.6%	26.1%	22.7%	33.3%	21.9%	49.0%	23.0%	28.8%	36.2%	16.4%
Peak Propulsion (% difference)	41.2%	<b>5.1%</b>	<b>5.0%</b>	<b>7.5%</b>	<b>6.6%</b>	31.8%	<b>1.6%</b>	<b>5.1%</b>	<b>0.6%</b>	20.8%
Peak Braking (% Difference)	<b>2.7%</b>	40.1%	46.4%	35.7%	49.9%	<b>9.7%</b>	42.1%	32.3%	26.8%	47.5%
Peak Vertical (% Difference)	22.8%	12.0%	<b>7.0%</b>	<b>7.5%</b>	20.9%	21.1%	<b>6.1%</b>	<b>3.0%</b>	<b>8.8%</b>	28.5%

In bold are values <10%

Muscle abbreviations are the same as those in Table A3.

†Data to be analyzed in future study.

**Table A7.** Summary of typical limb phase muscle activations during the stride cycle.

<b>Muscle</b>	<b>Action</b>	<b>Activations</b>
SRT	Hip Flexion/Abduction	Contact*
GLM	Hip Extension/Abduction	Contact/Swing
ADDL	Limb Adduction	Contact/Swing
BF	Hip extension/Knee flexion	Contact
VL	Knee Extension	Contact/Swing
TCN	Ankle Flexion/Foot Supination	Contact
LG/SOL	Ankle Extension	Contact/Swing
FDP	Digital Flexion	Contact*
LD	Vertebral Extension	Contact/Swing
RA	Vertebral Flexion	Contact

Muscle abbreviations are the same as those in Table A3.

\*Multiple bursts were measured over the course of one stride (not exclusive contact or swing phase bursts).



**Figure A1. Mean EMG burst duration (% stride) for hindlimb muscles during suspensory walking in *B. variegatus*.** Burst duration is expressed as a percentage of the stride (0–100%), with horizontal bars representing averages for each muscle during a stride. Values are means±s.e.m. (error bars) across individuals ( $N=5$  individuals per muscle) and represent the most typical pattern of EMG activations (biphasic activity for several muscles). The dashed vertical line marks the end of limb contact (lift-off) at a mean(±s.d.) duty factor of  $0.74\pm 0.11$  for SW three-toed sloths. Muscle abbreviations: SRT, sartorius; GLM, gluteus medius; ADDL, adductor longus; BF, biceps femoris; VL, vastus lateralis; TCN, tibialis cranialis; LG/SOL, lateral gastrocnemius/soleus; FDP, flexor digitorum profundus; LD, longissimus dorsi; RA, rectus abdominus. Data in green for PS (m. pectoralis superficialis) are taken from Gorvet et al. (2020).

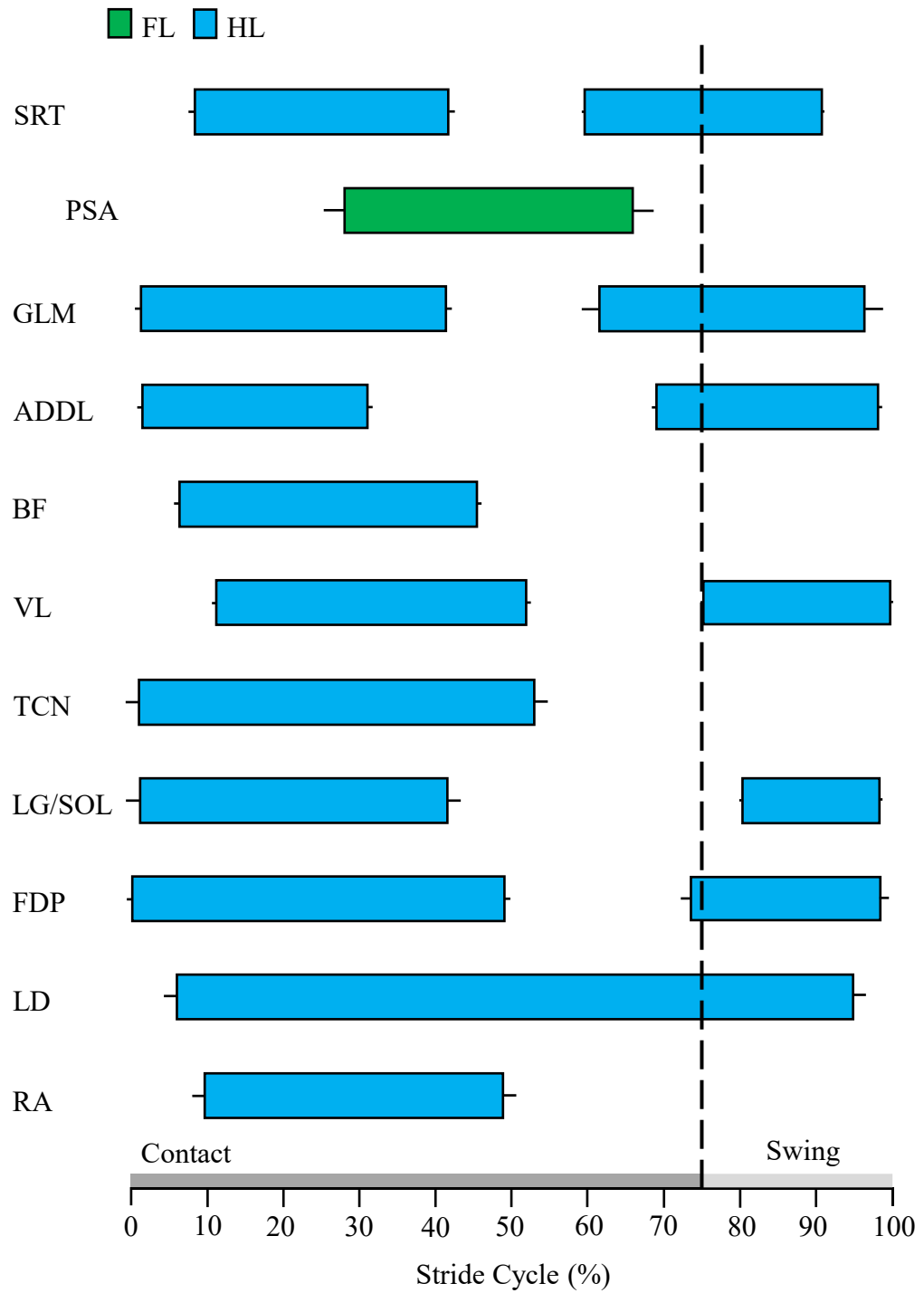
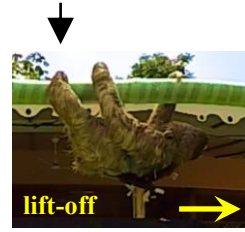


**Figure A2. Mean EMG intensity ratios for hindlimb muscles in *B. variegatus*.** Burst activity from major flexor/extensor muscles where mean EMG intensity was normalized to the single maximum EMG intensity recorded for each muscle during suspensory walking (SW). EMG intensity is expressed as ratios (0–1.0: Gillis and Biewener, 2001), with vertical bars representing means $\pm$ s.e.m. for each muscle across all individuals ( $N=5$ ) during contact of the right forelimb. Ratios near or equal to 1.0 indicate maximum activation observed during SW.

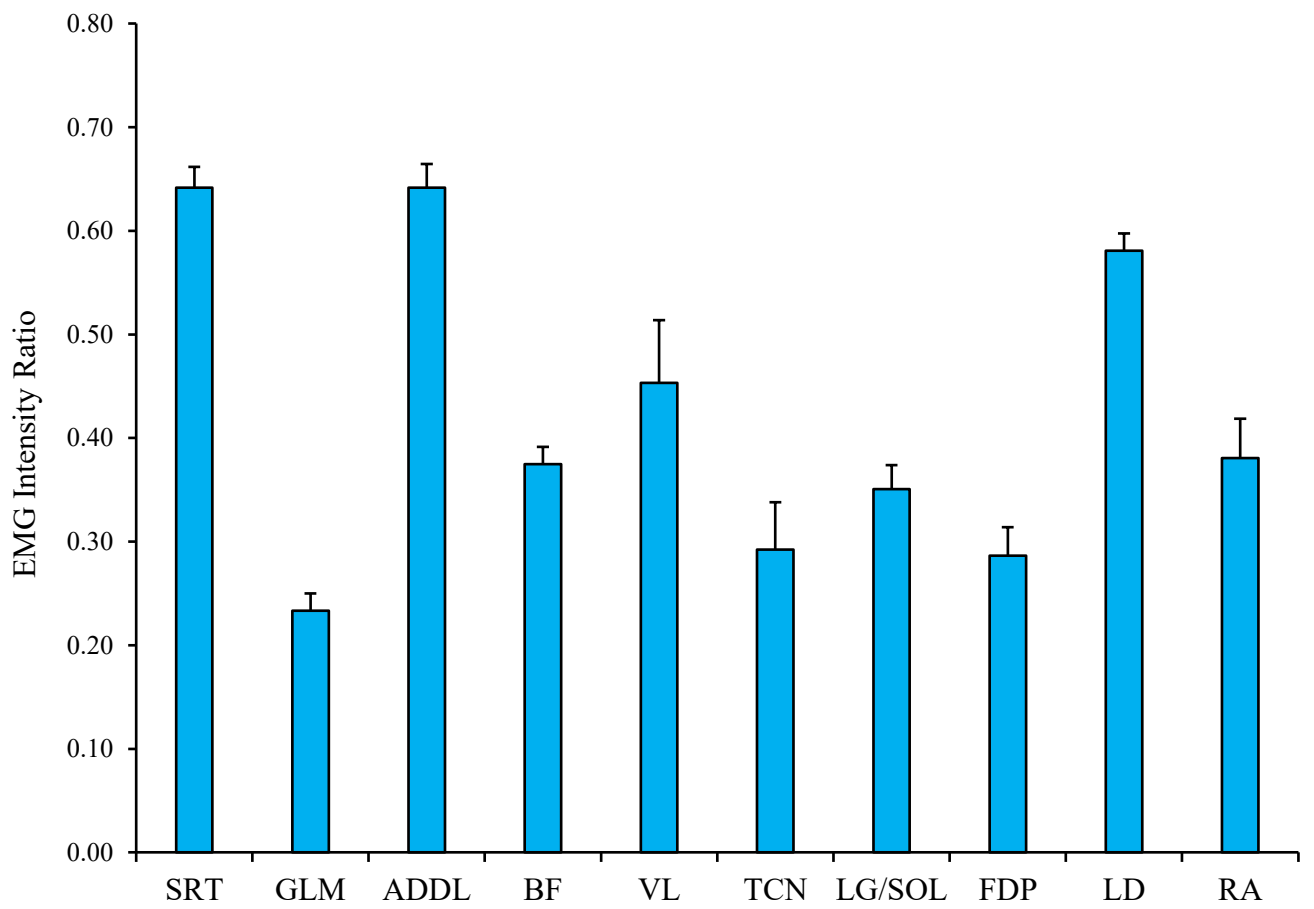
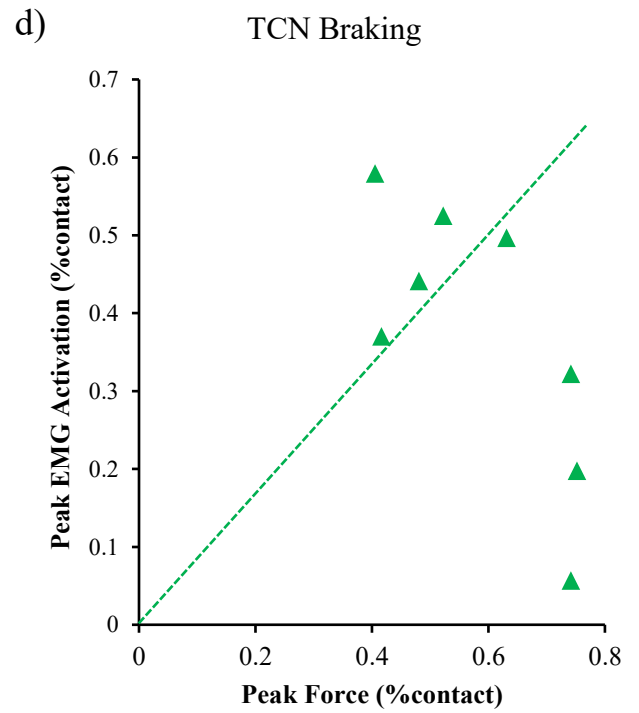
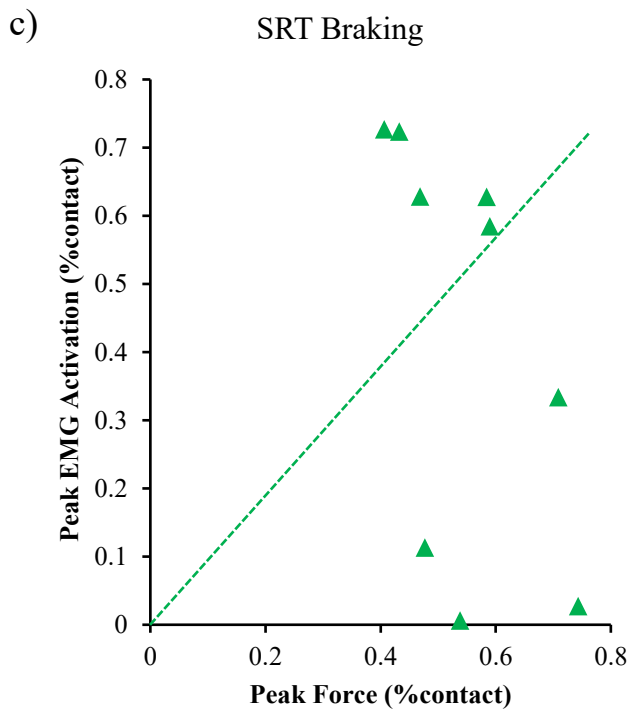
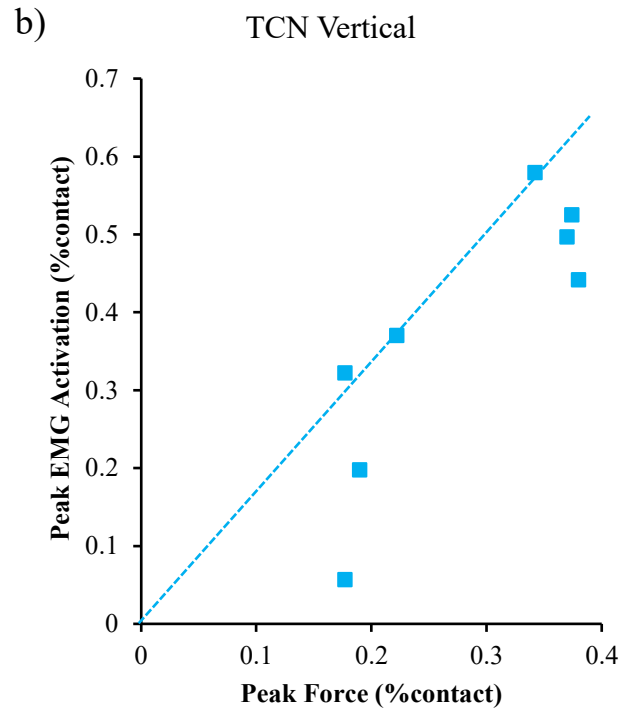
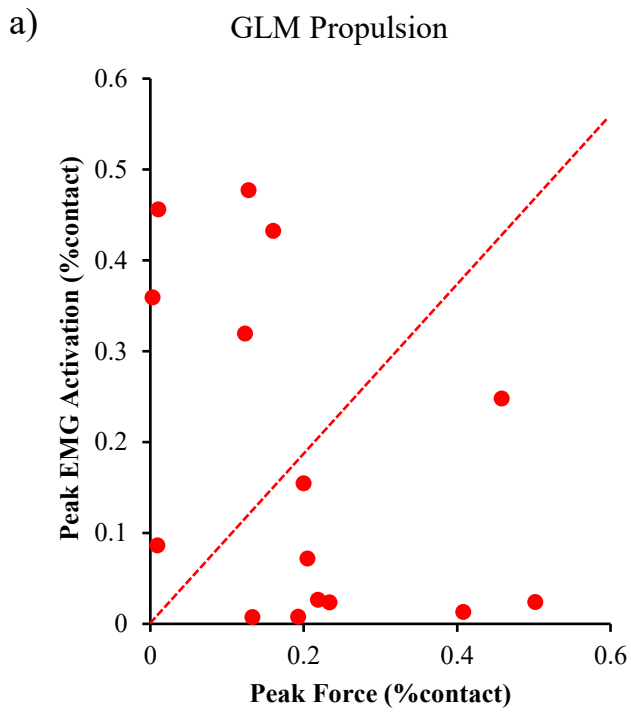


**Figure A3. Bi-plots of timing between peaks of muscle activation and limb loading during suspensory walking in *B. variegatus*.** **a**, bi-plot showing peaks of propulsive force and muscle activations for GLM with the relationship:  $y = -0.5199x + 0.2839$ ,  $R^2 = 0.1921$  (red circles and line); **b**, bi-plot showing peaks of vertical force and muscle activations for TCN with the relationship:  $y = 1.5572x - 0.0606$ ,  $R^2 = 0.7033$  (blue squares and line); **c**, bi-plot showing peaks of braking force and muscle activations for SRT and TCN (green triangles and lines) with the relationships:  $y = -1.3012x + 1.1344$ ,  $R^2 = 0.2604$  and  $y = -0.8693x + 0.8834$ ,  $R^2 = 0.5326$ , respectively. The dashed line represents a one-to-one relationship between the timing variables of the two muscles.



## APPENDIX II: LITERATURE REVIEW/PROPOSAL

### Evolution and Speciation

Xenarthra is a superorder of mammals endemic to the modern-day continent of South America. It consists of the orders Cingulata (Armadillos) and Pilosa (Sloths and Anteaters) (Gardner, 2008). The order Pilosa split nearly 40 million years ago into the suborders Folivora (Tree Sloths) and Verminlingua (Anteaters) (Gardner, 2005). The Folivora is further branched into two clades composed of the modern families of tree sloths, Megalonychidae (i.e., two-toed sloths) and Bradypodidae (i.e., three-toed sloths) (Gaudin, 2004). There are two extant species of two toed sloths (Genus: *Choloepus*): *Choloepus didactylus*, or the Linnaeus's two-toed sloth, and *Choloepus hoffmannii*, or Hoffmann's two-toed sloth, whereas there are four extant species of three-toed sloths (Genus: *Bradypus*). These include the pygmy three-toed sloth (*Bradypus pygmaeus*), the maned three-toed sloth (*Bradypus torquatus*), the pale-throated three-toed sloth (*Bradypus tridactylus*), and the brown-throated three-toed sloth (*Bradypus variegatus*).

Understanding of sloth phylogeny has recently been revised by a series of molecular studies, based on collagen and mitochondrial DNA sequences (Presslee et al., 2019). These investigations consistently place the relationship of extant two-toed sloths close to the extinct mylodonts and megalonychids. However, the three-toed sloths are placed within the Megatherioidea, the extinct lineage of giant ground sloths. Megatherioids (e.g., *Megatherium americanum*) once inhabited the Central America regions of North America where modern tree sloths are populous today. Moreover, the findings of these studies in addition to multiple morphological analyses in xenarthrans (see below) provide strong support for the hypothesis that arboreality arose separately in the two genera of modern tree sloths via the process of evolutionary convergence where the lineages split nearly 29MYA (Presslee et al., 2019). Therefore, *Choloepus* and *Bradypus* are very distant relatives and evolved their suspensory behaviors independently, making these unusual mammals one of the most remarkable known examples of convergent evolution (Nyakatura, 2012).

Xenarthrans share a number of distinct morphological traits: 1. The transverse processes of anterior caudal vertebrae are fused to the pelvis; 2. All species have xenarthrous or 'extra' zygapophyseal joints in their lumbar vertebrae in order to provide enhanced

stability to the trunk; 3. The scapula contains a well-developed secondary spine; and 4. Palatine vacuities (i.e., an incomplete septo-maxilla) may be present in the roof of the mouth. Additional features that xenarthrans may share include robust skeletons (e.g., armadillos and anteaters: Vizcaíno et al., 2008; Vizcaíno, 2009) and rudimentary teeth (e.g., armadillos and sloths), whereas the anteaters lack teeth in their jaws in favor of a specialized tongue for foraging on ants and termites (Gaudin and McDonald, 2008; Gaudin and Croft, 2015). Moreover, the incisors and true canines (except *Choloepus*) of extant sloths are absent (Pujos et al., 2012). Xenarthrans as a whole Superorder are also well known to have lower basal metabolism, lower body temperatures, and slower digestion rates in comparison to other placental mammals (Sunquist and Montgomery, 1973).

### **Ecology and Physiology**

Extant sloths are found in the neotropical rainforests of Central and South America (Britton, 1941). The species *C. hoffmanni* is found in two disjunct areas. The northern population ranges from Honduras and Nicaragua to western Venezuela, and the southern population ranges from north-central Peru through southwestern Brazil to central Bolivia (Hayssen, 2011). The species *B. variegatus* is distributed north in Nicaragua, Honduras, Ecuador, Colombia, Venezuela, and extends further south than *C. hoffmanni* into Brazil and northern Argentina. On average, *C. hoffmanni* has a larger home range of 1.97 hectares compared to the 1.59 hectares for *B. variegatus* (Montgomery and Sunquist, 1975). These distributions do overlap causing some sympatry primarily in the northern regions (e.g., Central America) of the geographic range, but species are disparately separated in southern regions (Hayssen, 2010).

Sloths are high canopy folivores whose diets are of low nutritional-energy value, consisting primarily of leaves (Montgomery, 1983). However, there are differences between the diets of both genera correlating with the native vegetation within regions of their home ranges. Notably, *Bradypus* is restricted to consumption of leaves from fifteen species of *Cecropia* trees (e.g., Gauramo), while *Choloepus* has a more diverse diet, including buds, flowers, fruits, and twig tips from 34 species of *Cecropia* trees (Meritt, 1985; Montgomery, 1983; Vaughn et al., 2007). Sloths descend their home trees an average of every 4-8 days to defecate (Voirin et al. 2013). However, sloths are most vulnerable



being on the forest floor. This is because a variety of carnivorous animals including margays, anacondas, ocelots, harpy eagles and jaguars all have a greater opportunity to prey on sloths during, but not limited to this period in time (Garla et al., 2001; Touchton et al., 2002). Jungle cats such as margays and ocelots are strong and capable of ascending trees to the level of the canopy, while hawks and harpy eagles (native to the neotropics) can detect a prey sloth from a position above the emergent tree line.

Sloths have little ability to evade predators and are essentially defenseless when on the forest floor. Interestingly, a contrast in tree descent is observed between *Choloepus* and *Bradypus*, and this pattern of movement is potentially due to predation avoidance strategies related to both their mobility and a stronger sense of sight or smell. For example, *B. variegatus* has a tail first descent, which may be due to its ability to rotate the head 180° (total range of motion: 270°, see below) in order to scan the surrounding area for any predators. The mobility of the head further relates to a reliance on sight in *Bradypus*. Sloths generally have poor eyesight, but it is suspected that three-toed sloth have better visual acuity than two-toed sloths (Mendel, 1985a). On the other hand, *C. hoffmanni* descends trees headfirst, and this could be related to its reliance on sense of smell for threat detection. *Choloepus* demonstrates some more overt threatening defense mechanisms than *Bradypus*, and these include forelimb claw slashing, hissing, and baring teeth. While *B. variegatus* may try to thwart an avian predator (e.g., harpy eagle) in the canopy with some slashing gestures, its main predatory defense strategy is stealth and/or camouflage (Enders 1935; Montgomery and Sunquist, 1978; Mendel, 1985a).

Slow, deliberate movement patterns are not only linked to predator avoidance, but also reflect an energy poor diet. Sloths have a low daily food intake an average of 17g dry weight per day, which is related to their low metabolic rates (Cliffe et al., 2015, 2018). For example, *B. variegatus* has the lowest recorded field metabolic rate ( $162 \text{ kJ/day} \cdot \text{kg}^{0.734}$ ) among non-hibernating mammals (Pauli et al., 2016). Sloths also have unusually low body temperatures for placental mammals, averaging only 32.7°C in *Bradypus* and 34.5°C in *Choloepus* (Pauli et al., 2016). In addition, adult *B. variegatus* has a smaller body mass range of 3.2–6.1 kg while that for *C. hoffmanni* is larger, averaging 7.0–9.0 kg (Genoways and Timm, 2003; Gillespie, 2003), and differences in body size can be correlated with differences in body temperature and thermoregulatory strategies of sloths. Thus, their

overall low body temperatures further indicates that they are heterothermic and must employ behavioral thermoregulation to conserve metabolic energy to cope with daily temperature fluctuations and diurnal versus nocturnal activity observed in different species of sloths (Cliffe et al., 2018). The species *B. variegatus*, for instance, will employ sun basking for warmth atop the canopies during the early morning hours, and they descend into the canopy's shade as the temperature rise throughout the day (Montgomery and Sunquist, 1978). In contrast, *C. hoffmanni* does not prefer the canopy and emergent levels of rainforest strata and mainly occupies the understory to canopy level in the trees and tends to be more active at night (see below) when temperatures are cooler. Having larger body mass means that two-toed sloths have a smaller surface area to volume ratio and can more easily retain body heat for internal warmth.

Last, different patterns of wakefulness are observed among species of sloths. *Bradypus* is diurnal meaning it is active both during day and night but spends 15–18 hours a day resting and/or sleeping (Sunquist and Montgomery, 1973). Additionally, *B. variegatus* is reported to have several modes of sleep/wake cycles including (a) “awake-exploring” where the animal is alert, moving the head, and blinking frequently, (b) “awake-alert” where the head is up and eyes open, blinking occasionally, (c) “awake-fixating” where the head is up and eyes open, but the animal shows a tonic immobility, (d) “behavioral sleep” where the animal sits in a reclined position (in a branch recess-elbow) with its head tucked or suspends (i.e., hangs) beneath a tree branch with its head down and eyes closed (Barratt, 1965). In contrast, *C. hoffmanni* is primarily nocturnal, being active ~11 hours during the night and sleeping beneath the canopies of trees during the day (Montgomery et al., 1973; Montgomery and Sunquist, 1975). The activity patterns of both genera demonstrate that sloths are not highly active animals, thereby reinforcing the supposition that their behavior, as well as their physiology, is correlated and modified in extreme ways to conserve metabolic energy (Cliffe et al., 2018).

### **Locomotion and Gait Patterns**

Sloths evolved a below-branch or anti-pronograde mode of locomotion making them one of a few taxa of mammals for which suspensory locomotion and posture is obligatory. Average velocity for suspensory walking in sloths was originally reported to be ~0.14 ms<sup>-1</sup>

(Britton and Atkinson, 1938). A recent study (Gorvet et al., 2020) found that *B. variegatus* moves slower ( $0.07 \text{ ms}^{-1}$ ) beneath a beam when allowed to freely choose their preferred speed, whereas velocities in *C. didactylus* have been reported to be considerably greater than average in studies using treadpoles for steady-state measurements (Nyakatura et al., 2010). Despite differences in absolute speeds, both species exhibit a lateral sequence diagonal-couplet (LSDC) gait (Cartmill et al., 2002; Usherwood and Davies, 2017) during suspensory walking but use a diagonal sequence gait with near diagonal couplets during vertical climbing. These patterns were most definitely determined by the work of Gorvet et al. (2020). Briefly, a diagonal-sequence gait is defined by consecutive footfalls (or grips onto a substrate) of contralateral fore- and hindlimb pairs (Muybridge, 1887; Hildebrand, 1985). A diagonal couplet is specifically a pattern of footfalls whereby contralateral pairs of feet (fore- and hindfeet) contact the substrate simultaneously (Hildebrand, 1985; Mendel, 1985a).

Diagonal-sequence gaits are most often employed by mammals (e.g., primates) that use pronograde (above branch) locomotion for stability on arboreal substrates. The diagonal pattern of footfalls prevents rolling off (via a large rolling torque) of branches that would otherwise occur by bearing the majority of weight on one side of the body as during a lateral sequence gait. Although sloths can perform both arboreal and terrestrial locomotion (akin to a crawl), they do not demonstrate a running gait during either mode of transport (Mendel, 1981a, 1985b). Moreover, whereas brachiating primates (e.g., gibbons and siamangs) use pendular mechanics via arm swinging to locomote at low metabolic costs (Bertram and Chang, 2001), such mechanisms are not available to sloths. In contrast, sloths must move in a manner that minimizes fluctuations of the dynamic forces exerted on the support (Nyakatura and Andrada, 2013) so as not to make the support unstable or oscillate thereby creating wasted effort when walking.

Another important distinction between pronograde versus anti-pronograde locomotion is that joint torques in upright quadrupeds reflect the need to counteract gravitational induced flexion of the limb (i.e., limb loading). Thus, the limb extensor muscles of pronograde arboreal mammals have an anti-gravity role to prevent limb collapse during weight bearing (Cohen and Gans, 1975; Jenkins and Weijstouch, 1979). However, since locomotion and posture in sloths is the inverse orientation, gravitational induced extensor

torques at the limb joints must be controlled by limb flexor muscles (Fujiwara et al., 2011). An anti-gravity role in the elbow of suspensory mammals has indeed been experimentally shown (see below) for brachiating primates and in lorises that use suspensory locomotion as well as slow, intermittent movement patterns (Jungers and Stern, 1980, 1981; Jouffroy and Stern, 1990). The slow and deliberate locomotion of sloths ( $0.07 \text{ ms}^{-1}$ : Gorvet et al., 2020) ( $0.02\text{--}0.47 \text{ ms}^{-1}$ : Nyakatura and Fischer, 2010) ( $0.04\text{--}0.19 \text{ ms}^{-1}$ : Granatosky et al., 2018) is emphasized when compared with higher speeds of agile primates that employ facultative suspensory locomotion, but primarily locomote above branch; including the grey mouse lemur ( $0.39\text{--}0.89 \text{ ms}^{-1}$ ) and squirrel monkey ( $0.39\text{--}1.00 \text{ ms}^{-1}$ ) (Schmitt, 2008), as well as the slow loris ( $0.73 \text{ ms}^{-1}$ : Schmitt and Lemelin, 2004).

### **Functional Morphology, Myology, and Muscle Physiology**

Sloths have notably reduced skeletal muscle mass. The skeletal muscle mass of sloths comprises only 23.6% of total body mass for *B. variegatus* and 26.2–27.4% for *C. hoffmanni* (Grand, 1978). For comparison, other arboreal mammals have an average skeletal muscle mass of 33% their body mass (Muchlinski et al., 2012). These data indicate that a reduction in muscle mass is representative of an adaptation for arboreal lifestyle. Other morphological features are somewhat unique (among mammals) to sloth form and include modifications to the neck and pectoral girdle as well as their feet. For example, *B. variegatus* notably has 8–9 cervical vertebrae, allowing for exaggerated rotation of the head up to  $180^\circ$  (in a cranial-caudal orientation), hence the ability to look forward while suspended below branch (Mendel, 1985a). *Choloepus*, on the other hand, has only 5–6 cervical vertebrae, which limits the rotation of the head/neck, and places more emphasis on hyperextension of the neck as the functional motion while in a suspensory posture. Whereas the unusual number of cervical vertebrae is a main example of the distinct morphology of sloths, it is also one of prominent differences between two-toed and three-toed forms. Additionally, *B. variegatus* has forelimbs that are longer than their hindlimbs and has a reduced tail. In contrast, *C. hoffmanni* has fore and hindlimbs that are equal length and it lacks a tail (Britton, 1941). The differences in limb length are evidence that further indicates ecological preferences among species. In this case, *C. hoffmanni* prefers a support that is parallel to the ground, and although *Choloepus* spends more time in suspension than

*Bradypus*, both genera independently evolved a suite of adaptations that allow for their arboreal-suspensorial lifestyle.

The structural requirement for suspension involves those of a tensile limb system. Sloths have modified pelvic and pectoral girdles with hip/shoulder joints that are able to support their limbs loaded in tension rather than in compression. In order for the pectoral girdle to efficiently rotate from a dorsal to more lateral position, the scapulae of both genera are reduced in size, and the thorax is reduced cranially and has a circular cross-section. In addition, sloths have a ligament of fibrous connective tissue that connects the clavicle to the sternum, which permits greater degrees of freedom for rotation at the sternoclavicular articulation (Nyakatura and Fischer, 2010). Evidence suggests that the greatest torque (or moment) occurs at the thoraco-scapular articulation and shoulder joint when the forelimb touches down during suspensory walking with the moment of nearly 1.0 N.m/kg. Therefore, the center-of-mass (CoM) does not accelerate, which allows the movement to be slow, controlled and the CoM is translated in a uniform manner (Nyakatura and Andrada, 2013). The forelimb flexor muscles of sloths must then provide support of their body weight at the digital/carpal, elbow and shoulder joints by some combination of active or passive means (via tensile loading) much like that observed in primates with suspensory habits (Granatosky et al., 2018). While tensile loading of distal flexor tendons or muscle-tendon units with adequate stiffness could be a major form of body weight support (Mendel 1981a, b; Mendel, 1985), activation of strong elbow flexors likely mitigates levels of limb loading (Granatosky et al., 2018; Gorvet et al., 2020), especially loading of the highly mobile shoulder joints in sloths. Overall, function of their tensile limb system (see below) is expected to reduce muscular recruitment (i.e., volume of active muscle) during postural suspension (Preuschoft and Demes, 1984; Gorvet et al., 2020).

All sloths have highly modified feet. Regardless of the number of digits remaining on their forefeet, all sloths have three digits on their hindfeet. The species *B. variegatus* has three functional digits on the forefeet that are partially fused – digits II, III, and IV. In general, *Bradypus* (sp.) has vestigial metacarpals I and V, which remain as splint-like bone appendages. Three-toed sloths also have long claws at the end of their curved distal phalanges and have volar pads that are covered with fur. Unlike *Bradypus*, *Choloepus* (spp.) has two functional digits on their forefeet – digits II and III. Metacarpals I and IV

are vestigial and splint-like in the two-toed sloth condition, with digit V being absent. The species *C. hoffmanni* also has long, recurved claws on their digits, but their volar pads are hairless and have thick, leathery skin. The claws of both genera act as hook-like projections which help them to perform their suspensory locomotion (Mendel, 1981a, b). Moreover, depending on the diameter of the arboreal substrate, *Choloepus* may grip the support mainly with its claws versus *Bradypus* that places a large area of its feet on the substrate. *Bradypus* may also prefer, or cope, with larger diameter supports better than *Choloepus* (Mendel 1981a, b; Mendel, 1985a; Granatosky et al., 2018; Gorvet et al., 2020).

Another source of passive aid to the suspensory apparatus in sloths is their tendons. Tendons in some terrestrial mammals are known to function as stiff elastic elements for joint position control and/or as efficient biological springs during locomotion to conserve energy (Alexander, 1984). For example, in horses and other ungulates, muscle-tendon units (both the internal and external tendon) are extremely modified to undergo large strain by having long, thin tendons capable of large energy elastic strain storage and recovery (Biewener, 1998). MTU tensile strain may also occur with little-to-no muscle activation, thus the resisting force is passive tension during postural behavior (Lieber, 2002; Hodson-Tole et al., 2016.) Notably, horses have a weight-bearing suspensory apparatus (Hildebrand, 1960) which allows them to remain standing for long periods of time without fatigue (Hermanson and Cobb, 1992). These specializations in distal MTU structure-function reduce metabolic energy expenditure that would otherwise need to be supplied by muscle work (Biewener, 1998). Sloth tendons tradeoff between stiffness and compliance to passively support body weight while still supplying precise joint position control. (Mossor et al., 2020) showed that sloth FDP tendons fall short on strength and elasticity and can be grouped completely opposite of specialized cursorial or saltatorial tendons. However, these tendons are not proposed to work as a biological spring as sloths cannot run or gallop; they are thought of as a suspensory apparatus for energy conservation (Mossor et al., 2020).

#### **a. Hindlimb Musculature**

The musculature of the pelvic (hind) limbs purportedly acts to keep hip (acetabulofemoral) joints stabilized in an extended position and the claws flexed. The actions of the respective functional muscle groups (hip extensor/knee flexors and digital flexors) is *a priori* based

on the locations of their origin and insertions reported in numerous historical volumes (Humphry, 1870; Macalister, 1869; Mackintosh 1875a, b; Windle and Parsons, 1899; Wislocki, 1928). This sub-section is not intended to be a thorough review of hindlimb myology but instead a summary of muscles and major functional muscle groups. However, where appropriate, individual muscles will be highlighted and detailed.

Hindlimb muscles originating from the hip region should act to protract and retract the femur (or limb) at the hip joint as well as stabilize the hip joint during suspensory locomotion and posture. The cranial region of the hip joint contains the *m. iliacus*, *m. psoas*, *m. sartorius* and *m. tensor fascia latae* (craniolateral) that can act as hip joint flexors. Along the caudal region of the hip joint the *m. gluteus superficialis* (caudolateral) should act to both flex the hip and abduct the hindlimb, whereas *mm. gluteus medius* and *gluteus profundus* (often inseparable) are positioned to act as the main hip extensors, and secondarily as hindlimb abductors. The *m. sartorius* is a bi-articular muscle that is expected to not only flex and the abduct femur at the hip joint, but also laterally rotate the thigh and flex the leg at the knee joint. There are five muscles with the potential to adduct the femur at the hip joint, including *m. pectineus*, *m. adductor brevis*, *m. adductor longus*, *m. adductor magnus*, and *m. gracilis*.

Along the cranial and caudal regions of the thigh are located the knee extensors and hip extensor/knee flexors, with the latter collectively called the ‘hamstring’ muscles. The quadriceps femoris is composed of four muscle heads: *m. rectus femoris*, *m. vastus intermedius*, *m. vastus lateralis*, and *m. vastus medialis*. With the exception of *m. rectus femoris* which is bi-articular and has a small muscle moment arm at the hip joint, the knee extensors originate from the proximal and/or mid-shaft region of the femur and all heads insert on the tibial tuberosity via the quadriceps tendon containing the patella. The *mm. semimembranosus*, *semitendinosus*, and *biceps femoris* along the caudal thigh are all bi-articular and act in hip extension and knee flexion. Additionally, the two medial muscles *m. semimembranosus* and *m. semitendinosus* may internally rotate the leg when the knee is flexed. However, the larger of the two heads of *m. biceps femoris* (or *m. flexor crurus longus*) that crosses the hip and knee joints to insert far distal onto the crural fascia may act to laterally rotate the hip joint and aid in adduction of the femur.

The muscles of the leg act to flex/extend the leg at the knee or to flex/extend the hindfoot at the ankle, in addition to resisting gravitational extension of both the knee and ankle joints (i.e., anti-gravity muscles). The bi-articular m. gastrocnemius (medial and lateral heads) are the most superficial muscle bellies along the caudal aspect of the leg and their actions are flexion of the leg at the knee joint and extension of the hindfoot at the ankle joint via the calcaneal tendon. The small m. soleus is deep to and inserts in common with the m. gastrocnemius onto the calcaneal tuberosity but acts in only ankle extension. The m. flexor digitorum superficialis is also a bi-articular muscle that inserts onto a robust common flexor tendon that crosses the ankle joint and then divides into three tendon slips, one for insertion onto the terminal phalanx (base of claw) of each digit. The common flexor tendon arises from the distal bellies of well-developed m. flexor digitorum profundus, which is the deepest muscle of the caudal leg. It is possible that M. flexor digitorum profundus facilitates ankle extension, whereas only the belly m. flexor superficialis can act to flex the knee. Collectively, the m. flexor digitorum profundus is a muscle complex with 4 heads total that provide for strong flexion of the metacarpophalangeal and interphalangeal joints to conform the feet into a hook-like appendage (Nyakatura and Andrada, 2013).

Ankle flexion is the main role of the m. tibialis cranialis (tibial and fibular heads). Ankle flexors also include m. fibularis longus and m. fibularis quartus, while the m. extensor digitorum longus likely facilitates flexion of the ankle joint. Muscles that perform ankle flexion/extension may also act the pronators and supinators of the hindfoot. For example, mm. fibularis longus and fibularis quartus, as well as m. fibularis brevis, and all act as pronators of the hindfoot, whereas the supinators of the hindfoot include m. tibialis cranialis and m. tibialis caudalis. The m. tibialis caudalis also likely acts to extend the ankle joint. Lastly, the intrinsic foot musculature is overall reduced due to the loss of digits. The main belly of the plantar aspect of the foot is m. quadratus plantae and it is a flexor of digits II-IV. On the dorsal side of the foot is m. extensor digitorum brevis that facilitates extension of digits II-IV. The mm. interossei are well-developed and due to the fused state of the metatarsals, they most likely act to flex the metacarpophalangeal joints and proximal interphalangeal joints (Mendel, 1985b) to a lesser extent abduct the digits. However, the mm. lumbricals are reduced in *B. variagatus*, where just one (Mendel, 1981) or two



(Humphry, 1869; Windle and Parsons, 1899) bellies were observed, while as many as 4 bellies were described in *C. hoffmanni* (Mackintosh, 1875b).

### **b. Muscle Fiber Architecture**

Muscle architecture is defined as the orientation of muscle fibers relative to the axis of force production (Lieber, 2002). There are several types of fiber architecture observed ranging from parallel-fibered to pennate-fibered muscles. Parallel-fibered muscles have long fascicles that may approximate the length of the muscle belly. Typically, the fascicles are orientated at low angles (0–15°) to the force axis of the muscle. As velocity of contraction is proportional to fascicle length, parallel-fibered muscles have the advantage of shortening excursion for work and power generation, but this mechanical output comes with the trade-off of reduced force production. Pennate-fibered muscles have short fascicles oriented at pennation angles of 15–45° relative to the force axis of the muscle. There are four types of pennation observed in mammal skeletal muscles: unipennate, bipennate, multipennate, and rarely circumpennate (Lieber, 2002). A unipennate muscle has fibers that are arranged obliquely and from the tendon of origin to the tendon of insertion (Musculino, 2011). A bipennate muscle has fibers arranged obliquely on both sides of a central tendon of insertion in a manner reminiscent of a bird feather (Lieber, 2002). Multipennate muscles have a central tendon that branches into two or more tendinous inscriptions that run longitudinally throughout the muscle belly with short muscle fibers arranged obliquely in between each division (Musculino, 2011). In circumpennate muscles, fibers are arranged radially and connected to all sides of the central tendon.

In general, as the degree of pennation (angle) increases, muscle fibers must become shorter, and this strategy allows for a maximum number of muscle fibers arranged in parallel per volume of muscle. This mechanical design is advantageous because it allows muscles, in particular those found distal in animal limbs, to be small, but strong, while sacrificing at most only 13% of translational force based on fiber pennation angle (Lieber, 2002). However, any loss of translational force is offset by enhanced physiological cross-sectional area (PCSA), which is proportional to isometric force production (Alexander, 1984). Pennate-fibered muscles typically produce large force economically by minimizing

shortening of their muscle fibers (Biewener and Roberts, 2000). Thus, the disadvantage of pennation is lower work and power performance compared with parallel-fibered muscles.

### **c. Muscle Fiber Type**

Muscle force production also depends on intrinsic fiber contractile properties, which are, in turn, dependent on myosin heavy chain (MHC) expression. Therefore, specialization of muscle fibers is reflective of their expression of MHC isoforms. And although the distribution of muscle fiber types and/or motor units is directed by the size and conduction velocity of their alpha motor neurons (see below), the contractile tasks routinely performed by a muscle or muscle group has the ability to modify the muscle fiber contractile and metabolic properties (Kohn, 2014; Thomas et al., 2017; Spainhower et al., 2018). This phenomenon is understood as functional adaptation. Indeed, Schiaffino and Reggiani (1996) found that functional behaviors are one of the main determining factors of the intrinsic properties of muscle fiber types.

Mammals may express four myosin fiber types in their skeletal muscles: MHC-1, 2A, 2X, and 2B (Bottinelli, 2001). Slow MHC-1 fibers are historically considered to be oxidative (aerobic), have low power, and are the slowest-contracting adult muscle fibers (Kohn et al., 2007, 2011). MHC-2A fibers are faster-contracting and produce higher and power than the slow MHC-1 isoform. Fast MHC-2A fibers can be highly oxidative despite having some glycolytic (anaerobic) enzymatic properties (Schiaffino and Reggiani, 1996) and have the lowest contractile velocity of the fast-contracting isoforms. When the MHC-2A isoform is expressed in mammalian muscle fibers, larger cross-sectional area (CSA) than MHC-1 fibers has been commonly observed (Kohn et al., 2007), hence the fast fiber types have the capacity to produce larger isometric force than slow MHC-1 fibers. However, findings in sloths (Spainhower et al., 2018) and primates (Sickles and Pinkstaff, 1981a) indicate that the predominant myosin fiber type expressed is often the largest, and thus produces the largest magnitude of force regardless of MHC isoform expression. MHC-2X fibers contract faster than MHC-2A isoform fibers and data from domesticated mammals show that they produce a greater force and have higher power output than MHC-2A fibers (Kohn et al., 2007). These same studies indicate that fast MHC-2X fibers are moderately oxidative-glycolytic in their fiber type metabolism. Last, the MHC-2B isoform is the fastest contracting and generate the highest power of all myosin fiber types. Fast

MHC-2B fibers are historically shown to be the most glycolytic in their metabolism and have low fatigue resistance (Kohn et al., 2007). Large distributions of fast MHC-2B fibers are most typically expressed in limbs of rodents and lagomorphs (Schiaffino and Reggiani, 1996). Small mammals have a large surface area to volume ratio and must have muscles high intrinsic power to provide heat as major factor in their thermoregulatory strategy (Clarke and Rothery, 2007).

MHC fiber type and metabolic properties are available for sloths. An important study by Spainhower et al. (2018) found that both *C. hoffmanni* and *B. variegatus* only express slow MHC-1 and fast MHC-2A fibers in their forelimb musculature. Moreover, there is predominant expression of slow MHC-1 fibers in all muscle functional groups, although a slower-to-faster contracting change in fiber type distribution is observed along the length of the limbs. The distal forelimb musculature (e.g., carpal and digital flexors) are the only functional groups where average proportion of slow MHC-1 fibers is exceeded by expression of the fast MHC-2A isoform (Spainhower et al., 2018). In the hindlimbs of sloths, there is also a relative increase in fast MHC-2A fibers in the digital flexors of both species, but slow MHC-1 fibers retain the largest percentage expression in all muscles studied (Spainhower et al., 2021). For example, *C. hoffmanni* and *B. variegatus* express similar large proportions of slow MHC-1 fibers in their hip flexors suggesting that the functional role of joint stability (i.e., anti-gravity muscles) of this muscle group is common to both species (Spainhower et al., 2021). Slow-contracting muscles are important to controlling acceleration of the center of mass (CoM) (i.e., minimizing destabilization of the body), which is related to the slow, deliberate locomotion of sloths (Nyakatura and Andrada, 2013).

Sloth limbs and those of primates, which share ecological and behavioral preferences, are extraordinarily similar in their myosin fiber type composition. For example, the fore- and hindlimbs of the slow loris (*Nycticebus coucang*) have a similar expression of overall slow-contracting muscle fiber types (identified as Type I and Type IIA) (Sickles and Pinkstaff, 1981a, b). Two- and three-toed sloths, as well as *N. coucang*, also lack expression of the fast MHC-2X and -2B isoforms and these findings are notably suggestive of parallel evolution of slower contracting fiber phenotypes in mammalian taxa that exhibit obligatory suspensory behaviors or those that require clinging during vertical climbing.

Strong, slow-contracting muscle fibers may therefore be a functional requirement for suspensory habits. Sustained activations of numerous limb flexor muscles (see below) are expected to be necessary for the prolonged gripping/grasping behaviors in sloths and slow lorises.

### **Muscle Contraction**

Skeletal muscle is voluntary contractile tissue that performs mechanical work when recruited by the nervous system. Excitation-contraction coupling (ECC) is the process by which an electrical impulse (i.e., action potential: AP) is transduced into the mechanical output of force by skeletal muscles. Briefly, the process begins when muscle fibers compartmentalized within motor units are stimulated by motor neurons. A motor neuron and the set of muscle fibers that it innervates form a motor unit (MU: Hill et al., 2004). An excitatory AP is generated at the motor end plate (via the synaptic transmission of acetylcholine across the neuromuscular junction) of each fiber within a MU, which results in an all-or-none contraction of the muscle fibers, and ultimately produces gross muscle contraction (Gans, 1982). Muscle fibers produce muscle tension when they are activated to contract, which is the sum of twitch force produced by each muscle fiber composing a MU type (slow versus fast). Furthermore, because muscle activation/contraction is an all-or-none response, each fiber in a MU is activated at the same threshold of depolarization and produces the same magnitude of force.

There are two different methods that the nervous system uses to control muscle tension: neuromuscular recruitment and temporal summation. First, neuromuscular recruitment is an increase in the number and size of the MUs that are activated (Size Principle: Henneman, 1957). The primary strategy of controlling the amount of tension produced by skeletal muscles is continuous recruitment of MUs. This means that the tension developed by the entire muscle increases as larger or a greater quantity of MUs are recruited. Varying the number of active MUs as well as the timing of their activation results in smooth, controlled movements (Hill et al., 2004). The size of the MUs differs by the amount of muscle fibers innervated, where MUs of a smaller size tend to contain slow-contracting MHC isoform fibers, while larger MUs are frequently composed of fast-contracting MHC fiber types (McPhedran et al., 1965a, b). Contractile velocity of muscle fibers is also matched with the

AP conduction velocity of their motor neurons, thus slow muscle fibers have smaller motor neurons with slow conduction velocities while the inverse is true for fast-contracting muscle fibers (Brooks and Faulkner, 1988). This feature is integral to Size Principle by indicating that smaller, slower-contracting MUs are recruited first, followed by activation of increasingly larger, faster-contracting MUs for increased mechanical work and power (Henneman et al., 1965 a, b). Henneman and Olson (1965) suggested that this order of recruitment guarantees that the slowest, most fatigue resistant MUs are recruited first, and the faster, more fatigable MUs are recruited as needed. The pattern of recruitment observed saves animals metabolic energy by matching the mechanical work and power demands to a given behavior (Rome et al., 1990). Second, muscle force can be modulated via temporal summation of the twitch response that can result in maximal stimulation and tension of muscle fibers known as tetanus or tetanic force. In essence, the force of individual twitches sum with increased frequency of stimulation by the nervous system and muscle tension increases progressively without relaxation between twitch responses. Total tension produced per MU then changes with the rate of APs conducted to the muscle via the motor neuron (Hill et al., 2004).

There are three types of contractions by which whole muscles produce force: lengthening, isometric, and shortening contractions. Lengthening (eccentric) contractions produce the greatest force while muscles perform negative mechanical work, meaning they absorb power as external work is done to elongate muscle fibers, and therefore hydrolyze the least amount of ATP. Isometric contractions are contractions of the same length. They produce a large amount of force while also performing no mechanical work and consequently, consume a moderate amount of ATP per unit force. Shortening (concentric) contractions produce the least amount of force, perform both mechanical work and power, and therefore hydrolyze the greatest amount of ATP per unit force (Abott et al., 1952; Beltman et al., 2004).

The nervous system has to recruit a reasonable number and size of MUs to meet the locomotor demands for force and power for each type of contraction. Habits involving high mechanical work/power require an increased volume of active muscle to be recruited (Roberts et al., 1997). Application of the force-velocity relationship of muscles during movement is the easiest way to understand this mechanical and metabolic requirement.

Animals must always maintain enough force to support their body weight as well as enough force to perform behaviors that require high power. Shortening of the muscle limits the force production of a muscle due to the tradeoff between isometric force and velocity of contraction. Therefore, a large volume of active muscle must be recruited in order to maintain support when animals demand work and power performance from their limb muscles (e.g., uphill running). In contrast, limb muscles may produce large force and perform little-to-no mechanical work via isometric, or lengthening contractions, and this type of muscle activation results in substantial metabolic energy savings (Butcher et al., 2009). This type of contractile behavior is more typical of distal limb muscle-tendon units (MTU) during level running (Biewener and Roberts, 2000; Biewener et al., 2004).

#### **a. EMG activation patterns**

Electromyography (EMG) is a well-established technique used to measure muscle activation and assess recruitment patterns of MUs in muscles. EMG signals recorded from live animals to study patterns of muscle activity is critical to understanding muscle function (Wakeling et al., 2001; Wakeling et al., 2012). The most accurate method of EMG is done by percutaneous implantation of fine-wire electrodes into limb muscles of live animals (DeLuca, 1997). Data about the relative timing and magnitude of MU recruitment patterns is communicated by onset-offset timing of the EMG burst and intensity of muscle activation (Gans, 1992). In particular, the intensity (i.e., amplitude or size) of an EMG burst infers the relative volume of muscle recruited, which reflects the metabolic energy cost of producing force (Roberts et al., 1997). Onset-offset time is used to determine EMG burst duration and these patterns of muscle activation timing during the gait cycle are important for understanding the role a muscle plays in locomotion. For example, whether a joint can be flexed or extended indicates if a muscle has a role in braking or propulsion during locomotion versus an anti-gravity role for support. During movement, low levels of muscle activation observed with tensile loading of tendinous and/or elastic elements of the MTU can serve as an economical means to maintain limb posture, and this mechanism may be equally important for mammals the use inverted behaviors, such as sloths (Nyakatura et al., 2010), as it is for upright mammals (e.g., ungulates) specialized for running (or cursorial habit).

Evaluation of neuromuscular control mechanisms has been greatly advanced by use of wavelet analysis to evaluate slow and fast MU recruitment patterns (Wakeling et al., 2012) during locomotor and posture behaviors. Wavelet analysis specifically adapted for EMG activity (von Tscharner, 2000) has been extensively tested across numerous taxa (e.g., Wakeling et al., 2002; Wakeling et al., 2012; Lee et al., 2013; Gorvet et al., 2020) over the last two decades. Whereas EMG activity is traditionally analyzed for crude intensity as rectified-integrated area via a root mean square (RMS) method (Jouffroy and Stern, 1990), wavelet determines the spectral properties (intensity-frequency) of each EMG burst in sequential time packets called wavelets. Briefly, mean normalized EMG intensity is evaluated across a frequency spectra for which contour plots are used to detect peak burst amplitudes, followed by extraction of EMG intensity values at 17 selected characteristic frequencies (range: 0–902 Hz) sampled in 0.5–1 sec packets of the EMG signal data (von Tscharner, 2000; Wakeling et al., 2012). Low intensity-frequency properties (e.g., 120–200 Hz) are typical of the recruitment of slow MHC-1 fibers or MU in mammals (Wakeling et al., 2001; Hodson-Tole and Wakeling, 2007; Lee et al., 2013), whereas characteristic frequencies for the recruitment of fast MHC-2A fibers have been shown to range from 200 to 350 Hz (Wakeling et al., 2012).

Most mammals have a heterogeneous distribution of slow and fast MHC fiber types in their limb muscles and wavelet analysis has the power to distinguish between activation of slow vs. fast fibers (or MU) based on consistently measured spectral properties that match fiber type distributions. In fact, wavelet analysis was previously used on EMG data from sloth forelimbs to determine recruitments patterns of slow vs. fast muscle fibers during suspensory locomotor and postural behaviors (Gorvet et al., 2020). The main findings from this study and those of Spainhower et al. (2018, 2021) are integrated below and these data help establish the basis for the future analyses proposed in this review.

### **b. Suspensory muscle function**

Understanding of muscle function during suspensory behaviors is derived from foundational work with primates. Numerous studies in primate taxa have shown a relationship between muscle fiber type and EMG intensity during postural suspension and suspensory modes of locomotion (Jouffroy and Medina, 2004, and references therein; Jouffroy et al., 1999). The prevailing finding from these studies is that a near homogeneous

expression of large, slow MHC-1 fibers is typical of a single belly (or muscle head) of each major extensor functional group (elbow, knee, and ankle extensors) in the limbs of primates sampled and has a postural function as an anti-gravity muscle. For example, m. vastus intermedius in a rhesus macaque is 90% slow contracting, a feature that notably correlates with its large fiber size and role in hindlimb joint stabilization (Jouffroy et al., 1999). During arboreal postural behaviors, these slow-contracting muscles show low-to-moderate levels of EMG activity while the fast-contracting muscles show low activity; however, all muscles show high-level activity during locomotion (Jouffroy et al., 1999; Jouffroy and Medina, 2004).

Direct evidence of EMG muscle activation in the limbs of suspensorial primates beyond monkeys includes lemurs, lesser apes, and great apes, although these taxa are not exhaustive. Patel et al. (2015) showed that the hindlimb digital flexor muscles in red-ruffed lemurs (*Varecia rubra*) have long activations and are activated at higher levels than the forelimb digital flexors during stance phase of arboreal pronograde walking. These functional data emphasize hindlimb-biased support that most typical of primates during horizontal and vertical locomotion (Hanna et al., 2017). However, primates show a broad range of behavioral flexibility with use of their limbs (Granatosky et al., 2019). For example, the forelimb digital flexors in chimpanzees (*Pan troglodytes*) show maximum and sustained activity during suspension when their forelimbs are loaded in tension. But, for the digits that bear weight in knuckle-walking, the digital flexors are not active during contact (i.e., stance phase) and are only recruited to help clear the digits from the ground as the forelimb begins swing phase (Susman and Stern, 1979). These data collectively indicate the importance of the digital flexor activations for a strong grip on the substrate during arboreal maneuvering.

Electromyographic recordings during brachiation in gibbons have also reported function of ‘suspensory muscle chains’ that are found in the forelimbs of hylobatids (Jungers and Stern, 1980). The forelimb of white handed gibbons (*Hylobates lar*) has a unique arrangement of the insertions of the m. pectoralis major (clavicular head) on the radius (i.e., ventral chain) and the mm. latissimus dorsi and tensor fasciae antebrachii on the antebrachial fascia (i.e., dorsal chain) all via the short head of biceps brachii (modified to originate from the proximal humerus), which enhances role of strong extrinsic muscle



in forearm flexion (Jungers and Stern, 1980). Similar arrangement of muscle chains among the mm. pectoralis superficialis (anterior and posterior heads), deltoideus, and biceps brachii long head are notably observed in *Choloepus*, although muscle chains are not as complex in *Bradypus* (Nyakatura and Fischer, 2011; Olson et al., 2018). Jungers and Stern (1981) reported that, in early support phase, gibbons and spider monkeys (the latter lacking muscle chains) alike recruit both heads of m. pectoralis major purportedly for shock absorption and/or controlled abduction of the shoulder during brachiation. EMG activity was more consistent and prolonged in *Hylobates*. However, the short head of biceps brachii is recruited less consistently during support phase in gibbons than in black-headed spider monkeys (*Ateles fusciceps*). A more primary role in propulsion for the spider monkey is suggested by the consistent post mid-support EMG activity of m. biceps brachii short head. In particular, the most intense activation of this muscle occurs mid-swing for both spider monkeys and gibbons. The m. deltoideus is active throughout the second half of swing phase to elevate the arm, while the m. flexor digitorum superficialis fires just prior to contact for the next grasp (Jungers and Stern, 1981). Interestingly, the mm. pectoralis superficialis and deltoideus of gibbons were not active during quiet hanging, whereas the m. deltoideus of the spider monkey showed some EMG activity as did their m. pectoralis. The latter finding may be related to more generalized pectoral girdle myology of spider monkeys (Jungers and Stern, 1981).

Among primates, however, functional muscle data for *N. coucang*, in particular, are the most informative for matching expectations of EMG activation during suspension with muscle fiber types expressed in sloths. Jouffroy and Stern (1990) showed that the fore- and hindlimb flexor muscles (e.g., m. brachialis, m. semitendinosus, and m. flexor cruris longus) are active when the feet are in contact with the substrate during suspensory walking, whereas the limb extensor muscles (e.g., m. triceps brachii medial head and m. vastus lateralis) are active either during late contact or swing phase only. As stated above, a nearly uniform distribution of slow-contracting fibers are observed in both the flexors and extensors of lorises (Sickles and Pinkstaff, 1981a, b), and by correlating a predominant slow fiber type expression (no fast MHC-2X, 2B isoforms) with EMG activation patterns in *Nycticebus* suggests specialization of their slow-contracting muscles

for their controlled, deliberate suspensory habits. Moreover, it is possible that the majority of their limb muscles are capable of playing an anti-gravity role in suspensory support.

The previous results for *Nycticebus* match well with an overall 89% fiber type distribution of the MHC-1 isoform in the limb musculature of three-toed sloths (Spainhower et al., 2018, 2021). Similarly, an extremely large percentage expression of slow MHC-1 fibers among the hindlimb flexors (88%) and extensors (93%) of three-toed sloths also suggests that their hindlimb muscles may collectively play a majority anti-gravity role. Support for this hypothesis is exemplified by the results of our previous study (Gorvet et al., 2020) that evaluated EMG activation in the forelimb muscles of *B. variegatus*. The four main findings are summarized as the following: (1) the lowest volumes of active muscle were recruited during suspensory hanging (SH), where the distal carpal/digital flexors consistently showed the lowest levels of EMG activity among all muscles sampled; (2) flexor muscle activations were long and most intense during suspensory walking (SW) and found to be maximal for the elbow flexors and smallest for the carpal/digital flexors in forelimb; (3) EMG onset of the elbow and carpal/digital extensors occurred near mid-stance and either showed bi-phasic contact/swing activations or remained active through early swing during suspensory walking, and showed greater relative activations during vertical climbing (VC); and (4) small, fast MHC-2A fibers were recruited at low intensities of activation during SH, whereas large, slow MHC-1 fibers were recruited at large intensities of activation during SW and VC.

The last finding listed from the study by Gorvet et al. (2020) is further suggestive of two major specializations to the tensile limb system of sloths. First, as previously hypothesized (Mendel, 1981b, 1985a), largely passive weight-bearing in sloths is possible due to the presence of a digital flexor tendon ‘suspensory apparatus’ that functionally analogous to that in upright ungulates (Mossor et al., 2020). Second, sloths appear to have neuromuscular modifications that can offset the cost of muscle contraction by selective recruitment of small, fast-contracting MU (EMG spectral properties = low intensity, high frequency) when less force is needed for postural support that shifts to recruitment of large, slow contracting MU (EMG spectral properties = high intensity, low frequency) when greater force is needed for locomotor behaviors. Three-toed sloths may also have several forelimb muscles with super slow contraction velocities (i.e.,  $V_{\max}$ ) based on their reported

low mean EMG frequencies (Gorvet et al., 2020). These would be the slowest values for  $V_{\max}$  yet to be reported in vertebrates.

### **c. Neuromuscular characteristics**

Data from Gorvet et al. (2020) relate to historical findings indicating that sloth muscles have slow muscle contraction durations, which is defined as the difference in time between the onset of tension and peak tension during isometric contractions. Comparisons of the m. thoracic diaphragm, a typically slow, rhythmically contracting skeletal muscle, among sloths and cats emphasize prolonged contraction times with intervals of 70–120 ms and 35 ms, respectively (Goffart et al., 1962). This dramatic difference is also evident in a number of muscles of the distal hindlimb. For example, the contraction duration of the m. gastrocnemius in sloths is, on average, 109 ms vs. 22.5–27 ms for cats. Thus, muscle contractions in sloths are at least four times slower than those of the homologous muscles in cat limbs, even when measurements are normalized to body temperature (i.e., sloths display a much lower basal temperature than most placental mammals). Among sloth genera and species, there are significant differences in muscle contraction times. Digital flexor muscle contraction times in *Choloepus* vary between 70 and 175 ms, whereas those of *Bradypus* take nearly twice as long to contract with contraction times of 140–300 ms (Goffart et al., 1962). The differences in contraction times between genera indicates there are inherent differences in neuromuscular properties across species of sloths.

The protracted muscle contraction durations in sloths are attributable to both the aforementioned myosin fiber composition and neuromuscular properties. Because sloths predominantly express the slow MHC-1 in their skeletal muscle fibers (Spainhower et al., 2018, 2021), their muscles undergo considerably slower contractions relative to those of other mammals, which typically have heterogeneous muscle fiber distributions and include larger proportions of fast-contracting fibers (see above). Again, an application of the force-velocity relationship (Hill, 1938), which demonstrates that slow contractions produce large force, indicates that sloth muscles, in principle, emphasize force production over velocity (Sugi and Haruo, 2019). Slow, prolonged contractions should allow their skeletal muscles to operate near isometric force (or maximal joint torque) to limit accelerations of the body below the substrate. Force-velocity curves are available for sloths, but only from the m. thoracic diaphragm. When compared to the maximum contraction velocity ( $V_{\max}$  in cm/s)

of cats, indeed sloths have a  $V_{\max}$  that is 50% slower; however, produce similar maximum force (in  $\text{kg}/\text{cm}^2$ ) to that of feline m. thoracic diaphragm (Marechal et al., 1976). These findings may be attributed to sloth muscles operating at lengths which are optimal for force production at the expense of contractile velocity.

Not only do sloth limb muscles typically contract slower than those of other mammals, but the mechanical latent period, or the time from the induction of a stimulus to the beginning of a muscle contraction, is also longer (Goffart et al., 1962). Moreover, dramatic differences between *Choloepus* (7.7–8.5 ms) and *Bradypus* (40–50 ms) are observed (Gordon and Holbourn, 1949; Enger and Bullock, 1965). The previous findings are attributable to differences in size of the motor neurons across taxa. Sloth muscles are innervated by proportionally smaller motor neuron axons compared to those of other mammals. For example, the axons of the m. gastrocnemius reach a maximum diameter of only 16  $\mu\text{m}$  (Goffart and Geretbzooff, 1964) compared to a maximal thickness of  $\sim 22 \mu\text{m}$  in cats (Goffart et al., 1967). Motor neuron axon diameter displays a positive linear relationship with conduction velocity, thus resulting in a shorter mechanical latent period (Seidl, 2014). Enger and Bullock (1965) previously reported values of  $25 \text{ ms}^{-1}$  (*Bradypus*) and  $35 \text{ ms}^{-1}$  (*Choloepus*) for conduction velocity from sloth motor neuron branches. Domestic cats, which are similarly-sized mammals by body mass (in kg), have conduction velocities which are 3 to 4 times faster than those in sloths.

The physical size of motor neurons also influences the latency period (i.e., delay) of reflexes, which is part of critical mechanical sensory/motor feedback loops activated during locomotion. A monosynaptic reflex arc involves only a single motor neuron and a single sensory neuron. The overall delay in the reflex arcs in sloths was found to be nearly twice as long (e.g., 3.2 ms) in *Bradypus* compared to *Choloepus*, both of which are well above the latency periods measured in other mammals that can be as short as 0.5 ms (Enger and Bullock, 1965; Malcolm and Saraiva, 1967). These findings indicate how slowly sloth motor units react to stimuli. The delay in reflex arcs can therefore, in part, be explained by the slower nerve conduction velocities in sloths. In addition, being that sloths have gracile motor neurons that innervate potentially large MHC-1 and small MHC-2A motor units, this would result in delayed temporal summations that become manifest during their slow, intermittent movements by use of prolonged high force contractions (Spainhower et al.,

2021). Taken all together, it is apparent that there exist a number of integrated neuromuscular properties that explain ‘super slow’ muscle contractions implicated for sloth muscles.

### **Suspensory Locomotor Mechanics in Sloths**

Original work by Nyakatura and Andrada (2013) correctly predicted that sloths do not use pendulum exchanges of energy when walking below-branch. Sloths are incapable of running gaits; thus, they also cannot take advantage of elastic energy storage and recovery mechanisms economize locomotion (Biewener, 1998). However, Granatosky and Schmitt (2017) recently reported the forces involved with suspensory locomotion in two-toed sloths (*C. didactylus*). Measurement of substrate reaction forces (SRF) are essential to understanding limb system function and suspensory mechanics in arboreal taxa. Three important initial observations were made from the patterns of SRF in sloths: 1. Vertical SRF predominated indicating suspensory body-weight support on arboreal substrates; 2. Horizontal forces were intermediate and largely vary in direction between the fore- and hindlimbs; and 3. Medial forces on the substrate were appreciable, whereas lateral forces were negligible (Granatosky and Schmitt, 2017).

In contrast to SRF patterns typical of primates, which show hindlimb-biased body weight support as well as net propulsive impulse by the hindlimbs during horizontal locomotion (Schmitt and Lemelin, 2004) and vertical climbing (Hanna et al., 2017), the forelimbs of two-toed sloths are the main propulsion elements, whereas their hindlimbs perform greater net braking (Granatosky and Schmitt, 2017). Moreover, hindlimb forces in quadrupedal primates are brought about by actively shifting weight off the forelimbs and onto the hindlimbs through use of hindlimb retractors to relieve stresses on the forelimbs, which may be less well-structured (e.g., bones weaker in compression) for body weight support (Reynolds, 1985; Hanna et al., 2017). SRF data from *C. didactylus*, however, also reveal that both pairs of limbs maintain equal body weight support during suspensory walking (Granatosky et al., 2018). Therefore, the position of the CoM in sloths remains constant with horizontal levering or shifting of body weight between forelimbs and hindlimbs. Primates typically shift to greater tensile weight bearing by the forelimbs during suspensory maneuvering (Reynolds, 1985; Schmitt and Lemelin, 2002).

The unusual mechanics of sloth locomotion are not fully understood, but it was previously hypothesized (Granatosky et al., 2018; Gorvet et al., 2020) that co-activation of a forelimb flexor/adductor and hindlimb flexor/adductor during the contact phase of a suspensory walking stride might explain the patterns of SRF observed. It is also possible to co-contraction of epaxial/hypaxial musculature, in addition to specific limb muscles, would make the long axis of the body rigid when walking beneath branch to prevent shifting of the body weight (i.e., horizontal levering) and this prevent sloths from oscillating the substrate. The main predatory defense of sloths is stealth and cryptic movements (Enders 1935; Montgomery and Sunquist, 1978; Mendel, 1985a) so minimizing wasteful energy fluctuations (by oscillating tree branches) or ones that could lead to a fatal fall (fracturing the tree branch) is critical to fitness in sloths.

Collectively, the previous findings (e.g., Nyakatura and Andrada, 2013; Granatosky and Schmitt, 2017; Granatosky et al., 2018; Gorvet et al., 2020) strongly suggest that locomotion in the limb system of tree sloths is entirely driven by muscle activation. Although, locomotor mechanics have yet to be studied in any species of *Bradypus*, and SRF are not available for vertical climbing in sloths. During vertical climbing, both pairs of limbs are expected to have both a support and propulsive function. This expectation is based on recent data from slow climbing lorids that use the forelimbs for propulsion (tensile loading) during the first half of a climbing stride and for support hindlimbs (compressive loading) over the second half (Hanna et al., 2017). In fact, the contribution to vertical propulsion was relatively greater in the forelimbs of lorises compared to their hindlimbs. Given the overall similarity in behavior between *N. coucang* and sloths, it is likely that the hindlimbs of two- and three-toed forms also have a greater anti-gravity role as when grasping/clinging or climbing in an upright position.

### **Objectives and Hypotheses**

This study aims to evaluate muscle activation using electromyography (EMG) and substrate reaction forces (SRF) in the pelvic limbs of sloths. To this end, the contributions of the musculature will be used to evaluate function in sloth limbs as a tensile load-bearing system. It is hypothesized that selected muscles (or muscle pairs) in the fore- and hindlimbs co-activate to balance the body weight while walking below the substrate. The expected

results will substantially improve understanding of sloth locomotor mechanics and suspensory adaptations; in particular, their ability to minimize the metabolic cost of muscle contraction despite the lack of energy exchanges by pendulum or elastic energy storage/recovery mechanisms (Nyakatura and Andrada, 2013; Biewener, 1998). Slow, deliberate placement of the feet in contact with the substrate should further help to minimize the collisional costs of locomotion in sloths.

The mechanism by which sloths maintain a constant horizontal position of their center-of-mass (CoM) is not fully understood. Importantly, simultaneous recordings of EMG and SRF in tree sloths will reconcile prior findings that are incomplete. Expanding on the co-activation proposals of Gorvet et al. (2018, 2020) and Granatosky et al. (2018), the MHC fiber type compositions of the well-developed *m. sartorius*, *m. iliopsoas*, and *m. adductor* (all heads: Spainhower et al., 2021) are comparable to the that of the slow-contracting *m. pectoralis superficialis* (PS: both heads). Specifically, I hypothesize that contraction of slow fibers (or MU) from either or all of these hindlimb muscles in coordination with activation of PS is the mechanism by which sloths balance their body weight distribution during suspensory locomotion. Moreover, slow MU in the *m. sartorius* could control forward motion of the body via lengthening contractions. The pattern of activation of an opposable fore- and hindlimb pairs of flexors (and/or ep/hypaxial muscles) may serve to make the body axis rigid, and substantially contribute to slow movement in tree sloths.

## **MATERIALS AND METHODS**

### **Study animals**

A total of  $N=5$  sloths will be used for this study at The Sloth Sanctuary in Penshurst-Limon, Costa Rica. No preference will be given to the sex of the animals, although adult (or sub-adult) individuals will be preferable to juveniles due to grasping abilities of adults on beam substrates of larger sizes. All individuals are housed and will be cared for at The Sloth Sanctuary.

### **Implantation of Electrodes**

Sloths will be sedated (0.1 ml/kg Dexdomitor + 0.1 ml/kg Ketamine, injected into the *m. gluteus medius*) prior to electrode implantation. Supplemental doses of ketamine in increments of 0.1 ml will be used as necessary to achieve the desired level of sedation.

While under sedation, custom fine-wire, bipolar EMG electrodes (0.002 bifilar: California Fine Wire, Grover Beach, CA, USA) will be implanted into selected muscles of the hip, thigh, and leg. Additional electrodes may be implanted into antagonistic epaxial (e.g., *m. longissimus dorsi*) and hypaxial (e.g., *m. rectus abdominus*) muscles. Specifically, electrodes (sterilized by hydrogen peroxide plasma) will be implanted into either of two suites of four muscles in the left or right hindlimb. Pairs of 4 electrodes will be implanted percutaneously into the center of each muscle belly by using gentle force with a 26g needle to penetrate the skin, then a one-half twist, and removal of the needle that will leave the barred-hooked electrode end anchored in the muscle belly. Target muscle locations will first be identified by prior dissection of cadaver sloths and then by palpation of the limb while live sloths are under sedation. Finally, EMG wires will be cabled, secured, and connected to a wireless EMG unit (BioRadio™, Great Lakes NeuroTechnologies, Cleveland, OH, USA) that will be harnessed to the thorax of the sloth. Sedation will be reversed with injection of Antisedan (0.1 ml/kg) again into the *m. gluteus medius*.

### **EMG recordings**

Upon recovery from sedation, the limbs of sloths will be handled and placed in position to grasp a horizontal beam apparatus (4.57m x 0.22m x 1.52m). The beam will be segmented into three sections with 45 cm gaps in between. The center section of the beam will be instrumented with strain gauges (i.e., force transducers) to allow for simultaneous recordings of SRF with hindlimb muscle EMG. Sloths will be required to both hang in a static suspensory posture and walk suspended below the beam. Several trials of suspensory hanging (SH) using four contact support by the forelimbs and hindlimbs will be performed first in intervals of 1–3 min. Locomotor trials will consist of repeated short bouts of suspensory walking (SW), long enough to sample 2–3 footfalls of the instrumented hindlimb. SRF recordings require one contact each from a forelimb and hindlimb on the center section of the beam apparatus during SW. Sloths will also perform short bouts of vertical climbing (VC) where individuals will be allowed to freely climb a vertical beam or up the outside of a fenced enclosure (2.00m x 3.97m x 3.12m). Trials of VC will immediately follow SW trials. For each locomotor behavior, sloths will be encouraged to move with the enticement of food (e.g., leaves or flowers) by the handler as needed, but will be free to select their preferred speed.



All behavioral trials performed will be videoed with a GoPro camera (HERO4: San Mateo, CA, USA) positioned far enough from the animal to visualize/capture the entire length (or height) of the beam apparatuses; in the sagittal plane for the SW trials and in a coronal plane for VC trials. Video data (100 Hz) will be synchronized with both EMG (2000 Hz) and SRF (2000 Hz) with an LED light in the field-of-view of the camera. EMG will be recorded via broadband streaming using BioCapture™ software (Great Lakes NeuroTechnologies) for one suite of four muscles (proximal vs. distal musculature) then the other on consecutive days for the same individual. Output from the strain gauges attached to the beam apparatus will be conditioned and amplified, and then sent through an A/D converter to be recorded as changes in raw voltage on a laptop computer running Excitex software.

Several measured variables associated with EMG, including onset and offset time (in sec), burst duration (in sec), and burst intensity-frequency properties (via wavelet analysis: Wakeling et al., 2012) will be analyzed and compared statistically between muscles, behaviors, and individuals/species. Patterns of three-dimensional SRF will be resolved and peak force magnitudes in the vertical, horizontal (propulsive vs. braking), and medial-lateral directions will be determined. At the completion of data recordings (~2 h total) the fidelity of each implant will be verified before the fine wire electrodes are removed. The animals will then be placed back in their enclosure and observed for 1–2 h post-experiment to ensure full recovery.

## **Data analysis**

### **a. EMG**

Analysis of EMG activations will follow the previous methods of Gorvet et al. (2020). Video data will be analyzed for frame numbers that corresponded to the beginning and end of SH intervals, or to foot-on (grasp) and foot-off (release) events during locomotor trials from the force records. Frame number will be calibrated to time in seconds in the EMG waveform records using the video frame marking the time that the LED light first illuminated. Next, EMG recordings will be exported from BioCapture™ as a series of .CSV files in MS Excel (Microsoft Corp., Redmond, WA, USA) that will be used as source data for quantitative EMG analysis. EMG recordings for SW and VC, in particular, will be analyzed as a series of strides consisting of consecutive pairs of limbs contact and swing

phases. Specifically, LabScribe software (iWorx Systems Inc., Dover, NH) will be used to measure and calculate all temporal variables (time in sec and % stride) associated with both the limb cycle and EMG recordings relative to the stride interval, where the sum of the contact and swing phases is 100% of the stride, and include duty factor, swing duration, EMG onset, EMG offset, and EMG burst duration. Velocity (in  $\text{ms}^{-1}$ ) for SW and VC will be calculated by using the software Tracker (<https://physlets.org/tracker/>) to digitize several strides of each individual through a calibrated distance (15 cm) in the frame of view. The BioRadio™ unit or a marker placed on the head of a sloth will be used as the mark to digitize through one stride per trial analyzed. Instantaneous velocity will be determined at 1 s intervals throughout a stride and averaged across data points where velocity is similar. All temporal measurements will be averaged for each muscle, behavior, and individual.

EMG intensity will be analyzed using custom code written for the software Mathematica© (Wolfram Research, Champaign, IL, USA). First, burst intensity will be quantified by the Root Mean Square (RMS) method on rectified EMG data (Wakeling et al., 2001; Hodson-Tole and Wakeling, 2007; Wakeling, 2009). The maximum activations (millivolts) will be measured from each burst and stride sampled for final analysis and averaged for each muscle and individual. Burst intensities for each muscle will be normalized by calculating a series of intensity ratios ranging from 0 to 1 to compare EMG activation across behaviors, where a ratio of zero is no activation and one is maximum activation (Gillis and Biewener, 2001, 2002). Specifically, mean burst intensities for each muscle and behavior will be divided by a recorded value of maximum voluntary contraction for each muscle.

Second, a subset of 2–3 bursts per muscle and individual will be chosen for wavelet analysis (von Tscharner, 2000; Wakeling et al., 2012), whereby mean normalized EMG intensity will be evaluated across a frequency spectra for which contour plots will be used to detect burst intensities, followed by extraction of EMG intensity at 17 selected characteristic frequencies (range: 0–902 Hz) sampled in 0.5–1 s packets (x5) of EMG signal data. Mean and peak frequencies then will be determined for each muscle and behavior across individuals in the format of binary data for low-end and high-end frequency characteristics present in the recorded EMG signals. Finally, the mean frequency

properties of wavelets will be output as a series eigenscores for Principal Components Analysis (PCA). PCA is a multivariate analysis defined in terms of eigenvector-eigenvalue pairs. The eigenvector represents the PC weighting, while the eigenvalue represents the PC loading score and is responsible for describing the amount of each eigenvector in each measured spectrum (Wakeling, 2004; Hodson-Tole and Wakeling, 2007). To quantify high frequency vs. low frequency components within the EMG signal, PC1 (y-axis) loading scores will be plotted against the PC2 (x-axis) loading scores, resulting in a vector angle ( $\theta$ ). A larger  $\theta$  has a negative contribution and specifies low-frequency content, while a smaller  $\theta$  has a positive contribution and characterizes higher-frequency content. These PC loading plots will be used to evaluate activation frequency grouping patterns for slow and fast motor units for each muscle across the three functional behaviors SH, SW, and VC.

#### **b. SRF**

Voltage output from the beam transducers will be calibrated to force in Newtons. Records of SRF in each dimension then will be normalized to body weight (%BW) with values <100% indicating applied SRF lower than body weight and values >100% indicating applied SRF above body weight. Support in sloths most commonly involves multiple limbs or limb pairs, thus peak SRF for a single is not expected to exceed BW force. Peak magnitudes of SRF in the vertical, horizontal, and mediolateral directions will be resolved. Vertical forces are positive by convention and represent body weight support and how the CoM is distributed between the fore- and hindlimb pairs in sloths (Granatosky et al., 2018); horizontal forces that have a positive sign are propulsive, whereas horizontal SRF that have a negative sign are braking; and medial forces are negative and lateral forces are positive. Contact intervals also will be normalized to percent stride (0–100%) to make equal comparisons in timing of peak SRF between fore- and hindlimbs possible (Granatosky and Schmitt, 2017).

#### **Statistics**

Values will be reported as means  $\pm$  s.d. (standard deviation) unless otherwise specified. ANOVA will be performed in SPSS (v. 20: IBM, Inc., Armonk, NY, USA) and used to assess differences for stride duration, duty factor, and velocity between SW and VC. Although patterns of SRF are most important for evaluation of locomotor mechanics, peak SRF between sloth forelimbs and hindlimbs also will be tested for statistical differences by

time of day that sloths will be required to perform locomotor trials, and this time interval may not coincide with a typical active period for *Bradypus*, which is diurnal however. In addition, measurements from some muscles may vary due to fatigue and because muscle suites from the same individual will be sampled on separate days. Second, it is also possible that sloths will not be fully recovered from sedation at the outset of the recording sessions. Sloths do not metabolize drugs quickly (Gorvet et al., 2020), and despite the administration of a reversal agent, individuals may perform better after multiple SW trials. For this reason, 10–15 records of each behavior are planned to ensure the sampling of optimum performance, which includes consecutive strides of near steady-state walking and climbing. A third possibility could be difficulty managing the diameter of the beam apparatus.

ANOVA. These tests will be used to mainly assess significant effects of fore- vs. hindlimbs in both weight-bearing support and propulsion/braking during locomotion (Granatosky and Schmitt, 2017).

Descriptive statistics for all temporal and EMG intensity measurements for each muscle will be pooled and averaged across individuals to account for variance associated with the typical patterns of EMG activation timing and EMG maximum activation. For additional statistical analysis, Coefficients of Variation (CV) will be calculated for each variable analyzed to justify use of mean data in multivariate testing. MANOVA will be performed (in SPSS) to evaluate statistical significance in both EMG burst duration (%) relative to the stride cycle and normalized EMG burst intensity, specifically how these activation parameters varied among muscles (effect: muscle) and the three behavioral conditions (effect: behavior). A significant MANOVA will be followed by a series of one-way ANOVAs with post hoc tests to determine all pair-wise significant outcomes (Gorvet et al., 2020). Significance for all tests will be accepted at  $p \leq 0.05$ .

### **Study Limitations**

The implantation of fine-wire electrodes has been approved as a recovery procedure with the stipulation that no animal will be sacrificed following experimentation. Thus, the exact placement of EMG electrode implantation cannot be verified. Moreover, there is no access to ultrasound or MRI to verify muscle identity *in vivo* or the depth/location of the electrode wire once implanted in a muscle mid-belly. However, despite the potential lack of placement details for electrode implants in some muscles, EMG activation broadly sampled from flexor and extensor musculature (per limb region) will be adequate to achieve our study objective and test our hypothesis and predictions. Also, EMG studies are often fraught with the inability to sample data from all muscles per behavior and individual due to electrode failure. There is not an option (or time) to record SW and VC on separate days because one of the goals of this study is to minimize stress to the animals. However, it may be advantageous to alternate the order of SW and VC trials, although suspensory walking is stereotypical in sloths and adequate sampling of this locomotor behavior *a priori* must be ensured.

Three other factors are suggested to be potential study limitations. First, all individuals may not be capable of performing all behaviors equally well. This may be attributed to the

**RESOLUCIÓN N°**  
**R-SINAC-PNI-ACLAC-012-2021**  
**Exp. Dig. N° M-PC-SINAC-PNI-ACLAC-013-2021**

Ministerio Del Ambiente y Energía, Sistema Nacional de Áreas de Conservación, a través del Programa de Investigación del Área de Conservación La Amistad Caribe, a las quince horas, cuarenta minutos del día primero del mes de setiembre del año dos mil veintiuno.

**RESULTANDO**

**PRIMERO:** Que el día décimo séptimo del mes de marzo del año dos mil veinte, se recibe vía electrónica solicitud de permiso de investigación y licencias de colecta científica de Michael Todd Butcher, estadounidense, biólogo, pasaporte N° 526175396, dirección permanente: Departamento de Ciencias Biológicas, sala 4011 – One University Plaza, Youngstown, Ohio 44555, USA. Dirección en Costa Rica: Santuario de perezosos, P.O. Box 23-702, Cahuita, Limón, Costa Rica, solicita permiso para desarrollar la investigación: “Activación de Hindlimb Muscle durante la suspensión en perezosos de árbol (*Xenarthra: Pilosa*)”.

**SEGUNDO:** Que la investigación es apoyada por el Departamento de Ciencias Biológicas, Universidad Estatal de Youngstown, Ohio, USA. Teléfono: 330-941-7177. Fax: 330-941-1483. Sitio Web: <https://www.yosu.edu>.

**TERCERO:** Que se solicita autorizar la participación en esta investigación científica a Dakota Martin D. Morgan, estadounidense, biólogo, pasaporte N° 597155810 y Michael C. Granatosky, estadounidense, antropólogo en biología, pasaporte N° 569573129, en calidad de coinvestigadores.

**CUARTO:** Que el día décimo séptimo del mes de julio del año dos mil veinte, el investigador Michael Todd Butcher, pasaporte N° 526175396, cumplió con los requisitos establecidos en el Decreto N°32553-MINAE (incluyendo la carta de visto bueno del Santuario de perezosos, donde se realizará la investigación científica).

**CONSIDERANDO**

**PRIMERO:** Que la Ley de Conservación de la Vida Silvestre No.7317 y sus reformas, en los artículos 1 y 3, establece que: “La vida silvestre está conformada por el conjunto de organismos que viven en condiciones naturales, temporales o permanentes en el territorio nacional...” que “Se declara de dominio público la fauna silvestre que constituye un recurso natural renovable,... De interés público la flora silvestre...” y que únicamente pueden ser objeto de apropiación particular y de comercio mediante las disposiciones contenidas en los tratados públicos, en los convenios internacionales y en la presente Ley N° 7317 y su reglamento, artículos 3 y del 36 al 50 y otras normativas vinculantes.

**SEGUNDO:** Que la Ley de Conservación de la Vida Silvestre N° 7317 y sus reformas, establece en el artículo 6° que el Sistema Nacional de Áreas de Conservación del Ministerio de Ambiente y Energía es el órgano competente en materia de planificación, desarrollo y control de la vida